THESIS APPROVAL

GRADUATE SCHOOL, KASETSART UNIVERSITY

Master of Engineering (Civil Engineering)

DEGREE

Civil Engineering | Civil Engineering
FIELD | **DEPARTMENT**

TITLE: Effects of Myanmar Volcanic Ash on Portland Cement Concrete Pavement

NAME: Miss Ei Ei Mon

THIS THESIS HAS BEEN ACCEPTED BY

______________________________ **THESIS ADVISOR**

(Associate Professor Chavalek Vanichavetin, Ph.D.)

______________________________ **THESIS CO-ADVISOR**

(Mr. Aswin Karnasuta, M.Eng.)

______________________________ **DEPARMENT HEAD**

(Associate Professor Korchoke Chantawarangul, Ph.D.)

APPROVED BY THE GRADUATE SCHOOL ON ______________________________

______________________________ **DEAN**

(Associate Professor Gunjana Theeragool, D.Agr.)

THESIS

EFFECTS OF MYANMAR VOLCANIC ASH ON PORTLAND CEMENT CONCRETE PAVEMENT

EI EI MON

A Thesis Submitted in Partial Fulfillment of
the Requirements for the Degree of
Master of Engineering (Civil Engineering)
Graduate School, Kasetsart University
2011

Ei Ei Mon 2011: Effects of Myanmar Volcanic Ash on Portland Cement Concrete Pavement. Master of Engineering (Civil Engineering), Major Field: Civil Engineering, Department of Civil Engineering. Thesis Advisor: Associate Professor Chavalek Vanichavetin, Ph.D. 117 pages.

Use of pozzolan substantially reduces cement requirement in construction leading to better economy and less environmentally adverse impact. But the utilization of Myanmar volcanic ash is still limited due to the lack of understanding of the characteristics of volcanic ash itself and the properties of concrete containing volcanic ash. Effects of pozzolan on properties of concrete vary with pozzolan type and volume. In this study, effects of Myanmar volcanic ash on Portland Cement Concrete Pavement (PCCP) were investigated. Twelve concrete mixes were produced in three levels (0.5, 0.55 and 0.6) of water to binder ratio (w/b) and four levels (0%, 15%, 30% and 45%) of cement replacement with volcanic ash by weight. Specimens were subjected to compressive strength, flexural strength and Los Angeles abrasion tests. Test results showed that optimum percent replacement of cement with volcanic ash was 15% for pavement. The compressive strength, flexural strength and abrasion resistance of volcanic ash concrete were slightly lower than the control concrete. Microstructures were examined using Scanning Electron Microscope (SEM) and Mercury Intrusion Porosimetry (MIP) and X-ray diffraction (XRD) analysis. Eight mortar mixes in four levels of cement replacement with volcanic ash and fly ash were mixed to get 100% flow. The water demand of fly ash was lower than volcanic ash and compressive strength of fly ash mortar was higher than that of volcanic ash mortar at early age. The results showed that the strengths of concrete with volcanic ash were correlated well with pore volume.

________________________ ________________________ ___ / ___ / ___

Student’s signature Thesis Advisor’s signature

ACKNOWLEDGEMENTS

I would like to give grateful appreciation to my advisor Associate Professor Dr. Chavalek Vanichavetin and my Co-Advisor Mr. Aswin Karnusata for their advice and valuable suggestions for the writing of this thesis. I am also grateful to Associate Professor Dr. Prasert Suwanvitaya, Associate Professor Dr. Warakorn Mairaing and Associate Professor Dr. Suvimol Sajjavanich for their encouragement and valuable technical guidance which enabled my study to be accomplished successfully.

I would like to express sincere thanks to Associate Professor Dr. Parames Kamhangrittirong, Associate Professor Dr. Duangrudee Chausuwan and Mr. Chatchawan Kanjanasuwan for their cooperation and help during my experimental work. Thanks are also given to Ms. Arunee Riandara and all staff of the International Graduate Program in Civil Engineering for their kind cooperation.

I gratefully acknowledge Thailand International Development Co-operation Agency (TICA) and the Ministry of Construction of the Republic of Union of Myanmar for awarding scholarship.

I am grateful to the officers of the Ministry of Electric Power for the supply of volcanic ash and the officers and the technical staff of the Road Research Laboratory of Public Work, Ministry of Construction for helping during experimental work in Myanmar.

Finally I deeply appreciate my parents for their encouragement throughout the course of my study.

Ei Ei Mon

June 2011

TABLE OF CONTENTS

	Page
TABLES OF CONTENTS	i
LIST OF TABLES	ii
LIST OF FIGURES	iv
INTRODUCTION	1
OBJECTIVES	4
LITERATURE REVIEW	7
MATERIALS AND METHODS	36
Materials	36
Methods	40
RESULTS AND DISCUSSION	49
CONCLUSIONS AND RECOMMENDATIONS	68
Conclusions	68
Recommendations	69
LITERATURE CITED	70
APPENDICES	75
Appendix A Results of the experiments	76
Appendix B Photos of the experiments	111
CURRICULUM VITAE	117

LIST OF TABLES

Table **Page**

Table		Page
1	Classification of pozzolan according to their chemical compositions	8
2	Approximate free water content required to give various levels of workability	21
3	Probability factor for various tolerances	23
4	Approximate compressive strength of concrete mixes with water cement ratio as 0.5	25
5	Assumed standard deviations	25
6	Minimum cement content, maximum water cement ratio and grading of concrete to ensure durability under special exposure with aggregate of 20mm nominal maximum size	28
7	Chemical composition of ASTM Type I ‘Horse Head’ brand cement	36
8	Physical properties of Myanmar volcanic ash and Mae Moh fly ash	37
9	Chemical compositions (%) of Myanmar volcanic ash and Mae Moh fly ash	37
10	Mineral constituents of Myanmar volcanic ash compared with ASTM C 618	38
11	Physical properties of aggregates	39
12	Consistency and Setting Times of cement pastes with different replacements of volcanic ash	49
13	Comparison of flexural strengths of volcanic ash concrete and control concrete	56
14	Test results of Mercury Intrusion Porosimetry (MIP)	59

Appendix Table

A 1	Mix Proportion per one cubic meter of concrete (slump 30-60 mm)	77
A 2	Summary of test results of average compressive strength	78

LIST OF TABLES (Continued)

Appendix Table		Page
A3	Compressive strength of specimens tested at 7 days	79
A4	Compressive strength of specimens tested at 14 days	80
A5	Compressive strength of specimens tested at 28 days	81
A6	Compressive strength of specimens tested at 56 days	82
A7	Summary of test results of average flexural strength	83
A8	Flexural strength of specimens tested at 7 days	84
A9	Flexural strength of specimens tested at 14 days	85
A10	Flexural strength of specimens tested at 28 days	86
A11	Flexural strength of specimens tested at 56 days	87
A12	Los Angeles Abrasion wear (%) of volcanic ash concrete at w/cm=0.5	87
A13	Pore Size Distribution of OPC by Volume – Intrusion	88
A14	Pore Size Distribution of 1VA45 by Volume – Intrusion	95
A15	Pore Size Distribution of 56VA45 by Volume – Intrusion	102
A16	Compressive strength of standard motor at 7 days	109
A17	Compressive strength of standard motor at 28 days	109
A18	Water demand for 100% flow standard motor for compressive strength and water absorption tests	110
A19	Water absorption of standard motor at 28 days	110

LIST OF FIGURES

Figure **Page**

1	Types of pozzolan	9
2	Location of pozzolan sources in Myanmar	14
3	SEM micrograph of volcanic ash	15
4	Relationship between compressive strength and free water cement ratio	24
5	Estimated wet density of fully compacted concrete	27
6	Recommended proportions of fine aggregate according to percentage passing a 600μm sieve	30
7	Testing equipment set for flexural strength	44
8	Effect of % replacement VA on compressive strength of concrete at w/b = 0.5	51
9	Effect of % replacement VA on compressive strength of concrete at w/b = 0.55	51
10	Effect of % replacement VA on compressive strength of concrete at w/b = 0.6	52
11	Effect of % replacement VA on flexural strength of concrete at w/b = 0.5	53
12	Effect of % replacement VA on flexural strength of concrete at w/b = 0.55	53
13	Effect of % replacement VA on flexural strength of concrete at w/b = 0.6	54
14	Relation between compressive strength and flexural strength of volcanic ash concrete and control concrete	54
15	Relationship between compressive strength and flexural strength of control concrete	55
16	Relationship between compressive strength and flexural strength of volcanic ash	56

LIST OF FIGURES (Continued)

Figure **Page**

Figure		Page
17	Effect of VA replacement on Los Angeles Abrasion wear (%)	57
18	Pore diameter and incremental pore volume of OPC and VA45 pastes at 1day and VA45 at 56 days	59
19	SEM micrograph of ordinary Portland cement paste at 1 day	60
20	SEM micrograph of cement paste with 45%volcanic ash at 1 day	61
21	SEM micrograph of cement paste with 45% volcanic ash at 56 days	61
22	XRD patterns of ordinary Portland cement paste at 1 day	62
23	XRD patterns of cement paste with 45% volcanic ash at 1 day	63
24	XRD patterns of cement paste with 45%volcanic ash at 56 days	63
25	Compressive strengths of mortars incorporating volcanic ash and fly ash at 7 days	65
26	Cement equivalent factors (n) of fly ash and volcanic ash at 7 days	65
27	Compressive strengths of mortars incorporating volcanic ash and fly ash at 28 days	66
28	Cement equivalent factors (n) of fly ash and volcanic ash at 28 days	66
29	Water absorption (%) of cement mortars incorporating fly ash and volcanic ash	67

Appendix Figure

Appendix Figure		Page
B1	Testing consistency of cement and volcanic ash mix paste	112
B2	Curing of specimens in water	112
B3	Testing Los Angeles abrasion of concrete	113
B4	Testing compressive strength of concrete with ELE testing machine	113
B5	Testing flexural strength of VA concrete	114
B6	Mixing mortar	114

LIST OF FIGURES (Continued)

Appendix Figure **Page**

B7	Measuring flow of mortar	115
B8	Testing compressive strength of mortar with Universal Testing Machine	115
B9	Photos of fly ash, volcanic ash and cement powders	116

EFFECTS OF MYANMAR VOLCANIC ASH ON PORTLAND CEMENT CONCRETE PAVEMENT

INTRODUCTION

Reducing poverty and environmental pollution are important goals for sustainable development of a country. Myanmar is one of the several developing countries where an abundance of volcanic ash can be found. Regions where poverty is prevalent and natural pozzolans are available can be targeted to develop more sustainable construction.

The manufacture of Portland cement is expensive, energy-intensive and generates harmful emissions. One way to reduce CO2 emissions related to cement manufacturing is simply to reduce the demand for Portland cement. Even small reductions of Portland cement content in concrete pavements will yield significant environmental savings. The strategy is to replace some Portland cement in concrete mixtures with pozzolanic material.

Using pozzolan in concrete mixtures can also yield other benefits, including increased economy and enhanced concrete durability, improvement in workability, reduction of heat of hydration, increased water tightness and ultimate strength, and enhanced resistance to sulphate attack. Therefore, their appropriate use should always be considered.

Compressive strength has been always regarded as an important index of the concrete quality. To ensure the construction safety and economy in engineering practice, it is important to know the strength development of concrete with pozzolan at various ages. The pozzolanic materials have been used widely in concrete construction because of its engineering benefits. The effects of properties of concrete will differ greatly on the kind of pozzolanic materials, its quality and its percentages of replacement of cement.

Flexural strength is a very important parameter for concrete in the design of concrete structures, such as concrete pavement, bridge, and building. The determination of flexural tensile strength is essential to estimate the load at which the concrete members may crack. As it is difficult to determine the tensile strength of concrete by conducting a direct tension test, it is computed by flexure testing. The flexure tensile test is useful in the design of pavement slabs and airfield runway as flexural tension is critical in these cases (Gambhir, 2006).

The scraping or sliding action of the vehicle movements results in wearing and abrasion on the surface layer of pavement structures due to friction between pavement surface and vehicle tyre. Abrasion and erosion resistance of concrete is of significance when concrete is to be exposed to abrasive force on road surface. So the abrasion resistance is also important for durability of pavement in surface layer (Berry, 1994).

The meaningful use of Myanmar volcanic ash (natural pozzolan) can not only transform it into a natural resource to produce low-cost construction materials but can also help to decrease environmental hazards leading to sustainable development. The development of less expensive and environmentally friendly VA-based concrete with acceptable strength and durability characteristics can be extremely helpful.

The objective of this study is to improve the understanding of the properties of volcanic ash and to implement the effective usage of Myanmar volcanic ash in concrete pavement.

Statement of the problems

Cement, an important part of concrete, comprises a substantial portion of the construction cost and its high cost can sometimes become a financial burden for project owner. In developing countries, the economical substitutes could satisfy the need of the people.

Natural pozzolans are found at extinct volcanoes in Myanmar. 74 million tons of natural pozzolan can be extracted. The pozzolan grinding plant started its production work in April 2005 and can produce 1,000 tons of finished goods daily. The usage of pozzolan in Myanmar is only on dam projects. Most of the dams in Myanmar are earth filled dam and only two Roller Compacted Concrete (RCC) dams currently use pozzolan.

Cement factories in Myanmar can produce about 1.4 million tons per year. The cement usage is about 2.0 million tons. Approximately 0.6 million tons of cement are imported from Thailand. By replacing a fraction of cement by locally available natural pozzolan, the imported cement from Thailand can be reduced. Pozzolans are alternative materials that are substituted for Portland cement. The local availability also reduces the material transportation and expenses that are required for imported cement.

The manufacturing process of pozzolan needs less process compared to cement production process. So the price of pozzolan is very low compared to cement price. In Myanmar, the price of pozzolan is about one third of cement price at factory. So the project cost can be reduced by using pozzolan.

OBJECTIVES

The objectives of this study are as follows:

1. To improve the understanding of the properties of Myanmar volcanic ash (natural pozzolan).
2. To implement the effective usage of Myanmar volcanic ash in concrete pavement.
3. To examine the optimum percentage replacement of Myanmar volcanic ash for pavement.
4. To compare the compressive strengths of volcanic ash and fly ash mortars.

Scope of Study

1. Consistency and setting times of volcanic ash concrete

Testing the consistency, initial and final setting times of volcanic ash and cement pastes were done according to ASTM C 187 and ASTM C 191.

2. Mechanical properties of volcanic ash concrete

- Myanmar volcanic ash was applied as partial replacement of cement in concrete specimen.
- The volcanic ash fractions were 0%, 15%, 30% and 45%.
- The water to binder (w/b) ratios were 0.5, 0.55 and 0.6.
- Slump range was 30 mm- 60 mm.
- 28-days characteristic strength was 28 MPa.
- Maximum aggregate size was 20 mm.
- Average of 3 test specimens was recorded as 1 data.
- Specimen sizes were:
    1. 150 mm x 150 mm x 150 mm for compressive strength test
    2. 150 mm x 150 mm x 600 mm for flexural strength test

3. Crushed specimens from compressive strength test and flexural strength test were used for abrasion resistance test.

- Curing of specimens was done in water.

- The tests were conducted at 7 days, 14 days, 28 days and 56 days for compressive and flexural strength tests. Abrasion resistance test was conducted at 28 days and 56 days.

3. Microstructure Investigations: Scanning Electron Microscope (SEM), X-ray Diffraction (XRD) and Mercury Intrusion Porosimetry (MIP)

- Volcanic ash and cement were used.
- Water to binder (w/b) ratio was 0.5.
- Specimen size was 50 mm x 50 mm x 50 mm.
- Ordinary Portland Cement (OPC) paste was tested at 1 day and 56 days.

4. Comparison of compression strengths of volcanic ash and fly ash mortars

- Myanmar volcanic ash and fly ash were applied as cement replacement in mortar specimens.
- The volcanic ash and fly ash fractions were 0%, 15%, 30% and 45%.
- 100% flow was applied.
- Specimen sizes were 40 mm diameter with 80 mm depth.
- Sand to binder ratio was 2.75:1.
- Curing of specimens was done in water.
- Mortar compressive strength tests were conducted at 7 days and 28 days.
- Average of 3 test specimens was recorded as 1 data.

5. Comparison of water absorption of fly ash and volcanic ash mortars

- Mix proportion for mortar was same as reactivity index test.

- Specimens with 50 mm diameter and 40 mm depth were use.

- Curing of specimens was done in water.
- Absorption test was conducted at 28 days.
- Average of 3 test specimens was recorded as 1 data.

LITERATURE REVIEW

1. Pozzolan

Fine volcanic ash, deposited by winds from the eruption of volcanoes, or pulverized volcanic pumice, is pozzolan. Pozzolan is defined as a siliceous or siliceous and aluminous material, which in itself possesses little or no cementitious value but will, in finely divided form and in presence of moisture, chemically react with calcium hydroxide at ordinary temperature to form compounds possessing cementitious properties (ASTM C 618).

Pozzolans have been in use for many centuries by the Greeks and the Romans. The Greek started to use pozzolans after noticing that certain types of finely ground volcanic deposits when mixed with lime and sand were highly resistance to the action of water. They obtained their best pozzolans from around the Bay of Naples and particularly in a town called Pozzoli. Consequently these early materials were known as pozzolans.

2. Usage of Pozzolan

Pozzolan have been used in the construction of many mass concrete and marine structures such as dams, harbours, bridge piers, heavy duty industrial pavements, airport runway pavements, bus terminals and parking lots, etc.

Pozzolan can be used as lime-pozzolana and OPC-pozzolana. In lime-pozzolana, the addition of pozzolan will decrease setting times and increase the strength of lime based concretes and mortars. It can produce hydraulic cement which has the ability to set under water. Lime-pozzolana cements can often be produced for less than half the cost of OPC. The use of low-cost lime-pozzolana cements in small scale building works is common in many parts of Asia.

In OPC-based concrete, pozzolans are used to replace up to 30 per cent of OPC for use in structural applications and up to 50 per cent for non-structural purposes. As OPC is expensive and sometimes scarce, this can represent a significant cost saving. In addition, Portland-pozzolana blended cement has a number of significant technical advantages over plain OPC. They are: improved workability, reduced bleeding, improved sulphate resistance, improved resistance to alkali aggregate reaction, lower heat of hydration and enhanced long term strength.

The only disadvantage of these blended cements is that their early strength gain is slightly lower. This might means that removal of formwork on structural concrete and opening of traffic on pavement may need to be delayed. But this disadvantage is far out weighed by the advantages.

3. Classification of Pozzolan

According to their source, pozzolan can be classified into two main groups, natural and artificial pozzolans. According to their chemical composition, ASTM C 618 classified pozzolan into three main groups; class F, class C and class N pozzolans. Detailed classifications are shown in Table 1 and Figure 1.

Table 1 Classification of pozzolan according to their chemical compositions

Properties of pozzolan		F	C	N
$SiO_2 + Al_2O_3 + Fe_2O_3$	min%	70	50	70
SO_3	max%	5	5	4
Moisture content	max%	3	3	3
Loss on Ignition	max%	6	6	10

Source: ASTM C 618 (1993)

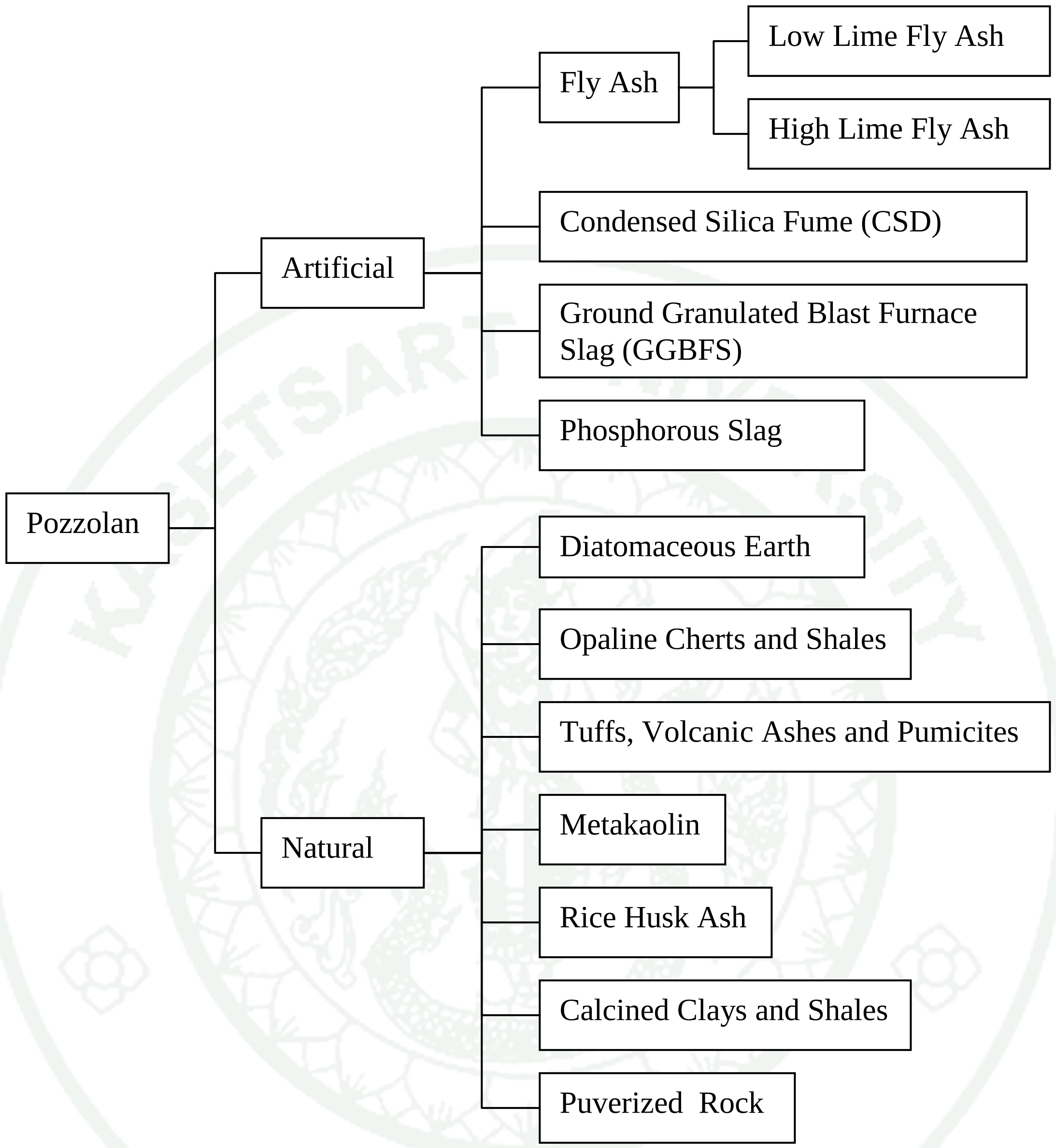

Figure 1 Types of pozzolan

Source: ACI 232 (1994)

4. Hydration Reaction and Pozzolanic Reaction of Volcanic Ash

The important chemical reactions involved with volcanic ash are:

4.1 Hydration reaction

This reaction is a consequence of $CaO.SiO_2$ plus H_2O. The product of the reaction is called cement gel. There are two chemical compounds which occur during the reaction. These compounds are Calcium Silicate Hydrate (C-S-H) and Calcium Hydroxide ($Ca(OH)_2$). Approximately 60% of cement gel is Calcium Silicate Hydrate (C-S-H) which is the main component of cement gel.

The chemical equations of hydration reaction are:

$$2(3CaO.SiO_2) + 6H_2O \longrightarrow 3CaO.\ 2SiO_2.\ 3\ H_2O + 3Ca(OH)_2 \qquad (1)$$

$$2(2CaO.SiO_2) + 4H_2O \longrightarrow 3CaO.\ 2Si\ O_2.\ 3\ H_2O + Ca(OH)_2 \qquad (2)$$

The reaction will continue while Calcium Oxide reacts with water and produces Calcium Hydroxide ($Ca(OH)_2$) until the reaction comes to the stable state or Calcium Silicate in the solution is totally used.

4.2 Pozzolanic reaction

This reaction is the second step continuing from the hydration reaction. In this step, Calcium Hydroxide ($Ca(OH)_2$) developed from the hydration reaction reacts with Silica (SiO_2) and Alumina (Al_2O_3) from volcanic ash.

The chemical equations of pozzolanic reaction are:

$$3Ca(OH)_2 + 2SiO_2 \longrightarrow 2CaO.2SiO_2.\ 3H_2O \qquad (3)$$

$$3Ca(OH)_2 + 2Al_2O_3 \longrightarrow 3CaO.2Al_2O_3.\ 3H_2O \qquad (4)$$

Calcium Silicate Hydrate ($CaO.2SiO_2$. $3H_2O$) and Calcium Aluminate Hydrate (CaO.2 Al_2O_3. $3H_2O$) strengthen the bond strength of concrete itself. These substances increase bonds between particles of cement paste increasing the strength of concrete. (Matee, 1992)

5. The Basic Properties of Volcanic Ash that should be Considered are:

1. The quantity of $SiO_2 + Al_2O_3 + Fe_2O_3$.

2. The quantity of CaO which has an effect on the hydration reaction. It increases the early strength development of concrete if there is an ample quantity. However it is not suitable for lower heat concrete.

3. The quantity of SO_3 and free lime will affect the expansion of concrete. The maximum quantity of SO_3 is 4% for class N pozzolan. (ASTM C 618)

4. The quantity of volcanic ash retained on sieve no 325. The fineness of volcanic ash has an effect on water content and pozzolanic activity index.

5. Pozzolanic activity index tells us about the rate of the pozzolanic reaction occurance.

6. The Advantages and Disadvantages of Natural and Artificial Pozzolan-Portland Cement Blended Mixes over Ordinary Portland Cement Mixes (Price, 1975)

6.1 Advantages

- Cheap (by-product or waste material).
- Slow hydration rate of reaction that leads to a reduced rate of heat development.

- Lower rate of thermal expansion by up to 10%.
- Good resistance to sulphate attack.
- Long term strength may be higher.
- Increased water tightness.
- Lower water requirement for fly ash.
- Increased workability.

6.2 Disadvantages

- Low specific gravity of pozzolans compared to cement increases the volume of material required for the same weight.
- Large quantities of fine materials may lead to increased handling, transportation and processing cost.
- Decreased rate of hardening and slow strength development.
- Resistance to freeze/thaw is slow to develop.
- For partial replacement of cement, the pozzolan and cement must be batched separately.
- Increased shrinkage during drying (expcept fly ash).
- Increased water requirement for pozzolans other than fly ash.

7. Natural Pozzolan Search, Investigation and Exploration in Myanmar

The feasibility study of Yeywa Hydropower Project in Myandalay Division was carried out by Nippon Koei Co. Ltd. The consultant had recommended to use the imported fly ash for construction of RCC dam. Importing fly ash from Mae Moh thermal power station in Thailand involves extreme land and sea transport routes. Significant cost saving can be achieved if domestic pozzolanic material from volcanic area is substituted. In order to search for indigenous pozzolanic material, a joint mission of Department of Hydroelectric Power and Colencol Power Engineering Ltd. visited central Myanmar in early December 2000. Successive investigations were followed up to the regions of upper Myanmar as shown in Figure 2. After intensive study, Popa (Pozzolan area No.1, i.e. P1) and Monywa (Pozzolan area No.2, i.e. P2) were selected as promising sites for further study.

Mt. Popa in central Myanmar is the southernmost existing volcanic cone on the Myanmar arc and is composed of pyroclastic rocks with associated minor and esitac lava flows.

There are significant deposits of very good natural pozzolans near Mount Popa and at Lower Chindwin. It can be used as cement replacement in the cementitious materials required in RCC dams. Exploration of the resources at Mount Popa area was decided upon for the Yeywa Hydro Power Project, it being accessible also to areas, south of Mandalay and the milling facilities now installed at Mount Popa. Pozzolans from Popa natural pozzolan grinding plant are presently providing the pozzolan being used in Yeywa dam.

It was learnt that 66% of the cement is replaced with natural pozzolan in constructing Roller Compacted Concrete Dam of ongoing Yeywa Hydropower project. The main purpose of using natural pozzolan in Yeywa dam is to avoid unnecessary cracks in concrete works by reducing the heat (Win Kyaw, 2006).

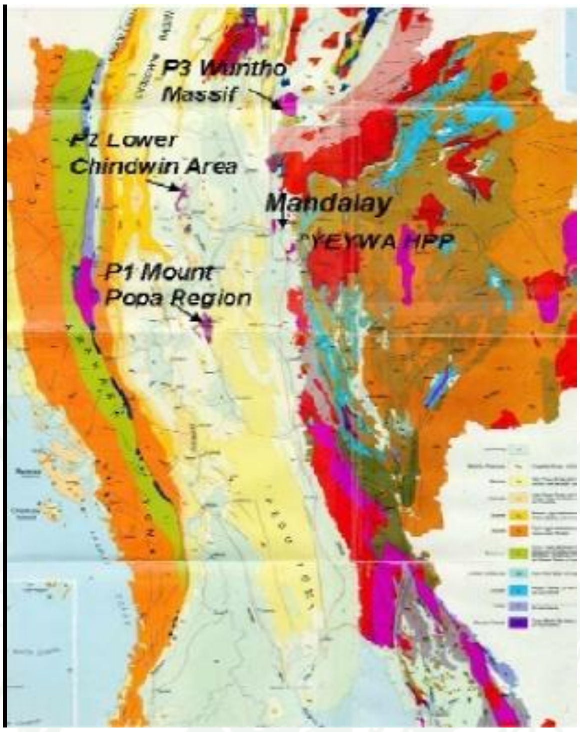

Figure 2: Location of Pozzolan Source in Myanmar

Source: Win Kyaw (2006)

8. Production of Volcanic Ash

The volcanic ash is a kind of natural pozzolan manufactured by grinding and calcination of naturally occurring minerals in the volcanic areas. It may also be heat treated in a kiln (calcined) or processed and then ground to a fine powder. Deposits of volcanic ash are likely to be found wherever there are active or recently active volcanoes. The most common natural pozzolans used are calcined clay, calcined shale, metakaolin and diatomaceous earth (ASTM C 618).

Lea (1974) stated that if the ash is carefully mined, with no admixture of sand or shale, the volcanic ash needs only to be dried at 100 C (212F) and finely ground to comply with ASTM C 618.

9. Comparison Between Myanmar Volcanic Ash (natural pozzolan) and Fly ash

The main difference between volcanic ash and fly ash is particle shape. The SEM micrograph of Myanmar volcanic ash is shown in Figure 3. Particle shape of volcanic ash is sharp angular shape and porous particles of siliceous glass but that of fly ash is spherical. CaO content of volcanic ash is lower than that of class C fly ash and SiO_2 content of volcanic ash is higher than that of class C fly ash. Lower CaO content will affect the early age hydration. But higher SiO_2 content gives a better pozzolanic reaction. According to Lea (1974), the partial replacement of Portland cement by pozzolan of high SiO_2/R_2O_3 (R_2O_3= Al_2O_3+Fe_2O_3) ratio has been found to increase the resistance of concrete to sulphate and sea water attack.

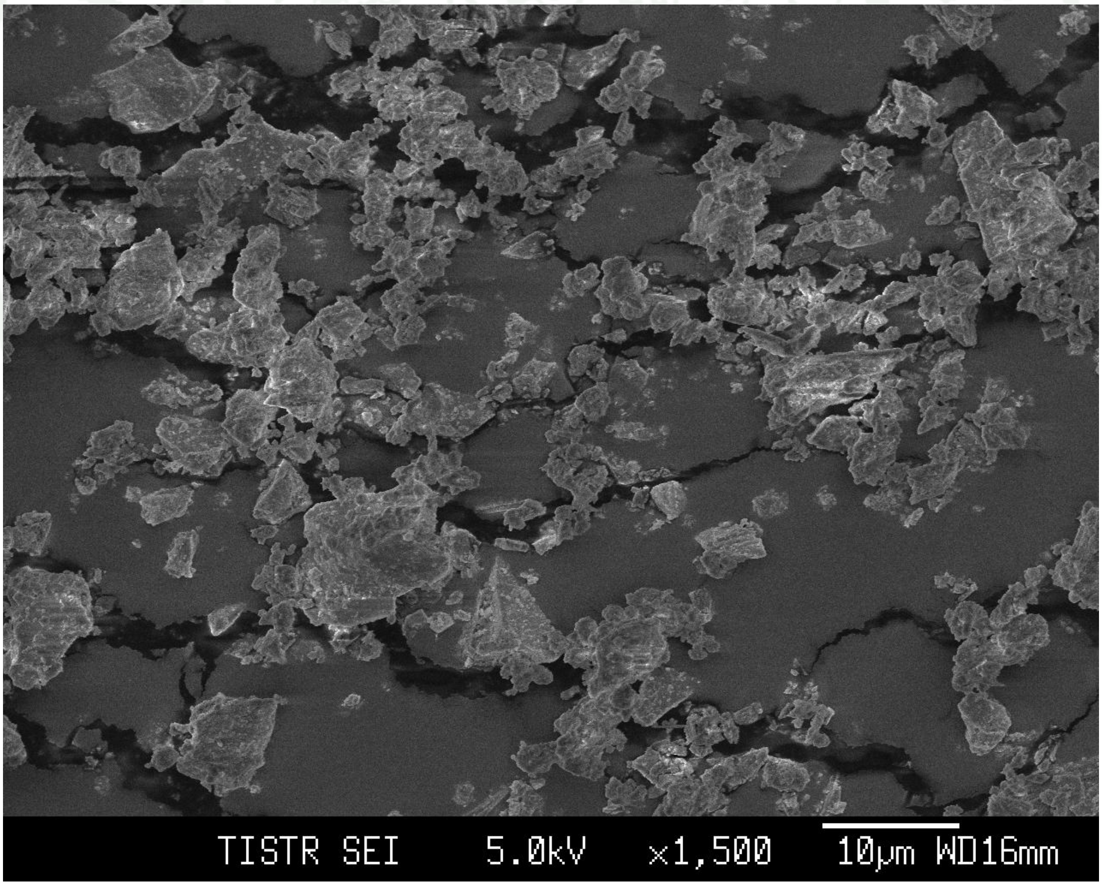

Figure 3 SEM Micrograph of volcanic ash

ACI 232 (1994) stated that the shape, fineness, particle-size distribution, density, and composition of natural pozzolan particles influence the properties of freshly mixed concrete and the strength development of hardened concrete. Most natural pozzolans tend to increase the water requirement in the normal consistency test as a result of their microporous character and high surface area. Natural pozzolans can improve the performance of both fresh and hardened concrete when used as an ingredient of Portland-pozzolan cement or as an admixture to Portland-cement concrete.

10. Mercury Intrusion Porosimetry (MIP) Method

The porosimetry method is a non destructive method used to investigate any type of porous materials, including soft, frail, and powders. This includes the quantification of pore diameter, total pore volume, bulk density and absolute density. This method provides the widest range of measurable pore radii from 0.3 nm to 300,000 nm (Volfkovich *et al*., 2005).

The mercury intrusion porosimetry method is based on the measurement of the volume of mercury intruded or extruded into the pores of the samples. According to Washburn equation, which represents the capillary flow in porous materials, the pore diameter is calculated as a function of the pressure given by the following:

$$\mathrm{D} = -\left(\frac{1}{P}\right)4\gamma\cos\theta \qquad (5)$$

Where:

P = the pressure

D = the pore diameter

γ = the surface tension of the mercury

θ = the contact angle between mercury and sample

A rearrangement of the equation in terms of r leads to the following expression.

$$|r| = \frac{(2900.753\gamma)cos\theta}{P} \qquad (6)$$

Where the pressure is in PSIA, r is the pore radius, θ is in degrees and γ is in erg/cm^3.

The volume of mercury intruded/extruded can be normalized by dividing the mercury (Hg) volume by the sample weight (cm^3 Hg/g of sample). In addition, the percent volume of mercury intruded/extruded is the volume of mercury intruded/extruded normalized 100% (full scale).

The first derivative of the volume vs. pressure data is represented as dV/dP. This value is used in the calculation of the distribution function. It can be calculated by using the following expression.

$$\frac{dV}{dP} = \frac{[\text{volume(i)} - \text{volume(i} - 1)]}{[\text{pressure(i)} - \text{pressure(i} - 1)]} \qquad (7)$$

Finally, these quantities are used to estimate the porosity, pore size distribution and pore number fraction of the sample.

The porosity is evaluated by measuring the total volume of mercury intruded up to the maximum pressure, and calculated using the following equation;

$$\text{Porosity(\%)} = \frac{Vt}{Vb} \times 100 \qquad (8)$$

Where:

Vt = the total volume of mercury intruded

Vb = the bulk volume of the sample

The pore number fraction is found by dividing the number of pores in a small interval by the total number of pores. The value obtained is a dimensionless quantity and represents the fractional amount of pores which are found in that particular interval.

The pore size distribution is determined by the calculation of volume pore size distribution function (Dv(r)), which is defined as pore volume per unit interval radius. It is estimated using the following equation.

$$\mathrm{Dv(r)} = \frac{P}{r} \times \frac{\mathrm{dV}}{dP} \tag{9}$$

Where:

Dv(r) = the volume pore size distribution function
dV/Dp = the first derivative (slope) of the volume vs. pressure data
P = the pressure applied
r = the pore radius

11. Scanning Electron Microscope (SEM)

SEM is a scanning electron microscope that uses electrons instead of light to form an image. Since their development in the early 1950's, SEM has developed new areas of study in the medical and physical science communities. The SEM has allowed researchers to examine a much bigger variety of specimens.

The SEM has many advantages over traditional microscopes. It has a large depth of field, which allows more of a specimen to be in focus at one time. It also has much higher resolution, so closely spaced specimens can be magnified at much higher levels. Because the SEM uses electromagnets rather than lens, the researcher has much more control in the degree of magnification. All of these advantages, as well as the actual strikingly clear images, make the SEM one of the most useful instruments in research today.

12. SEM for concrete

A foreknowledge of the basic microstructure of concrete is essential for understanding its mechanical behaviour and long term performance. It can be obtained from examination of a normal concrete under SEM. The introduction of SEM into concrete research has provided much greater insight into the kinetics of cement hydration, the morphology and chemical composition of hydration products, the microstructure of hydrated cement paste, the importance of paste aggregate interface, matrix densification and the reduced permeability of hydrated cement paste resulting from the addition of mineral and chemical admixtures. In other words, most of the factors that control the durability and mechanical properties of concrete can be ascertained by SEM.

13. X-ray Diffraction (XRD)

XRD is a common analytical technique used to measure the mineral content of cement. The X- rays are fired onto the material and they diffract off each lattice layer. The diffraction pattern is then used to identify the mineral as each mineral has a characteristic diffraction pattern. The angle (2Ө) of each peak can be used to identify the material. The intensity of the peak will indicate the relative amount present.

14. Basic Considerations for Concrete Mix Design

The concrete mix design is a process of selecting suitable ingredients for concrete and determining their proportions which would produce, as economically as possible, a concrete that satisfies the job requirements, i.e. concrete having a certain minimum compressive strength, workability and durability. The proportioning of the ingredients of concrete is an important phase of concrete technology as it ensures quality and economy (Gambhir, 2006).

15. The DoE (British) Mix Design Method

The traditional British mix design method of grading curve called Road Note No. 4 has been replaced by a general method developed by the Department of the Environment for normal concrete mixes. The method uses the relationship between water-cement ratio and compressive strength of concrete depending on the type of cement and the type of aggregate used. The water contents required to give various levels of workability, namely, very low, low, medium and high are determined from Table 2 for the two types of aggregates, viz. crushed (angular) and uncrushed (gravel).

Table 2 Approximate free water content required to give various levels of workability

	Level of Workability	Very Low	Low	Medium	High
Description	Slump, mm	0-10	10-30	30-60	60-180
	Vee-Bee, s	>12	12-6	6-3	3-0
	Compacting factor	0.75-0.85	0.85-0.90	0.90-0.93	>0.93
I. Water content:					
Maximum size of aggregate, mm	Type of aggregate	Water content kg/ m^3			
10	Uncrushed	150	180	205	225
	Crushed	180	205	230	250
20	Uncrushed	135	160	180	195
	Crushed	170	190	210	225
40	Uncrushed	115	140	160	175
	Crushed	155	175	190	205
II. Reduction in water content when fly ash is used					
Percent of fly ash in cementitious material		Reduction in water content, kg/ m^3			
10		5	5	5	10
20		10	10	10	15
30		15	15	20	20
40		20	20	25	25
50		25	25	30	30

This method is suitable for design of normal concrete mixes having 28-day cube compressive strength as high as 75 MPa. This method can also be used for concrete containing fly ash or GGBFS. The step-by step procedures of mix proportioning are as follows:

(1) Determination of Free water-cement Ratio

For the stipulated characteristic strength at a specified age, the target mean compressive strength at that age is first determined. The values of probability factor (k) are shown in Table 3 and the values of assumed standard deviations are shown in Table 5. The value of S in Table 5 shall be increased by 1 MPa whenever there is a deviation from quality of production such as proper storage of cement, periodic checking of workability and strength etc.

$$f_t = f_{ck} + kS \tag{10}$$

Where:

f_t = target mean strength
f_{ck} = characteristic strength
k = probability factor
S = standard deviation

According to IS: 456-2000, the term characteristic strength indicates value of strength of material, below which not more than 5 per cent of the test results are expected to fall. In the design of concrete mixes, the average strength to be aimed for the target mean strength that should be appreciably higher than the minimum or characteristic strength if the quality of concrete is to comply with the requirements of the specification.

Table 3 Probability factor for various tolerances

Percentage of results below characteristic strength	50 (1in2)	20 (1in5)	10 (1in10)	5 (1in20)	2.5 (1in40)	1.0 (1in100)	0.5 (1in200)	0.0
Probability factor(k)	0.00	0.84	1.28	1.65	1.96	2.33	2.58	Infinity

For the given type of cement and aggregate, the compressive strength at the specified age corresponding to a free water-cement ratio of 0.5 is obtained from Table 4. The water-cement ratio is determined from Figure 4 by using the compressive strength from Table 4 and the computed target mean strength. The resulting water cement ratio from Figure 4 should check with the value of cement content and maximum water cement ratio according to exposure condition shown in Table 6.

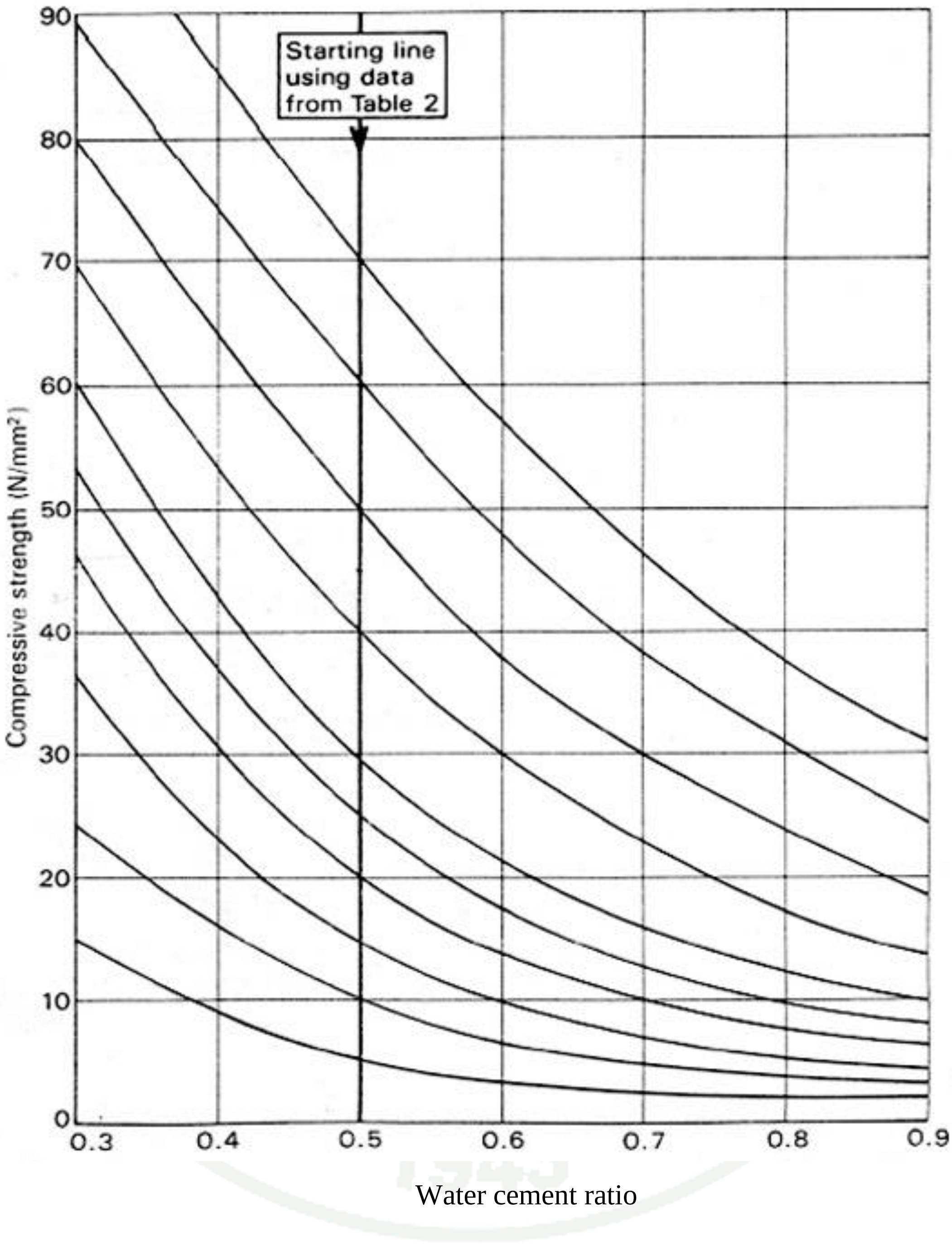

Figure 4 Relationship Between Compressive Strength and Free-water/ Cement Ratio

Table 4 Approximate Compressive Strength of Concrete Mixes with Water-cement Ratio as 0.5

Type of cement	Type of coarse Aggregate	Compressive strength, MPa Age (days)			
		3	7	28	91
Ordinary or sulphate-resisting Portland cement	Uncrushed	22	30	43	49
	Crushed	27	36	49	56
Rapid-hardening Portland cement	Uncrushed	29	37	48	54
	Crushed	34	43	55	61

Table 5 Assumed Standard Deviations

Grade of Concrete	M_{10}	M_{15}	M_{20}	M_{25}	M_{30}	M_{35}	M_{40}	M_{45}	M_{50}
Standard deviation, S (MPa)	3.5		4.0				5.0		

(2) Determination of Water Content

Depending upon the type and maximum nominal size of aggregate, and workability (specified in terms of slump or Vee-Bee time) the water content is determined from Table 2.

(3) Determination of Cement Content

The cement content of the mix is calculated from the selected water-cement ratio (Step 1) and the water content (Step 2) using equation 11.

$$\text{Cement Content} = \frac{\text{water content}}{\text{water} - \text{cement ratio}} \qquad (11)$$

The above value of cement content is checked against any maximum or minimum cement content shown in Table 6 that may have been specified for durability. If the computed cement content is below the specified minimum, this minimum must be used, which results in a reduced water-cement ratio and hence in a higher strength. However, if the calculated cement content is higher than the specified maximum, then the specified strength and workability cannot simultaneously be achieved with selected materials. In such a situation the process is repeated by changing the type of cement, the type and maximum size of aggregate.

(4) Determination of the Total Aggregate content

This stage requires the estimate of the density of fully compacted concrete which is obtained from Figure 5. This value depends on the free water content and the relative density of the combined aggregate in the saturated surface dry condition. If no information is available regarding the relative density of aggregates, an approximation can be made by assuming a value of 2.6 for un-crushed aggregate and 2.7 for crushed aggregate. The total aggregate content is obtained by using equation 12.

$$\text{Total Aggregate Content} = \text{D} - \text{C} - \text{W} \qquad (12)$$

Where:

D = wet density of concrete (kg/m^3)

C = Cement content (kg/m^3)

W = Free water content (kg/m^3)

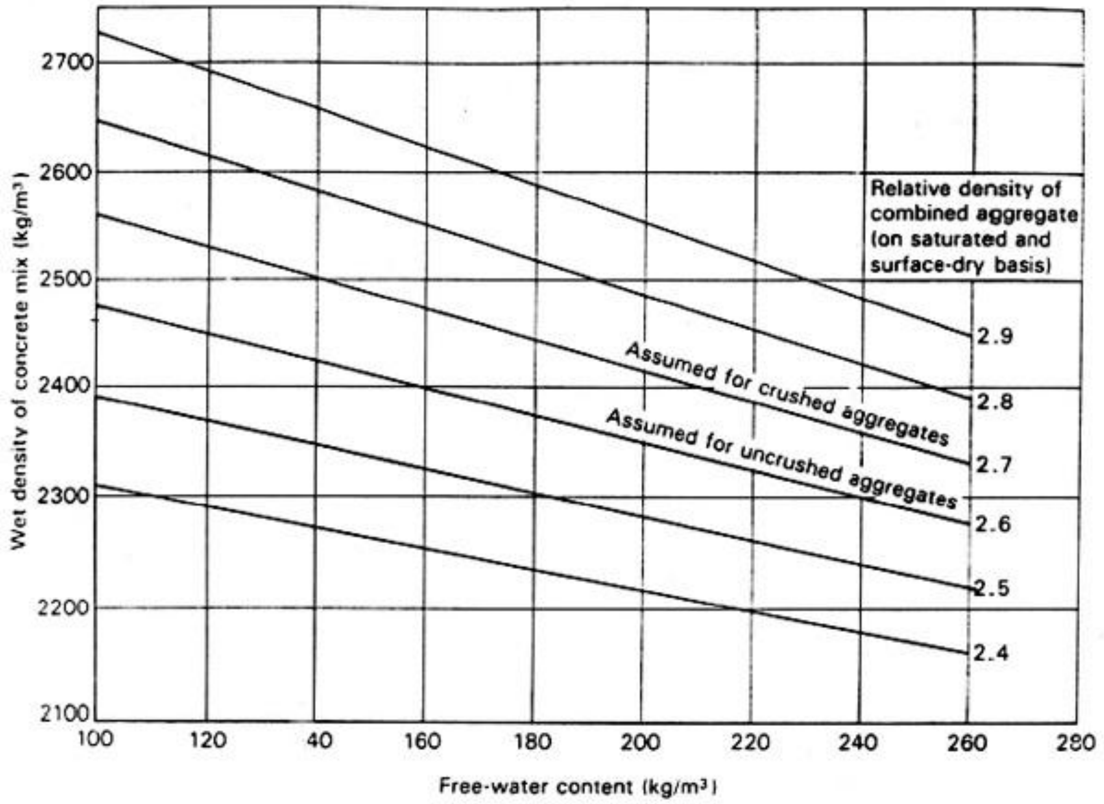

Figure 5 Estimated wet density of fully compacted concrete

(5) Determination of fine and coarse aggregate content

This stage involves deciding how much of the total aggregate should consist of materials smaller than 5mm, i.e. fine aggregate content. Figure 6 shows recommended values for the proportion of fine aggregate depending on the maximum size of aggregate, the workability level, the grading of fine aggregate and free water cement ratio. The best proportion of fines to use in a given concrete mix design will depend on the shape of the particular aggregate, the grading and the usage of the concrete. Equation 13 is used to determine the fine and coarse aggregate proportion by using the proportion of fine aggregate proportion obtained from Figure 6 and the total aggregate derived from Step 4.

Table 6 Minimum cement Content (kg/m^3), Maximum water Cement Ratio and Grading of Concrete to Ensure Durability under Special Exposure with Aggregate of 20mm Nominal Maximum Size

General Environment	Exposure conditions	Plain Concrete			Reinforced Concrete		
		Minimum cement content, kg/m^3	Maximum free water cement ratio	Minimum grade of concrete	Minimum cement content, kg/m^3	Maximum free water cement ratio	Minimum grade of concrete
Mild	Concrete surfaces protected against weather or aggressive conditions, except those situated in coastal area.	220	0.60	-	300	0.55	M20
Moderate	Concrete surfaces sheltered from severe rain or freezing whilst wet, Concrete exposed to condensation and rain. Concrete continuously under water. Concrete in contact or buried under non-aggressive soil/ground water. Concrete surfaces sheltered from saturated salt air in coastal area.	240	0.60	M15	300	0.50	M25
Severe	Concrete surfaces exposed to severe rain, alternate wetting and drying or occasional freezing whilst wet or severe condensations. Concrete completely immersed in sea water. Concrete exposed to coastal environment.	250	0.50	M20	320	0.45	M30

Table 6 (Continued)

General Environment	Exposure conditions	Plain Concrete			Reinforced Concrete		
		Minimum cement content, kg/m^3	Maximum free water cement ratio	Minimum grade of concrete	Minimum cement content, kg/m^3	Maximum free water cement ratio	Minimum grade of concrete
Very severe	Concrete surfaces exposed to sea water spray, corrosive fumes or severe freezing condition whilst wet. Concrete in contact with or buried under aggressive sub-soil/ground water.	260	0.45	M20	340	0.45	M35
Extreme	Members in direct contact with liquid/solid aggressive chemicals.	280	0.40	M25	360	0.40	M40

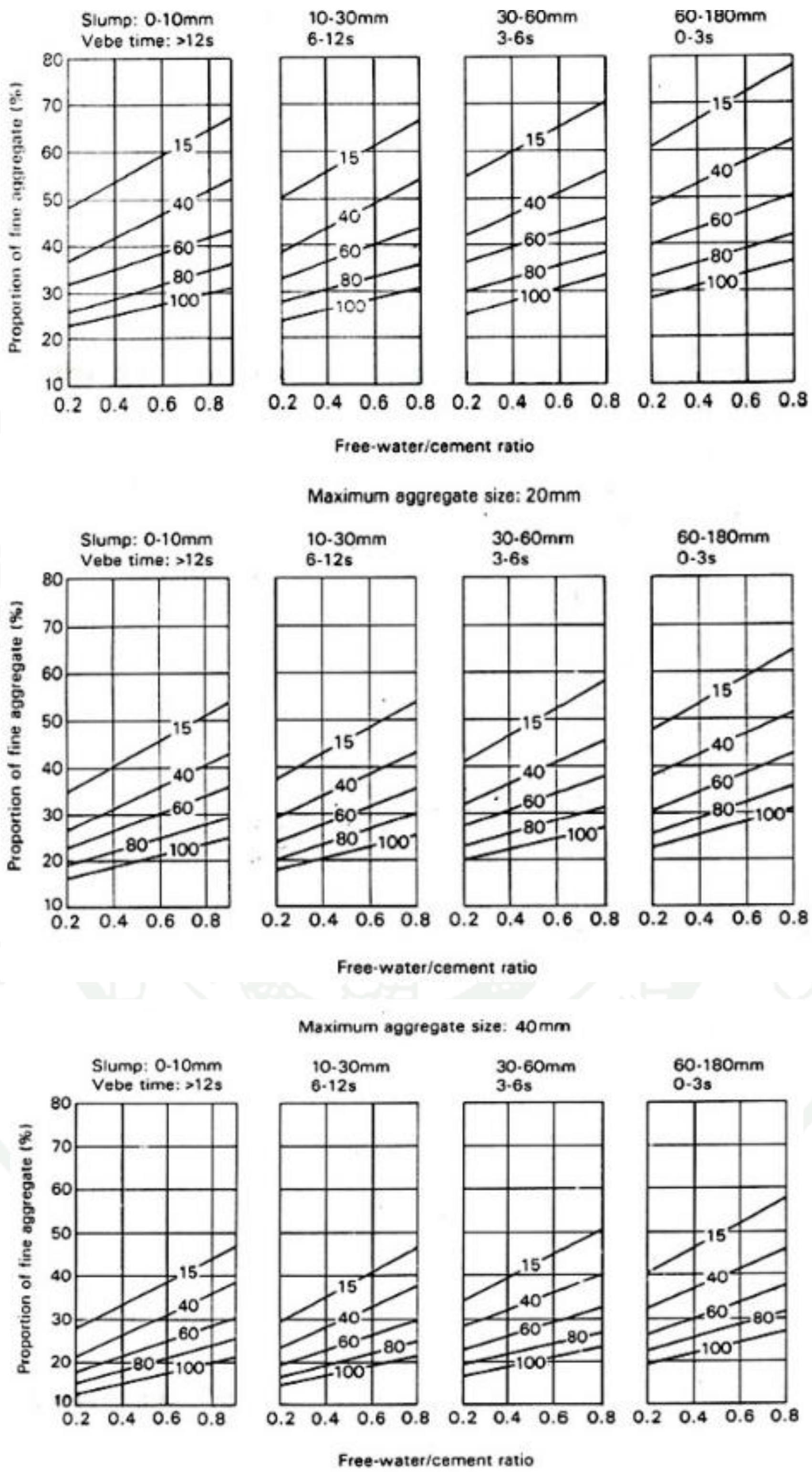

Figure 6 Recommended proportions of fine aggregate according to percentage passing a 600μm sieve

$$\text{Fine Aggregate Content} = \text{Total Aggregate Content} \times \text{Proportion of Fines} \quad (13)$$

$$\text{Coarse Aggregate Content} = \text{Total Aggregte Content} - \text{Fine aggregate} \quad (14)$$

16. Water absorption

The pore structure of concrete is known to be of high importance for the durability of the concrete. A characterisation of the pore structure by means of a simple test is often investigated, in order to find a very simple compliance criterion with respect to concrete durability. Water absorption test is adopted for checking the quality of concrete in terms of density and imperviousness. The water absorption by immersion is considered to be a relevant parameter in this respect. It gives an estimation of the total (reachable) pore volume of the concrete and their connectivity.

17. Loss on Ignition

Loss on ignition is essentially a measure of the unburnt carbon content in volcanic ash. It may affect quality of concrete by increasing the water requirement and reducing pozzolanic activity (Minnick *et al.*, 1971).

18. Effect of Chemical Composition on the Strength Development of Pozzolanic Concrete

Experiment conducted by Hassan (2006) stipulated that the major difference between cement and volcanic ash is calcium oxide content. Volcanic ash has calcium oxide content of 11.6% while Portland cement has 66% calcium oxide. That discrepancy in calcium oxide content was responsible for the slow setting and low strength in volcanic ash concrete at early age.

Tangtermsirikul *et al.* (2004) also investigated the effects of quantities of concrete ingredients, chemical compositions and physical properties of cement and fly ash on compressive strength of concrete. Their results concluded that the effectiveness of fly ash on 28 day compressive strength was proposed to be functions of calcium oxide in fly ash and fineness of fly ash. Fly ash with higher values of calcium oxide content and/or blaine fineness gives higher effectiveness than that with lower values. Loss on ignition of fly ash affects 28 day compressive strength adversely. However, this effect was reduced in fly ash with higher calcium oxide content.

Strength at any age and rate of strength development of fly ash concrete are affected by the characteristics of the fly ash. SiO_2 and CaO are regarded as the main chemical compositions influencing hydration reaction and pozzolanic reaction, which are the major contributions to the strength development of fly ash concrete. CaO mainly affects the hydration reaction and the product from the hydration reaction $Ca(OH)_2$ reacts mainly with SiO_2 in fly ash during the pozzolanic reaction. However, the amount of $Ca(OH)_2$ produced in concrete is time dependent. When using the same amount of fly ash and same replacement ratio, fly ash with higher CaO content gives better strength development at early age than that with lower CaO content since high calcium fly ash usually contains some hydraulic cementitious materials.

19. Mechanical Properties of Pozzolanic Concrete

Lane and Ozyildirim (1999) studied the effects of pozzolan and ground granulated blast furnace slag on concrete properties and their influence on durability. Their results indicated that the compressive strengths of fly ash concrete up to 56 days were lower than no fly ash concrete as a consequence of the slowly hydrating phase in fly ash concrete. However, by 1 year, the depression in strength level resulting from high amounts of fly ash had dissipated and the compressive strength of all concrete mixtures greatly exceeded the design strength of 30 MPa.

Lynn *et al.* (1962) investigated the effect of pozzolan on compressive strength and flexural strength of concrete. They reported that the ratio of flexural and splitting tensile strength to compressive strength at 28 days was either comparable or higher than those of Portland cement concrete. In conventional concrete flexural strength reached a maximum value between 14 and 28 days and beyond this, there was no significant increase. On the contrary, in high volume fly ash concrete (HVFAC) the flexural strength keeps on increasing with age because of the pozzolanic reaction of fly ash and strengthening of interfacial bond between cement paste and aggregate. This gives HVFAC a significant advantage over conventional concrete for use in pavements. They concluded that Portland-pozzolan concrete can exhibit higher flexural to compressive strength ratios than normal Portland cement at later ages.

Yetgin and Cavdar (2011) investigated the abrasion resistance, compressive strength and flexural strength of cement mortars having different pozzolanic composition and matrix. They found that the abrasion resistance, compressive strength and flexural strength increase while the curing time elapses. Moreover, the increase of the clinker, limestone, and silica fume ratios increase the abrasion resistance at the end of the year. On the other hand, blast furnace slag, natural pozzolan and fly ash conversely affect the abrasion resistance. Finally the CaO components increase the abrasion resistance of the mortars over the course of a year. However, SiO_2 and Al_2O_3 components decrease the abrasion resistance of the sample.

Gwbler and Klieger (1986) studied the abrasion resistance of concrete containing ten different sources of class C and class F fly ashes. Concrete mixtures were proportioned to have 25% fly ash by weight of total cementitious materials. The authors reported that the abrasion resistance of class C fly ash concrete was generally superior to class F fly ash concrete.

Naik *et al.* (1995) investigated the abrasion resistance of concrete proportioned to have five levels of cement replacements (15%, 30%, 40%, 50% and 70%) with one source of class C fly ash. Test results showed that abrasion resistance of concrete having cement replacement up to 30% was comparable to the reference concrete without fly ash, but beyond 30% cement replacement, fly ash concrete exhibited slightly lower resistance to abrasion to non-fly ash concrete.

20. Microstructure of Cement Paste

Mindess *et al.* (1981) reported that pore volume and pore size distribution of hydrated cement paste were the most important factors affecting durability, low permeability, strength, creep and shrinkage. To achieve high strength, low permeability and durable concrete, it is necessary to minimize porosity in cement paste. It is well known that the incorporation of pozzolanic materials as a partial replacement of cement affects the pore volume and pore size distribution of blended cement paste.

Struble and Brown (1987) stated that in cement paste, the glassy component of the fly ash undergoes a pozzolanic reaction with the calcium hydroxide produced by the cement to give C-S-H (calcium-silicate-hydrate) and C-A-H (calcium-aluminate-hydrate). The partial replacement of cement by fly ash allows the production of concretes with relatively high strength and low permeability.

At the micrometer scale, the cement paste is a composite of unhydrated residues of cement grains and hydration products which are C-S-H, $Ca(OH)_2$ and capillary pores. Hydrated cement paste contains large capillary pores with diameter between 50-10,000 nm, medium capillary pores with diameters of 10-50 nm and gel pores with diameters of less than 10 nm. (Mindess *et al.*, 1981)

21. Effect of Pozzolan on Temperature (thermal) Cracking

Pozzolans have been used in mass concrete as a partial replacement of Portland cement to reduce the temperature rise, as compared to that of a comparable concrete mixture containing Portland cement as the only cementing material. According to Townsend (1968), the heat of hydration that a pozzolan will contribute is approximately 50% of that would have been developed by an equal amount of Portland cement.

The rate of heat development of concrete closely parallels to the rate of compressive strength development of concrete as both are functions of the same chemical reactions. The lower rate of heat development of concrete containing pozzolan permits lowering the temperature rise at lower cost (Elfert, 1974).

22. Reactivity index of Cement-pozzolan Mixture

Strength activity index with Portland cement with pozzolan should not be less than 75% of 28-day strength of standard mortar (ASTM C 618).

The pozzolanic activities of natural pozzolans and their compressive strengths are directly proportional to the increase in SiO_2 ratio and inversely proportional to Al_2O_3 and Fe_2O_3 ratios. Again increase in the MgO and K_2O ratios decrease the pozzolanic activity. According to this, it is once again seen that the most important component of pozzolan is SiO_2 and it can provide contributions to pozzolanic activity in both crystalline form and non-crystalline form (Cavdar, 2007).

MATERIALS AND METHODS

Materials

1. Cement

The cement used in this study was locally manufactured ASTM Type I Portland cement called “Horse Head”. The chemical composition of cement is shown in Table 7.

Table 7 Chemical Composition of ASTM Type I ‘Horse Head” brand Cement

Chemical composition	“Horse Head” (%)
Silicon Dioxide (SiO_2)	21.83
Aluminum Oxide (Al_2O_3)	6.18
Ferric Oxide (Fe_2O_3)	2.79
Magnesium Oxide (MgO)	1.98
Sulphur Trioxide (SO_3)	2.35
Tricalcium Silicate & Aluminate (C_3S & C_3A)	61.61

Sources: Ministry of Electric power No. 1, Myanmar (2010)

2. Volcanic Ash and Fly Ash

Volcanic ash used in this experiment was taken from Popa Natural Pozzolan Grinding plant. Mae Moh fly ash from thermal power plant in Thailand was used for comparison with volcanic ash in compressive strength and water absorption of mortar. Its physical and chemical properties are presented in Tables 8 - 10.

Table 8 Physical Properties of Myanmar Volcanic Ash and Mae Moh Fly Ash

Properties	Volcanic ash	Fly ash
Specific gravity	2.84	2.12
Blaine specific surface area, (cm^2/g)	4090	2655

Sources: Ministry of Electric power No. 1, Myanmar (2010)
Ministry of Science and Technology, Thailand (2010)

Table 9 Mineral Constituent of Myanmar Volcanic Ash Compared with ASTM C 618

Properties of volcanic ash	Class N	Myanmar volcanic ash
SiO_2+ Al_2O_3+ Fe_2O_3 not less than (%)	70	76.92
SO_3 not exceed (%)	4	0.02
Loss on ignition not exceed (%)	10	1.69

Sources: Ministry of Electric power No. 1, Myanmar (2010)

Table 10 Chemical Compositions (%) of Myanmar Volcanic Ash and Mae Moh Fly Ash

<table>
<tr><th>Chemical composition</th><th>volcanic ash</th><th>fly ash</th></tr>
<tr><td>SiO_2</td><td>52.10</td><td>35.3</td></tr>
<tr><td>Al_2O_3</td><td>16.19</td><td>21.5</td></tr>
<tr><td>Fe_2O_3</td><td>8.63</td><td>14.2</td></tr>
<tr><td>CaO</td><td>10.15</td><td>18.7</td></tr>
<tr><td>K_2O</td><td>1.20</td><td>2.0</td></tr>
<tr><td>MgO</td><td>6.05</td><td>3.0</td></tr>
<tr><td>Na_2O</td><td>2.48</td><td>2.5</td></tr>
<tr><td>SO_3</td><td>0.02</td><td rowspan="4">2.4</td></tr>
<tr><td>TiO_2</td><td>0.81</td></tr>
<tr><td>P_2O_5</td><td>0.18</td></tr>
<tr><td>Free lime</td><td>0.02</td></tr>
<tr><td>Loss on ignition</td><td>1.69</td><td>0.4</td></tr>
</table>

Sources: Ministry of Electric power No. 1, Myanmar (2010)
Ministry of Science and Technology, Thailand (2010)

3. Aggregates

Coarse aggregate used was granite crushed rock (from Mon state) with nominal maximum size of 20 mm and fine aggregate used was locally available river sand. Physical properties of aggregates are shown in Table 11.

Table 11 Physical properties of aggregates

Properties	Fine aggregate	Coarse aggregate
Specific gravity	2.6	2.62
Moisture content (%)	2	0.05
Absorption (%)	1.5	0.65
Fineness modulus	2.4	-

4. Water

Water for the mixing and curing purpose was obtained from ordinary tap which was usually for drinking and domestic purpose, free from organic matter and acidic materials.

Methods

The experimental investigation is to examine the effect of volcanic ash on Portland cement concrete pavement. The experimental program in this study can be divided into five parts.

1. Consistency and setting times of cement paste containing volcanic ash

Consistency and setting times of volcanic ash and cement mixture pastes were determined by ASTM C187 and ASTM C191. The water requirement of binder was done by mixing water with binder and measuring the time for a vicat needle to penetrate 5-7 mm of the paste with 10 mm diameter needle.

The setting time was performed on volcanic ash and cement mixture paste which was obtained by mixing binder with water and measuring the time required for a needle to penetrate 3-5 mm of the paste with 1 mm diameter needle for initial setting time.

The needle with a metal attachment hollowed out so as to leave a circular cutting edge 5 mm diameter and 0.5 mm behind the tip of the needle was used for final setting time. The elapsed time from mixing the water with dry binder till only the needle makes an impression on the paste surface but the cutting edge fails to make on impression.

2. Mechanical Properties of Volcanic Ash Concrete

2.1 Mix Design

The mix proportions are based on the British Department of the Environment (DoE) to get the characteristic strength of 28 MPa at 28 days (Gambhir, 2006). Water to binder ratios (w/b) of 0.5, 0.55 and 0.6 with required slump of 30-60mm were used. The mix design data are shown in Appendix Table 1. VA was introduced as cement replacement material and control mixture incorporating ordinary Portland cement (OPC) was also prepared for comparison purpose. Air-entraining admixtures and high-range water reducing admixtures were not used in all the concrete mixes.

2.2 Mixing procedure

The concrete was mixed on a water tight, non absorbent platform with a shovel and trowel. The cement and fine aggregate were mixed dry until the mixture were thoroughly blended and was uniform in colour. The coarse aggregate was then added and the entire batch mixed until the coarse aggregate was uniformly distributed throughout the batch and the water was then added and the entire batch mixed until the concrete appears to be homogeneous and obtained the desired slump.

2.3 Specimen Details

The specimens for Compressive strength were 150mm x 150mm x 150mm cube moulds and flexural strength were beam specimens of 150mm x 150mm x 600mm.

In assembling the mould for use, the joints between the sections of the mould were coated with mould oil and a similar coating of mould oil was applied between the contact surfaces of the bottom of the mould and the base plate in order to ensure that no water escapes during the filling. The interior surfaces of the assembled mould are coated with mould oil to prevent adhesion of the concrete.

2.4 Compacting and curing of specimens

When compacting, the standard tamping bar with 16mmΦ×600mm length was used and the strokes of the bar were distributed in a uniform manner over the cross-section of the mould. The concrete was subjected to 35 strokes per layer for cubical specimens and 135 strokes per layer for beam specimens. The strokes penetrated into the underlying layer and the bottom layer was rodded throughout its depth. Where voids were left by the tamping bar, the sides of the moulds were tapped to close the voids.

The test specimens were stored in a place at room temperature for 24 hours. After that period, the specimens were marked and removed from the moulds and immediately submerged in water and kept there until taken out just prior to test. The water in which the specimens were submerged was renewed every 7 days and maintained at a temperature of 27±2ºC.

2.5 Testing procedure

2.5.1 Compressive Strength Test

The machine for compressive strength was ELE hand testing machine. Prior to testing, specimens were removed from the curing tank for about 3 hours. The specimens were placed in the machine in such a manner that the load was applied to the opposite of the cubes as cast, that is, not to the top and bottom. The load was applied in a uniform rate without shock until the resistance of the specimen to the increasing load breaks down and no greater load could be sustained. Compressive strengths of specimens were tested at 7, 14, 28 and 56 days. Average result was computed from 3 test specimens at each testing age.

The compressive strength was calculated as follows:

$$f_c' = \frac{P}{A} \tag{15}$$

Where :

f_c' = Ultimate compressive strength of concrete, MPa (psi)

P = Maximum applied load, lb

A = Cross section area of specimen, in^2

2.5.2 Flexural Strength Test

Preparation and curing of the specimens for flexural strength were the same as for the compressive strength. The diagram of flexural strength testing equipment is shown in Figure 7. The third point loading method was used in making flexure test. The bearing surfaces of the supporting and loading rollers were wiped clean. The specimens were turned on their side with respect to then position as moulded and centred on the support block. The specimens were then placed in the machine in such a manner that the bearing block would be perpendicular to the face of specimen and applied without eccentricity. The load-applying and support blocks would be maintained in a vertical position and in contact with the rods. The specimens were loaded continuously without shock at a constant rate. Testing the flexural strengths of concrete was made at 7, 14, 28 and 56 days. Average result was computed from 3 test specimens.

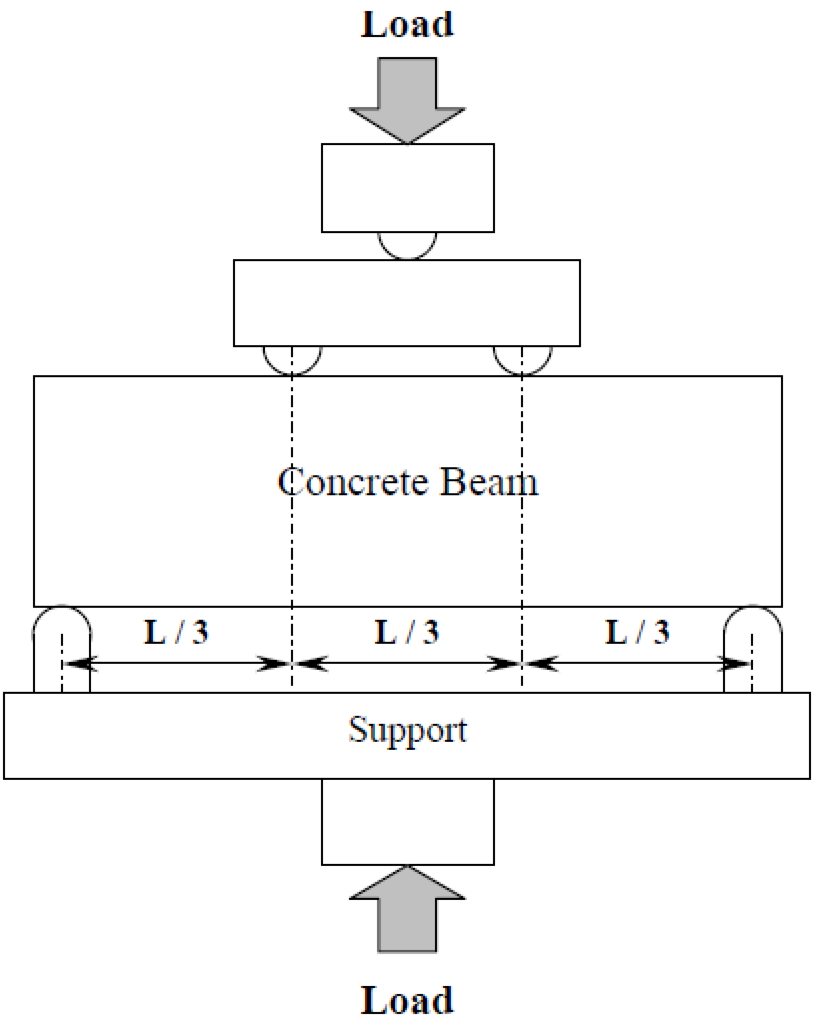

Figure 7 Testing equipment set for flexural strength test

When fracture initiated in the tension surface in the middle of span length, the flexural strength was computed as

$$R = \frac{PL}{bd^2} \quad (16)$$

Where:

R = Flexural strength, MPa (psi)

P = Maximum applied load, KN (lb)

L = Span length, mm (in)

b = average width of specimen, mm (in)

d = average depth of specimen, mm (in)

2.5.3 Los Angeles Abrasion resistance

The specimens tested in compressive strength and flexural strength were crushed to get the required sizes for Los Angeles abrasion machine according to ASTM C131. The samples (3/4”-1/2”=2500 gram and 1/2”-3/8”=2500 gram) were washed and oven dried at 105°C to 110°C. The crushed samples of concrete were weighed and filled in Los Angeles abrasion machine. This machine was rotated at speed of about 30-33 rpm for 500 revolutions. After complete number of revolutions test samples were discharged from the machine and sieved. After that test samples remaining on sieve No. 12 were washed and oven dried at 105°C to 110°C. Finally dried test samples were weighed. The percentages of wear were calculated by the difference between the original weight and the final weight of the test sample as a percentage of the original weight of the test sample.

$$\text{Abrasion }\% = \left(\frac{W_1 - W_2}{W_1}\right) \times 100 \qquad (17)$$

Where:

W_1 = Original weight of test sample

W_2 = Final weight of test sample

3. Microstructure of volcanic ash and cement mixture paste

The volcanic ash replacements of 0% and 45% were used to replace Portland cement for Mercury Intrusion Porosimetry (MIP), Scanning Electron Microscope (SEM) and X-ray diffraction (XRD) analysis. The water to binder ratio (w/b) was 0.5. The paste cubes were cast in 50mm cube moulds. After 24 hour casting, the specimens were removed from the moulds. The MIP, SEM and XRD analysis were made at 1 day and 56 day-age pastes.

3.1 Mercury Intrusion Prosimetry (MIP)

The porosity and pore size distribution were measured using MIP which had a measuring pressure ranging from 1.5 to 33000 PSIA capable of the measuring pore size diameter down to 0.006 µm. The contact angle selected was 140 degree and a constant surface tension of mercury of 480 dynes/cm was used for pore size calculation. The Washburn equation was used to calculate the pore radii. By carefully breaking the hardened cement paste cubes with a chisel, the representative sample of 3-6 mm pieces weighing between 1 and 1.5 g were taken from the middle of the specimen. The samples were dried in an oven at 105 degree Celsius for 24 hours before testing.

$$D = -\left(\frac{1}{P}\right) 4\gamma\cos\theta \qquad (18)$$

Where:

D = pore diameter, µm
P = applied pressure, MPa (psi)
γ = the surface tension, dynes/cm
θ = the contact angle, degree

3.2 Scanning Electron Microscope (SEM)

Paste cubes at the required ages of 1 day and 56 days were broken from the centre into small fragments. Hydration of the paste was stopped by drying as prepared in the MIP examination. The fractured surface was observed by using SEM (JOEL JSM-6040F). All samples were also coated with gold before SEM analysis.

3.3 X-ray diffraction (XRD)

The hydration of cement pastes were investigated by XRD analysis. All samples were cured in water before testing. At 1 day and 56 days, samples from crushed paste cubes and dried samples were tested for degree of hydration, as prepared in the MIP examination. The dried sample pasted were ground using a ball mill and sieved through a sieve No. 100 (opening 150 µm). The powder sample weighing 1 g was used to determine the amount of $Ca(OH)_2$ in the XRD analysis (Shiamadzu XD 6000).

4. Comparison of Strength Activity Index of cement mortars containing volcanic ash and fly ash

Volcanic ash and fly ash were used to replace Portland cement at the rates of 0%, 15%%, 30% and 45% by weight of cement. 1375 grams of sand and 500 grams of binder were mixed with water to get 100% flow for all mixes. The mortars were mixed in a mixer and were cast in 1.5 in (40mm) diameter with 3 in (80mm) length cylinder moulds and compacted by tamping rod. After casting 24 hours, specimens were removed from the moulds and cured in water. Average result was computed from 3 test specimens at 7 days and 28 days. Compressive strengths were tested with Universal testing machine. Cement equivalent factor (n) was calculated as follows.

$$\text{Cement equivalent factor (n)} = \left(\frac{A}{B}\right)100 \qquad (19)$$

Where:

A = average compressive strength of test specimens, MPa

B = average compressive strength of control mix specimens, MPa

5. Comparison of absorption of cement motor containing volcanic ash and fly ash

Water absorption can also be designated as open porosity. In testing absorption of mortar, material and mix proportion are the same as in the compressive strength testing of mortars. The mortars are cast in 50 mm diameter and 40 mm high moulds. After 24 hours casting, the specimens were removed from the moulds and immersed in water 28 days before testing age. The specimens were oven dried for 24 hours at 105 degree Celsius. The specimens were weighed (oven dry) after 1-2 hour at room temperature to cold. After that the specimens were immersed in water for 24 hours. The specimens were weighed (SSD) again after 1-2 hours at room temperature for surface dry. Absorptions of the specimens were calculated as follow.

$$\text{Absorption}(\%) = \frac{(B - A)}{A} \times 100 \qquad (20)$$

Where:

B = saturated surface dry weight

A = oven dry weight

RESULTS AND DISCUSSION

The experimental results are organized and presented in the subsequent sections as follows.

1. Consistency and Setting Times of volcanic ash and cement mixture pastes

Consistency and the setting times of cement pastes with different percentage of replacement with volcanic ash are shown in Table 12 and the SEM photo of volcanic powder is shown in Figure 3. It can be seen that volcanic ash powder was irregular shape with sharp angles which was different from the shape of fly ash. The results in Table 12 indicate that the consistency was slightly increased as volcanic ash replacement was increased. The setting times increased with an increase in volcanic ash content. The initial setting time was increased by 32 minutes and final setting time was increased by 50 minutes while the VA content was increased from 0-45%. This result was in agreement with the research of Helmuth (1987). He reported that the increase in setting time was probably due to the increase in the water to Portland cement ratio. This longer setting time was beneficial for saw cutting of the pavement slab and transporting concrete mix to a long distance site.

Table 12 Consistency and Setting Times of Cement Pastes with Different Replacements of Volcanic Ash

Mix no	Cement : Volcanic ash (%)	Initial setting time hr : min	Final setting time hr : min	Consistency %
1	100:0	2:28	3:35	28.0
2	85:15	2:40	3:45	28.3
3	70:30	2:52	3:50	28.9
4	55:45	3:00	4:25	29.5

2. Mechanical Properties of Volcanic Ash Concrete

2.1 Compressive Strength

The compressive strengths at 7 days, 14 days, 28 days and 56 days are shown in Figures 8-10 and Appendix Table 2-6. It can be seen that the compressive strength of concrete decreased as the w/b ratio increased. The strength of OPC was the highest and that of 45% volcanic ash concrete was the lowest. The compressive strength was found to decrease with an increase of VA content. At 45% volcanic ash replacement, the compressive strengths were dramatically decreased. This is reasonable due to the reduction of cement content in the mix with an increase of VA. A similar result was reported by Hossain (2003).

At the age of 56 days, the strengths of volcanic ash concrete showed significant improvement but were still lower than OPC. The improvement could be contributed to the pozzolanic reaction of VA. The rate of strength gained strongly dependent on volcanic ash replacement. Compressive strength of 15% VA concrete was slightly lower than the control concrete up to 56 days. This result supports the finding of Khan *et al.*, (2011). They reported that the strength of concrete with 15% natural pozzolan demonstrated low compressive strength when compared to that of plain concrete mix up to 90 days. At 180 days the strength of plain concrete mix and the mix containing 15% pozzolan had almost similar strength. According to the results in Figures 8-10, it is possible to substitute up to 15% of OPC by VA and obtained adequate early age strengths.

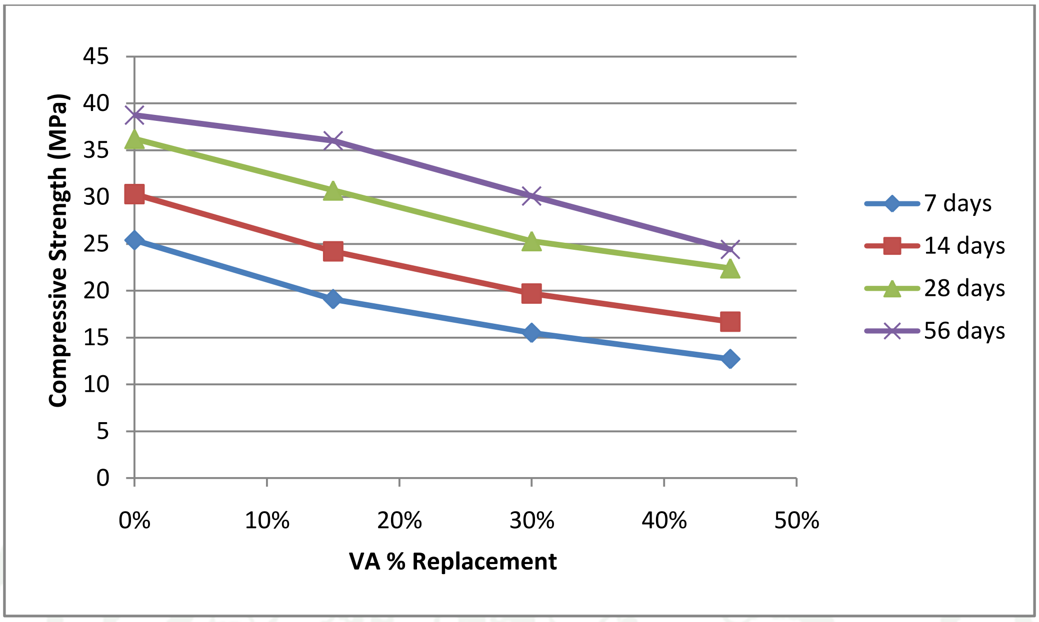

Figure 8 Effect of % replacement VA on compressive strength of concrete at w/b = 0.5

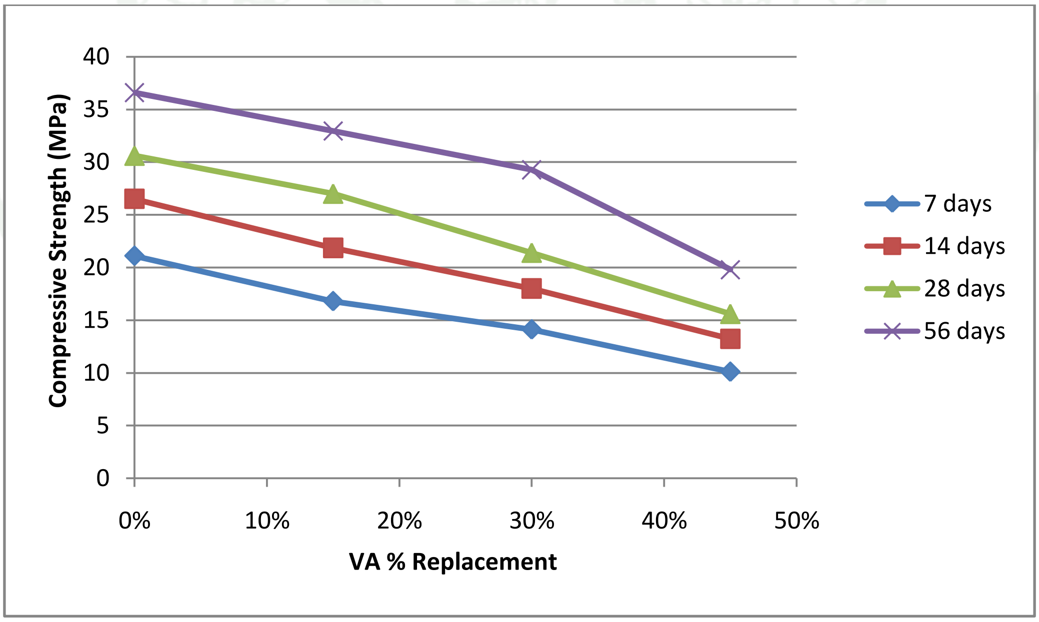

Figure 9 Effect of % replacement VA on compressive strength of concrete at w/b = 0.55

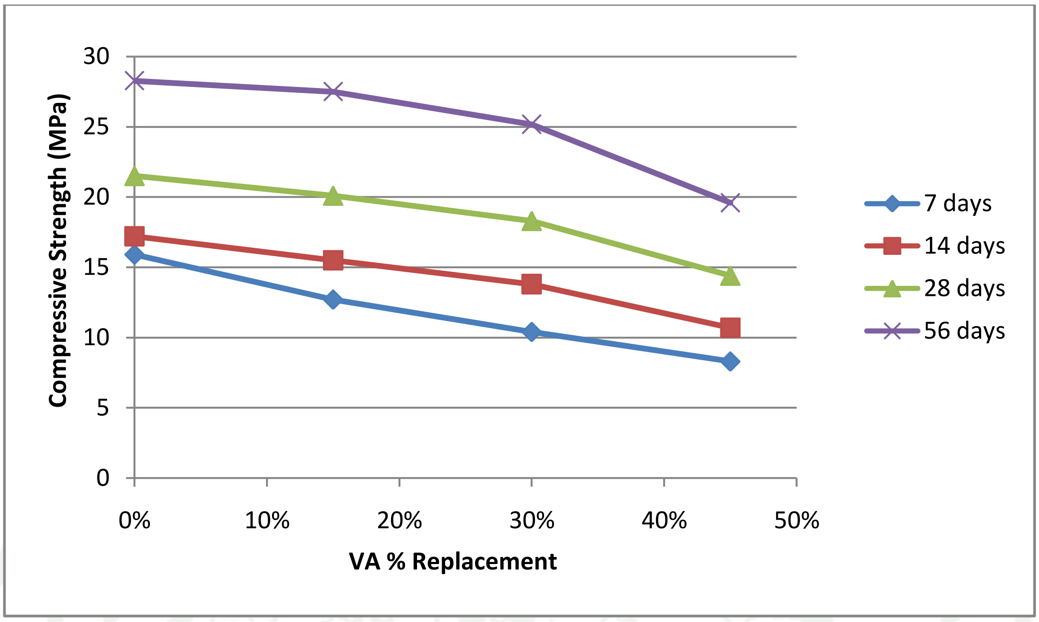

Figure 10 Effect of % replacement VA on compressive strength of concrete at w/b = 0.6

Normalized compressive strengths at 56 days were higher than that of 7, 14 and 28 days at three levels of w/b ratio. This is probably due to the pozzolanic reaction of VA which is slower at early age and faster at later ages. It can be concluded that the higher the age of concrete, the higher the normalized compressive strength of VA concrete compared to control concrete. The strength of volcanic ash concrete may be comparable or higher than the control concrete for long term strength.

2.2 Flexural strength

Test results of flexural strength are shown in Figure 11-13 and Appendix Table 7-11. The flexural strength of the concrete under investigation followed a similar trend to compressive strength. Figure 14 shows that as the compressive strength increased, the flexural strength also increased, but at a decreasing rate. Cengiz (2005) stated a similar result. The value of R^2 =0.9301 showed that compressive strengths were correlated well with flexural strengths. This result is in agreement with the statement of FHWA (2001). FHWA (2001) stated that in general, there was a relationship between the compressive and flexural strengths of concrete. Concrete which had a higher compressive strength would have a corresponding higher flexural strength.

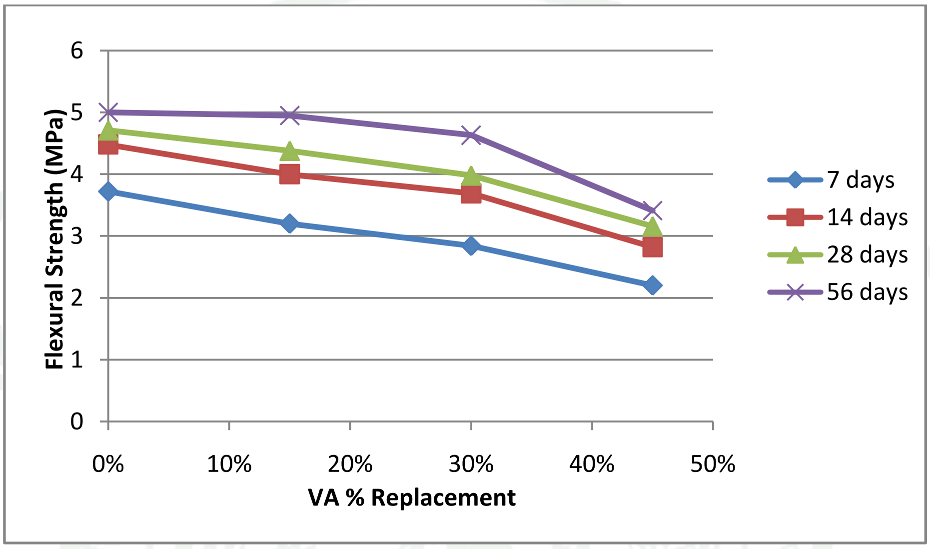

Figure 11 Effect of % replacement VA on flexural strength of concrete at w/b = 0.5

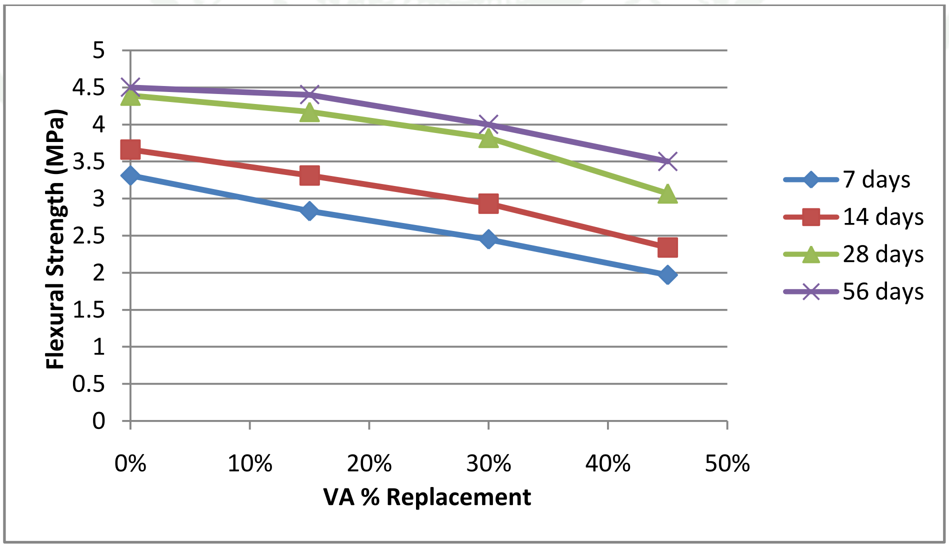

Figure 12 Effect of % replacement VA on flexural strength of concrete at w/b = 0.55

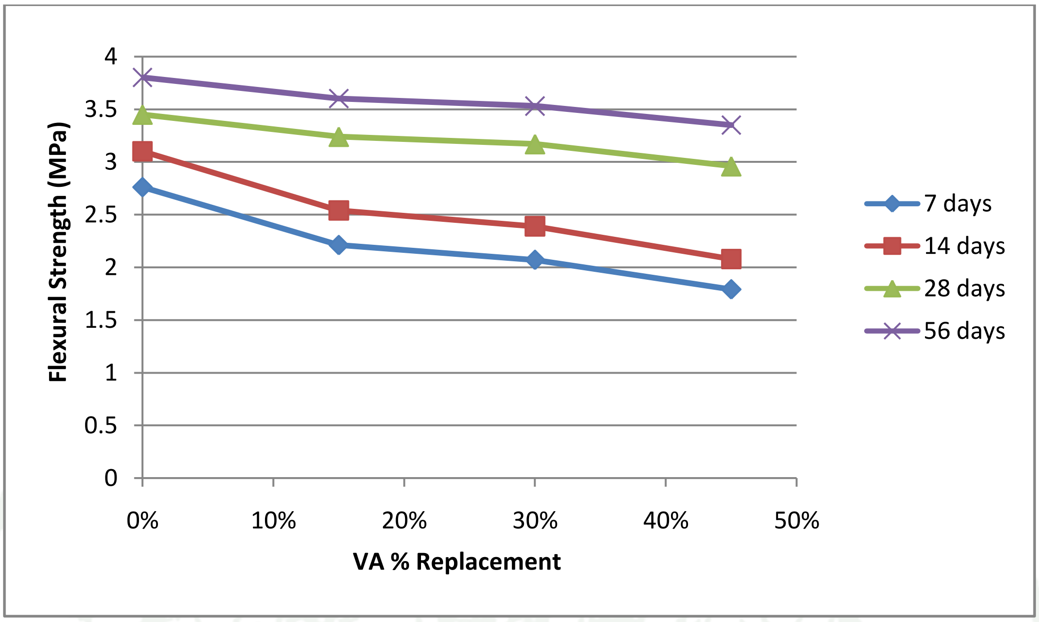

Figure 13 Effect of % replacement VA on flexural strength of concrete at w/b = 0.6

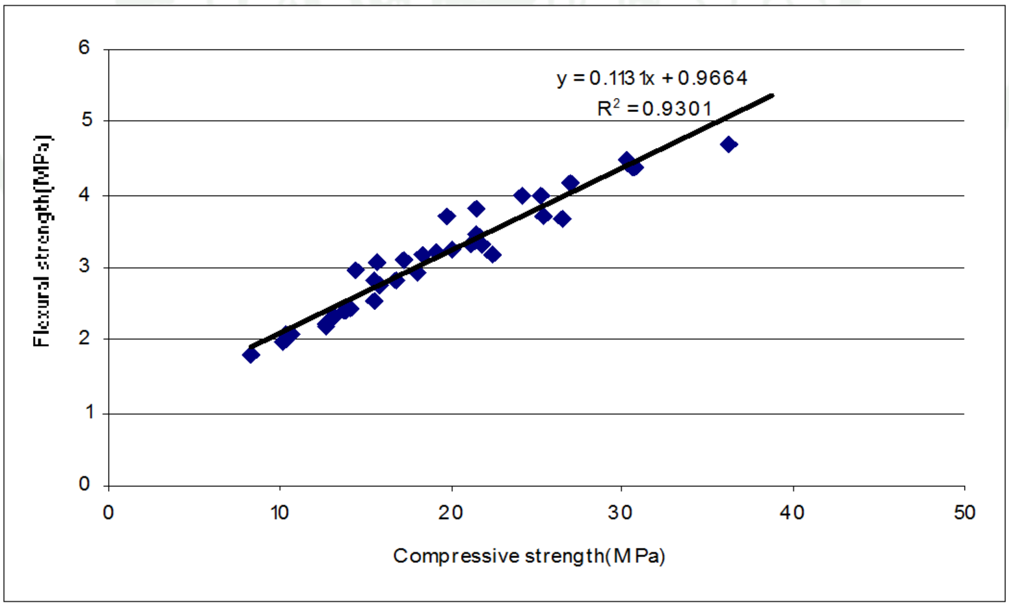

Figure 14 Relationship between compressive strength and flexural strength of volcanic ash concrete and control concrete

The relationship between compressive strengths and flexural strengths of control concrete are shown in Figure 15 and that of volcanic ash concrete are shown in Figure 16. Their relationships were significant with R^2 values of 0.955 and 0.92. The same compressive strengths were substituted in these equations to compare their flexural strengths. The values of compressive strengths and flexural strengths are shown in Table 13. It showed that flexural strength of control concrete was higher than that of VA concrete at lower compressive strength. But the flexural strength of VA concrete was higher when the compressive strength was higher. From this result, it can be concluded that the flexural strength of VA concrete may be comparable or higher than control concrete at later age. This result is consistent with the finding of Lynn *et al.* (1972). They stated that Portland-pozzolan concrete could exhibit higher flexural to compressive strength ratios than normal Portland cement at larger ages. This higher flexural strength is valuable for pavement.

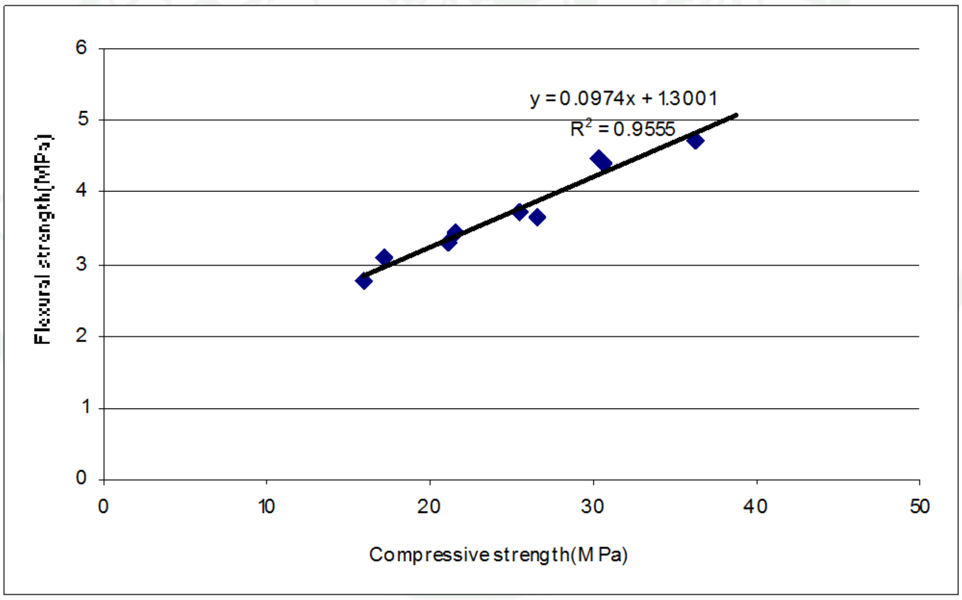

Figure 15 Relationship between compressive strength and flexural strength of control concrete

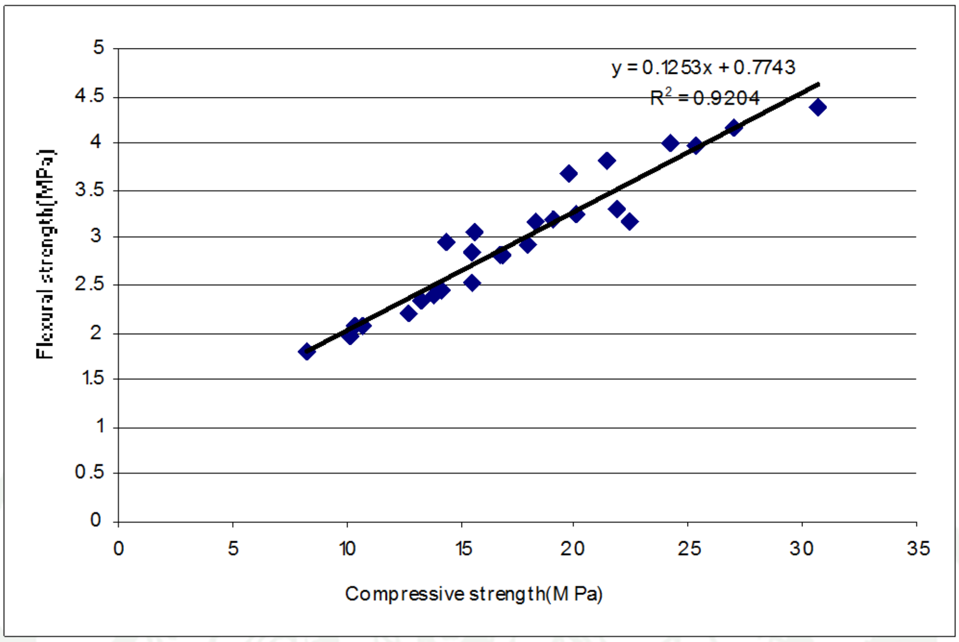

Figure 16 Relationship between compressive strength and flexural strength of volcanic ash concrete

Table 13 Comparison of flexural strengths of volcanic ash concrete and control concrete

Compressive strength (x)	Flexural strength of volcanic ash concrete (y_1) y_1=0.125x+0.7743	Flexural strength of control concrete (y_2) y_2=0.097+1.3001
10	2.0273	2.2741
15	2.6538	2.7611
20	3.2803	3.2481
25	3.9068	3.7351
30	4.5333	4.2221
35	5.1598	4.7091
40	5.7863	5.1961

2.3 Abrasion resistance

Results of Los Angeles Abrasion are shown in Figure 17 and Appendix Table 12. It is observed that the more abrasion wear was found as VA replacement was higher. Figures 8-10 also show that when the VA replacement was increased, the compressive strength was decreased at all w/b ratios. From these results, it can be concluded that there was a relationship between abrasion resistance and the strength characteristic of concrete. Abrasion wear of VA concrete slightly increased as the VA replacement increased at 28 days. VA replacement up to 15% cement exhibited similar abrasion resistance to the control concrete, but 45%VA showed significantly lower abrasion resistance than control concrete at 56 days. Present result supports the findings of Naik *et al*. (1994) and Laplane *et al.* (1991).

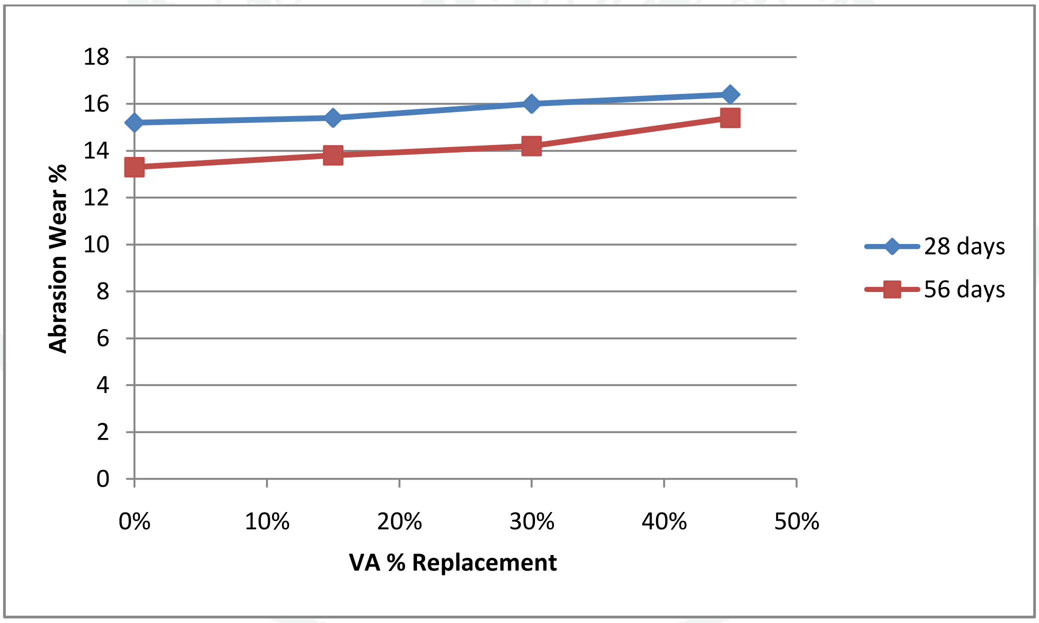

Figure 17 Effect of VA replacement on Los Angeles Abrasion wear (%)

3. Microstructure of cement pastes with volcanic ash

3.1 Mercury Intrusion Porosimetry (MIP)

The results of mercury intrusion porosimetry (MIP) analysis are shown in Figure 18 and Table 14. The critical peaks of OPC and VA45 at 1 day-age occurred at 0.123 µm and 0.288 µm diameter with 0.201 cc/g and 0.225 cc/g incremental pore volumes respectively. Total intruded pore volumes of OPC and VA45 at 1 day-age were 0.265 cc/g and 0.375 cc/g respectively. It is clearly indicated that VA45 was more porous than OPC. This is the result of the slow hydration process of VA45 at early age. The slow hydration process results in a low rate of heat development. This is of great importance in mass concrete construction such as dams and pavements. The cumulative effects of both the slower hydration and the higher porosity contribute to the decrease in compressive strength with the addition of volcanic ash.

At 56 days, the diameter at peak pore volume of VA45 is 0.0507 µm with incremental pore volume of 0.477 cc/g. From the results in Figure 18, it is clearly noted that the diameter of capillary pores significantly decreased with an increase in curing ages. The diameter of capillary pore at peak volume shift towards smaller pore diameter. This is probably due to the filling of large capillary pore with the hydration product. Theerawat *et al*. (2004) reported a similar result.

From the summary of MIP results shown in Table 14, it is noticed that the total intruded pore volume and total porosity of VA45 were significantly higher than OPC at 1 day. This may be the result of higher voids around volcanic ash particles and the porous structure of some volcanic ash particles resulting in an increase in the total pore volume. This high total pore volume has a marked effect on the strength resulting in a consistently low strength of volcanic ash concrete at early age. Total porosity of VA45 reduced to 46% at 56 days from that of 49% at 1 day. This small amount of reduction in porosity indicated the slow degree of hydration of volcanic ash. Density of VA45 paste was lower than that of OPC which is due to the lower specific gravity of VA than that of OPC.

Table 14 Test results of Mercury Intrusion Porosimetry (MIP)

	unit	OPC 1 day	VA45 1 day	VA45 56 days
Diameter at peak pore volume	(µm)	0.123	0.288	0.051
Total intruded pore volume	(cc/g)	0.265	0.375	0.325
Density	(cc/g)	2.795	2.608	2.702
Total porosity	(%)	42.6203	49.4904	46.7367

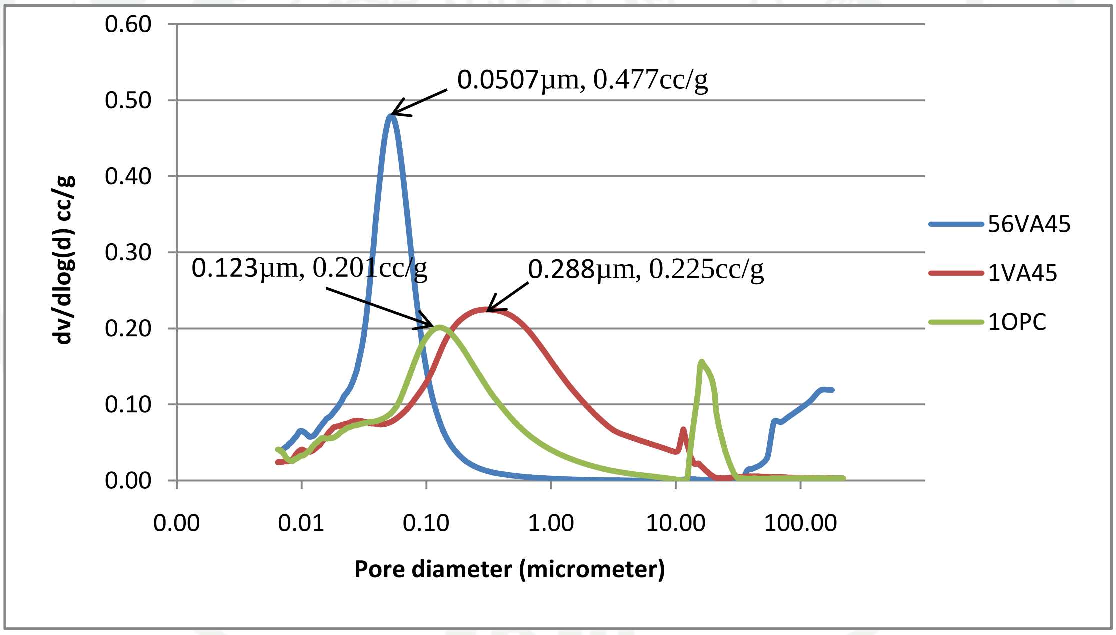

Figure 18 Pore diameter and incremental pore volume of OPC and VA45 pastes at 1day and VA45 at 56 days

3.2 Scanning Electron Microscope

The SEM photos of fractured surface pastes at 1 day age are shown in Figures 19-21. The microstructure of ordinary Portland cement (OPC) paste and cement paste with 45% volcanic ash (VA45) were porous and VA45 had more voids.

More ettringite needles were found in OPC (upper part of Figure 19) than VA45. This is probably due to the slower hydration in the volcanic ash cement mix. This result agrees with the finding of Isaia (2003). The slower reaction can reduce the heat of hydration and lower strength at early age.

The SEM photo of VA45 paste at 56 days is shown in Figure 21. It is observed that most volcanic ash particles were covered by a layer of hydration product and pozzolanic reaction. It is found that the quantity and the pore size were decreased as compared to that of 1 day-age paste. It is also noticed that some un-reacted VA particles still existed in the sample although it was cured for 56 days, which indicated the slow reaction of volcanic ash.

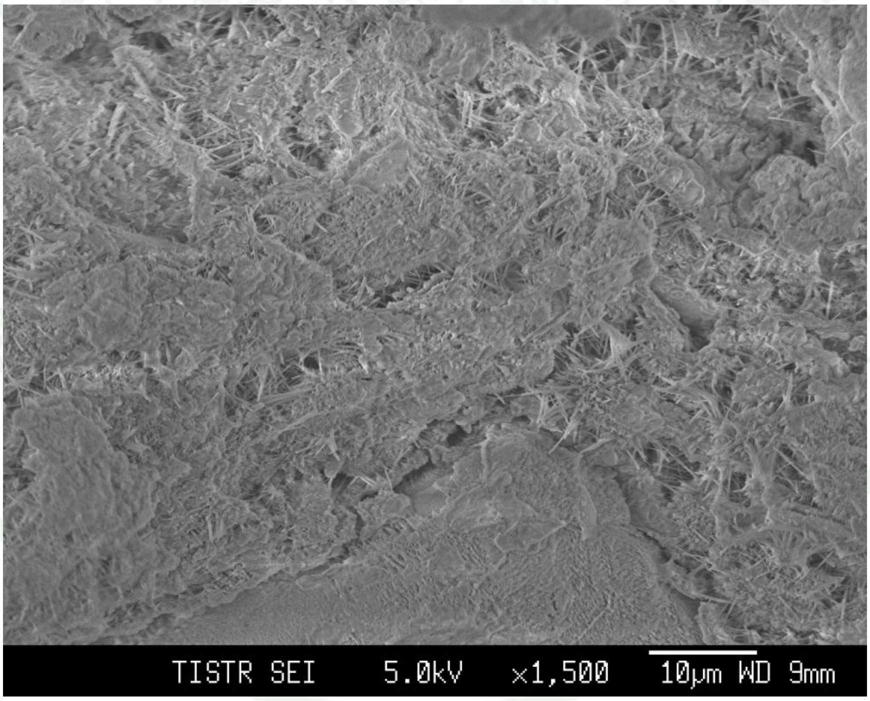

Figure 19 SEM micrograph of ordinary Portland cement paste at 1 day

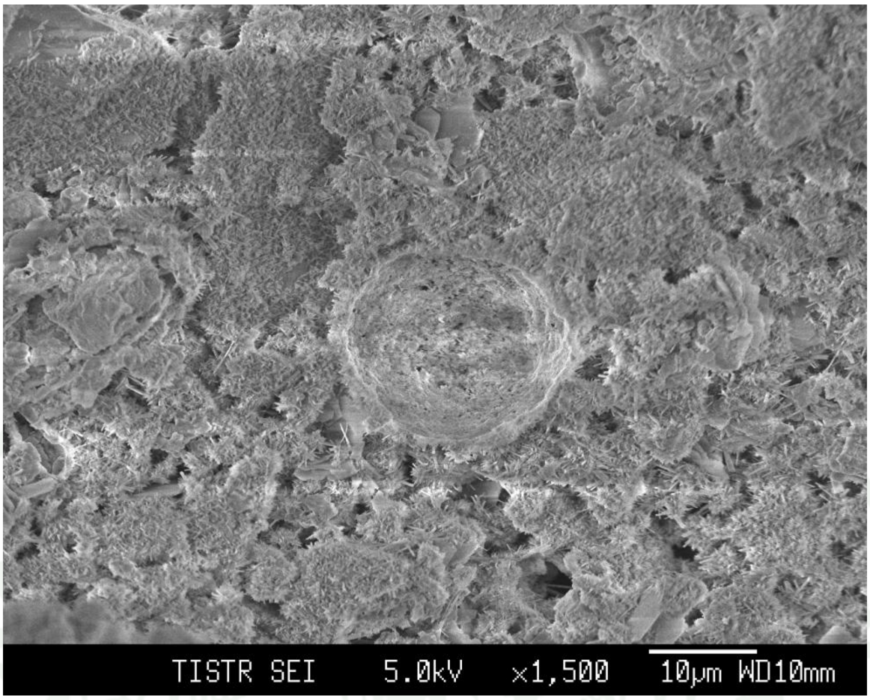

Figure 20 SEM micrograph of cement paste with 45%volcanic ash at 1 day

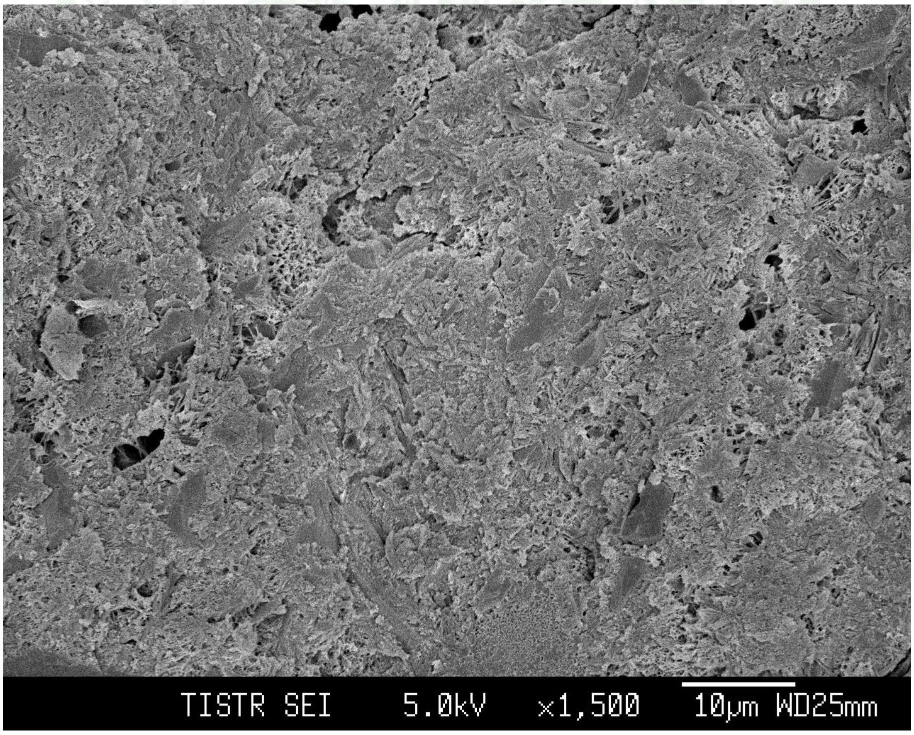

Figure 21 SEM micrograph of cement paste with 45% volcanic ash at 56 days

3.3 X-ray Diffraction (XRD)

The XRD patterns of OPC and VA45 at 1 day-age pastes and 56 day-age paste are shown in Figures 22-24. Figures show that the XRD pattern of VA45 was different from that of OPC. It is easily noticed that C-H or $Ca(OH)_2$ was one of the hydration products during the hydration reaction in OPC. In VA45, there were more products which were Potassium Calcium Magnesium Phosphate ($Ca_9MgK(PO_4)_7$) and Calcium Aluminum Silicate Hydroxide ($Ca_2Al_2SiO_6(OH)_2$) than OPC. According to Figure 23 and 24, the intensity peaks of $Ca(OH)_2$ in VA45 was significantly lower than that of OPC at 1 day. The reason is that the CaO content of volcanic ash (10%) was significantly lower than that of cement (66%) and the decrease in cement content in VA45. ($Ca_9MgK(PO_4)_7$) and ($Ca_2Al_2SiO_6(OH)_2$) products were significant in XRD pattern of VA45 at 1 day and 56 days. This is because of higher MgO and SiO_2 contents in volcanic ash than in ordinary Portland cement. It is found that the intensity peaks of C- H and ($Ca_9MgK(PO_4)_7$) products in VA45 were slightly lower in 56 days than 1 day. This suggests that there was a slight change of the crystalline phase into amorphous phase due to the pozzolanic reaction. This result is in agreement with the results of Khan *et al.* (2011).

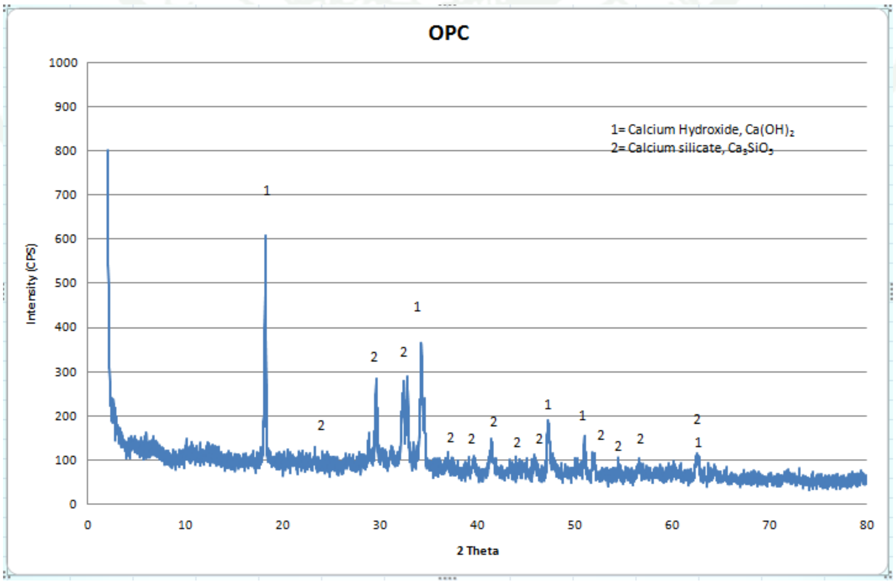

Figure 22 XRD patterns of ordinary Portland cement paste at 1 day

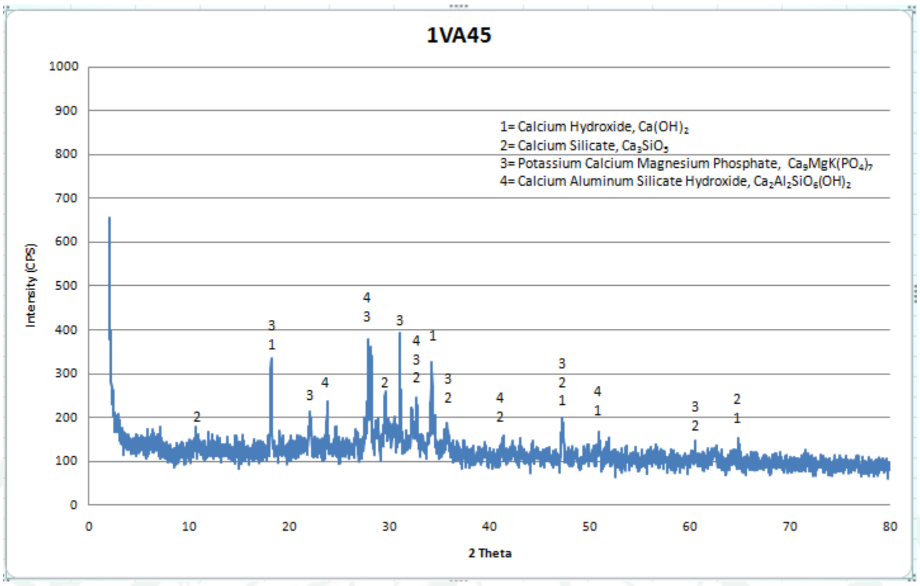

Figure 23 XRD patterns of cement paste with 45% volcanic ash at 1 day

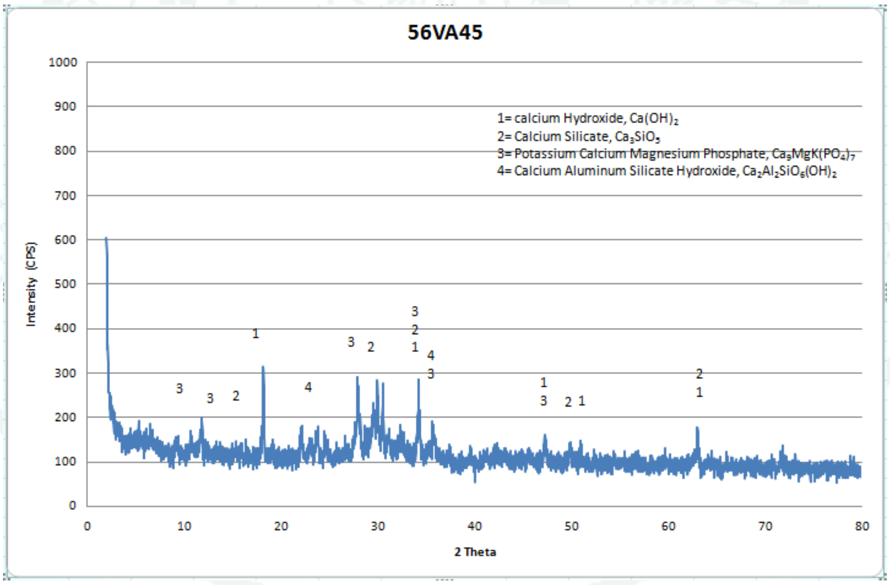

Figure 24 XRD patterns of cement paste with 45%volcanic ash at 56 days

4. Compressive strength of cement mortars incorporating volcanic ash and fly ash

Compressive strength and cement equivalent factor (n) of cement mortars containing volcanic ash and fly ash at 7 days are shown in Appendix Table 16 and Figures 25-26. From this result, compressive strength of all the fly ash mortar and volcanic ash mortar were lower than ordinary cement mortar at 7 days. It is recognized that n values of fly ash mortars were higher than that of volcanic ash mortars. At 15% cement replacement, n values of FA and VA mortars were more than 0.90. But at 30% cement replacement, n value of FA is more than 0.8 and that of VA is less than 0.75. It can be seen that n values of fly ash and volcanic ash mortar decreased as cement replacement with fly ash and volcanic ash increased at 7 days.

Compressive strength and cement equivalent factor (n) of volcanic ash and fly ash mortars at 28 days are shown in Appendix Table 17 and Figure 27-28. All the compressive strengths and cement equivalent factor (n) at 28 days were higher than that of 7 days. This is due to the pozzolanic reaction of volcanic ash and fly ash. Compressive strengths of mortars with 15% and 30% fly ash were higher than ordinary cement mortar(10% and 26%) and that of 45% fly ash mortar was slightly lower than ordinary cement mortar (about 3%). All the compressive strengths of volcanic ash mortars were lower than ordinary cement mortar. But compressive strength of 15% volcanic mortar was comparable to the control mortar. Cement equivalent factor (n) of 45% VA mortar was dramatically reduced to 52% at 28 days.

It is observed that cement equivalent factor (n) of volcanic ash was significantly lower than that of fly ash. It is probably due to lower CaO content of volcanic ash than that of fly ash. An irregular shape with porous particles of volcanic ash leads to increase in the water demand than that of fly ash with spherical shape for the same workability. It is reasonable that strength of volcanic ash-cement blended mortar with higher w/b ratio was lower than that of fly ash-cement blended mortar. SiO_2 content of volcanic ash was higher than that of fly ash. As a sequence, pozzolanic reaction of volcanic ash may be better than that of fly ash at the later ages.

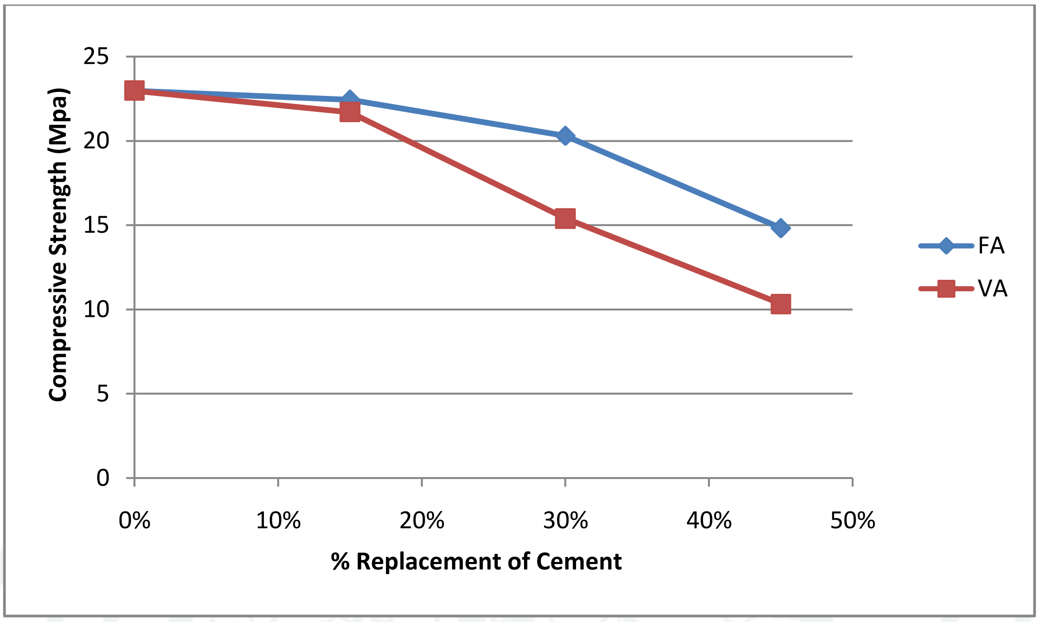

Figure 25 Compressive strengths of mortars incorporating volcanic ash and fly ash at 7 days

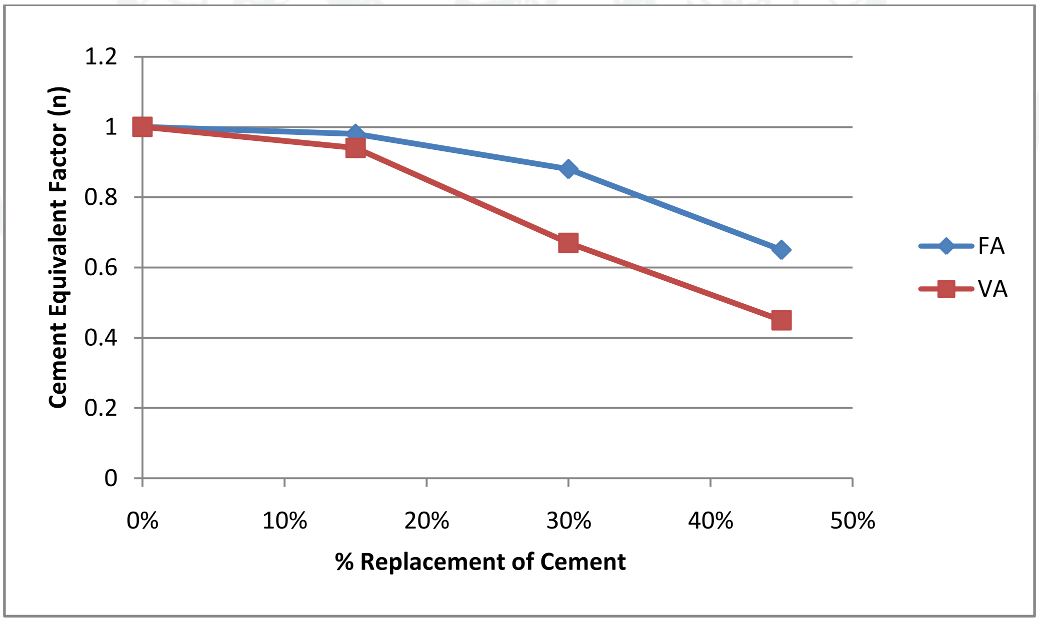

Figure 26 Cement equivalent factors (n) of fly ash and volcanic ash at 7 days

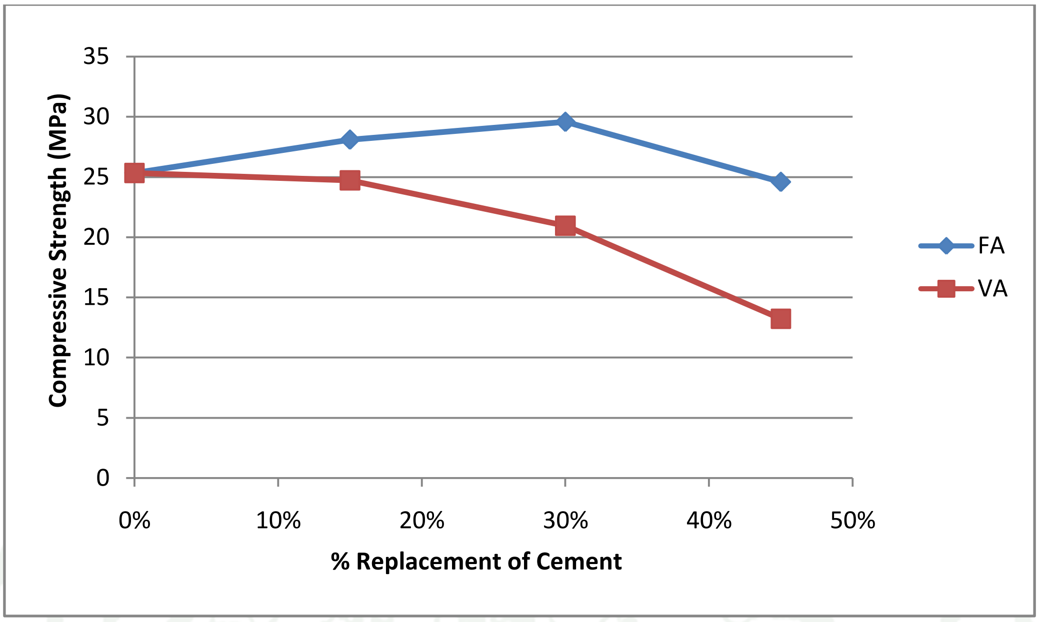

Figure 27 Compressive strengths of mortars incorporating volcanic ash and fly ash at 28 days

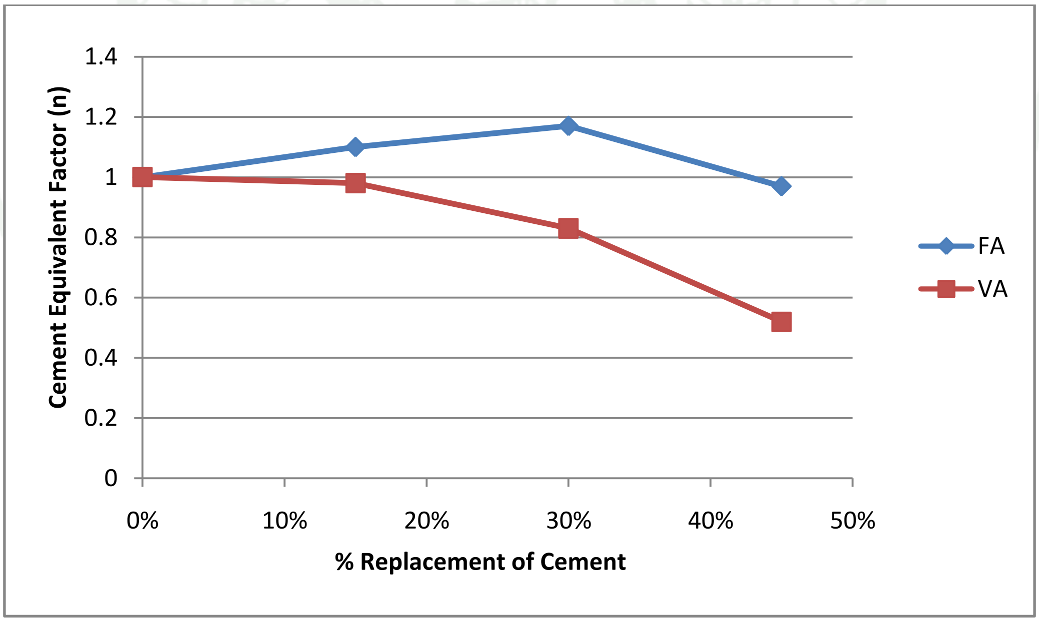

Figure 28 Cement equivalent factors (n) of fly ash and volcanic ash at 28 days

Water requirement for 100% flow standard cement mortars with various volcanic ash and fly ash replacements are shown in Appendix Table 18. Water requirement for blended Portland cement mortar with fly ash significantly reduced as the fly ash replacement increased but that of mortar with volcanic ash slightly increased as the volcanic ash replacement increased. This is in accordance with the finding of Colak (2003) who reported that the replacement of Portland cement by natural pozzolan caused an increase in the water content required for obtaining a constant workability.

5. Water absorption of cement mortars incorporating volcanic ash and fly ash

Water absorption of standard mortars with various fly ash and volcanic ash at 28 days are shown in Appendix Table 19 and Figure 29. Absorption of fly ash mortars slightly increased compared to the control mortar. But this slight increase in absorption was nearly the same for all fractions of the fly ash mortars. Absorption of volcanic ash mortars increased slightly as the volcanic replacement increased but that of 45% volcanic ash mortar increased significantly. Absorption of 15% volcanic ash mortar was comparable to the control mortar. According to this result, it can be concluded that volcanic ash be replace up to 15% of the cement.

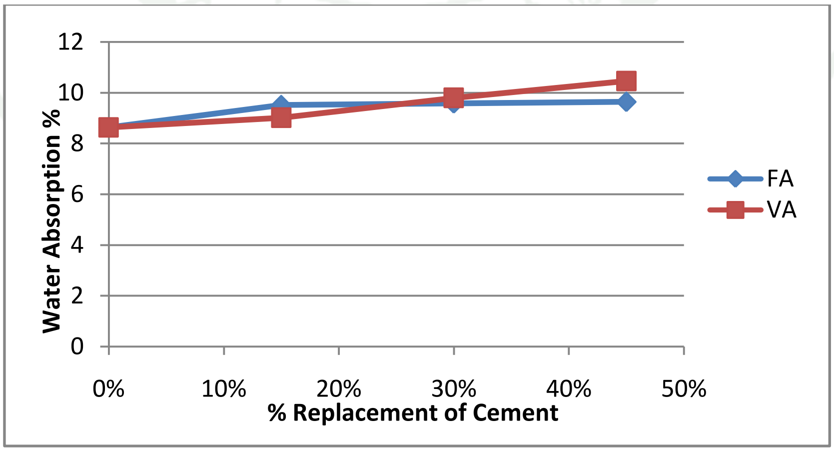

Figure 29 Water absorption (%) of cement mortars incorporating fly ash and volcanic ash at 28 days

CONCLUSIONS AND RECOMMENDATIONS

Conclusions

1. The consistency and setting times of cement paste containing volcanic ash slightly increased as the percentage of cement replacement increased. Increasing setting times was beneficial for saw cutting of pavement slab and transporting of concrete mix to a long distance site.

2. The incorporation of volcanic ash in concrete reduced the compressive strength at early age but there was an increase in the compressive strength at the later ages. The early age strengths were reduced further if the percentage of cement replacement with volcanic ash were increased.

3. The flexural strength of volcanic ash concrete correlated well with the compressive strength of concrete. The flexural strength of volcanic ash concrete may be comparable or higher than the control concrete at the older ages.

4. The abrasion resistance of volcanic ash was slightly lower than the control concrete. The percentages of abrasion wear decreased as the curing time increased. The increase in abrasion wear percentage was significant at 45% of volcanic ash replacement with cement although abrasion wear percentage at 15% of volcanic ash replacement was comparable to the control concrete.

5. The cement equivalent factor (n) of volcanic ash was lower than that of fly ash. The cement equivalent factor (n) at 28 days was significantly higher than that of 7 days. The pozzolanic reaction of volcanic ash was faster as the curing age was older.

6. The water absorption of mortar with volcanic ash was slightly increased as the volcanic ash replacement was increased. The water absorption of mortar at 15% cement replacement with volcanic ash was comparable to that of the control mortar.

7. This is expected as the pozzolanic reaction of VA was a slower process than cement hydration, resulting in a slower strength development of volcanic ash concrete compared to control concrete at early ages, but faster at later ages. This is beneficial for the construction of mass concrete such as pavements and dams.

8. Volcanic ash should be used as a cement replacement up to 15% of cement for surface layer of pavement. The opening for traffic will be delayed because of lower early age strength. Design age should be changed from 28 days to 90 days.

Recommendations

Myanmar volcanic ash is suitable for use as a partial replacement of cement in mass concrete construction such as large bridge pier, abutment of bridge, roller compacted concrete dam, highway and airport pavements etc.

Further research is needed, especially in the microstructure of cement pastes with various percentage of replacement cement with volcanic ash at 7, 28 and 90 days. Shrinkage and expansion tests, sulphate resistance test and chloride permeability tests should also be carried out for future research.

LITERATURE CITED

American Concrete Institute. 1994. Use of Natural Pozzolans in Concrete. ACI Committee 232. **ACI Material Journal**. 91(4): 410-426.

American Society for Testing Materials. 1992. Standard Test Method for Normal Consistency Test of Portland Cement. ASTM Designation C187-92. **Annual Book of ASTM Standards**, 4(02).

American Society for Testing Materials. 1992. Standard Test Method for Initial and Final Setting Time of Portland Cement. ASTM Designation C191-92. **Annual Book of ASTM Standards**, 4(02).

American Society for Testing Materials. 1992. Standard Test Method for Sampling and Testing of Fly Ash or Pozzolans for Use as a Mineral Admixture in Portland Cement Concrete. ASTM Designation C311-92. **Annual Book of ASTM Standards**. 4(02).

American Society for Testing Materials.. 1993. Standard Specification for Coal Fly Ash and Raw or Calcined Natural Pozzolan for Use as a Mineral Admixture in Portland Cement Concrete. ASTM Designation C618-93. **Annual Book of ASTM Standards**. 4(02).

Bergman, L.A. 1962. **Optimization of Portland-pozzolan Concrete, Airport Runways.** Construction Materials, ND Ready Mix Concrete Products Association.

Berry, E.E., R.T. Hemmings, M.H. Zhang, B.J. Cornelious and D.M. Golden. 1994. Hydration in High Volume Fly Ash Binders. **ACI Materials Journal**. 91: 382-389.

Cavdar, A. and S. Yetgin. 2007. Availalility of Tuffs from Northeast of Turkey as Natural Pozolan on Cement, some Chemical and Mechanical Relationships. **Journals of Construction and Building materials**. 21(12): 2066-2071.

Cengiz, D.A. 2005. Strength Properties of High-volume Fly Ash Roller Compacted and workable concrete, and influence of curing condition. **Cement and Concrete Research**. 35: 1112-1121

Colak, A. 2003. Characteristics of Pastes from a Portland Cement Containing Different Amounts of Natural Pozzolan. **Cement and Concrete Research**. (33): 585-593.

Elfert, R.J. 1974. **Bureau of Reclamation Experiences with Fly ash and other Pozzolans in Concrete.** Information Circular. 8640: 80-93. U.S Bureau of Mines, Washington, D.C.

Federal Highway Administration (FHWA). 2001. **The Effect of Higher strength and Associated Concrete Properties on Pavement Performance**. FHWA RD-00-161. US Department of Transportation.

Gambhirm, M.L. 2006. **Concrete Technology.** Third Edition. McGraw-Hill Publishing Company Limited, New Delhi.

Gelber, S.H. and P. Klieger. 1986. Effect of Fly Ash on Physical properties of Concrete. **ACI Special publication**. SP-91: 1-50.

Helmuth, R. 1987. **Fly Ash in Cement and Concrete**. Portland Cement Association, Illinois.

Hossain, K.M.A. 2003. Blended Cement Using Volcanic Ash and Pumice. **Cement and Concrete Research**. 33:1601-1605.

Isaia, G.C., A.L. Gastaldini and R. Moraes. 2003. Physical and pozzolanic action of mineral additions on the mechanical strength of high-performance concrete. **Cement and Concrete Composition**. 25:69–76.

IS: 456. 2000. **Code of Practice for Plain and Reinforced Concrete**. Bureau of Indian Standards, New Delhi, India.

Khan, M.L. and A.M. Alhozaimy. 2011. Properties of Natural Pozzolan and its Potential Utilization in Enviromentally Friendly Concrete. **NRC research, Canadian Journal of Civil Engineering.** 38: 71-78.

Kyaw, W., M. Zaw, A. Dredge, P. Fischer and K. Steiger. 2006. **Yeywa Hydropower Project Overview.** Department of Hydropower. Ministry of Electric Power 1, Myanmar.

Lane, D.S. and C. Ozyildirim. 1999. **Combination of Pozzolan and Ground Granulated Blast Furnace Slag for Durable Hydraulic Cement Concrete.** Final Report, VTRC 00-R1. Virginia Transport Research Council.

Laplante, P.C. and A.D. Vezina. 1991. Abrasion resistance of concrete. **Journal of Material in Civil Engineering**. 3(1):19-28.

Lea, F.M. 1974. **The chemistry of cement and concrete**. Third Edition. Edward Arnold, New York.

Mindess, S. and J.F. Young. 1981**. Concrete**. Prentice-Hall Inc., Englewood Cliffs, N.J.

Minnck, L.J., W.C. Webster and E.J. Purdy. 1971. Predictions of the Effects of Fly Ash in Portland Cement Mortar and Concrete. **Journal of Materials**. 6: 163-187.

Ministry of Electrical Power No.1 (MOEP 1). 2010. **Chemical and Physical Properties of Natural Pozzolan (Popa)**. MOEP 1. Yangon, Myanmar.

Naik, T.R., B.W. Ramme, and J.H. Tews. 1994. Abrasion Resistance of Concrete as Influenced by Inclusion of Fly Ash. **Cement and Concrete Research**. 24(2): 303-312.

Naik, T.R., B.W. Ramme and J.H. Tews. 1995. Pavement Construction with high volume Class C and Class F Fly Ash Concrete. **Cement and Concrete Research**. 92(12): 200-210.

Naik, T.R., S.S. Singh. and M.M. Hossain. 1995. Abrasion Resistance of High Strength Concrete made with Class C Fly Ash. **ACI Material Journal**. 92 (6): 649-659.

Price,W.H. 1975. Pozzolans- a review. **Journal of American Concrete Institute**. 65:225-232.

Sinsiri, T., C. Jaturapitakkul and P. Chindaprasirt. 2004. Effect of Fly Ash on Pore Size and Microstructure of hardened Cement Paste. **Processings of the First International Conference of Asian Concrete Federation**. Thai Concrete Association (TCA). Chiang Mai, Thailand.

Struble, L. and P. Brown. 1987. Microstructure Development During Hydration of Cement. **Materials and Research Society Symposia Preceeding**. 85:106-201.

Tangtermsirikul, S., T. Kaewkhluab and P. Jitvutikrai. 2004. A Compressive Strength Model for Roller Compacted Concrete with Fly Ash. **Magazine of Concrete Research**. 56 (1): 35-44.

Townsend, C.L. 1968. Control of Temperature Cracking in Mass Concrete. **Causes, Mechanism and Control of Cracking in Concrete.** SP-20: 119-139. American Concrete Institute, Farmington Hills, Michigan.

V. Matee and M. Moranville. 1992. Durability of Reactive Powder Composites: Influence of Silica Fume on the Leaching Properties of very Low Water Binder Pastes. **Magazine of Concrete Research**. 44 (161): 291-309.

Volfkovich, Y.M., A.V. Sakars and A.A. Volinsky. 2005. The Method of Standard Porosimetry and Automated Standard Porosimetry. **International Journal of Nanotechnology.** 2(3): 292-302.

Yetgin, S. and A. Cavdar. 2011. Abrasion Resistance of Cement Mortar with Different Pozzolanic Compositions and Matrices. **Journal of Materials in Civil Engineering.** 23(2): 138-145.

APPENDICES

Appendix A

Results of the experiments

Appendix Table A1 Mix Proportion per one cubic meter of concrete (slump 30-60 mm)

Mix no	VA %	w/b	Water (kg)	Volcanic ash (kg)	Cement weight (kg)	Aggregate weight (kg)	Sand weight (kg)
1	0	0.5	210	0	420	1173	577
2	15	0.5	210	63	357	1173	577
3	30	0.5	210	126	294	1173	577
4	45	0.5	210	189	231	1173	577
5	0	0.55	210	0	382	1180	608
6	15	0.55	210	57	325	1180	608
7	30	0.55	210	115	267	1180	608
8	45	0.55	210	172	210	1180	608
9	0	0.6	210	0	350	1183	637
10	15	0.6	210	52	298	1183	637
11	30	0.6	210	105	245	1183	637
12	45	0.6	210	157	193	1183	637

Appendix Table A2 Summary of test results of average compressive strength

w/b	VA (%)	Average compressive strength (MPa)			
		7 days	14 days	28 days	56 days
0.50	0%	25.4	30.3	36.2	38.74
0.50	15%	19.1	24.2	30.7	36
0.50	30%	15.5	19.7	25.3	30.1
0.50	45%	12.7	16.7	22.4	24.4
0.55	0%	21.1	26.5	30.6	36.59
0.55	15%	16.8	21.85	27	32.95
0.55	30%	14.12	18	21.4	29.27
0.55	45%	10.11	13.23	15.6	19.8
0.60	0%	15.9	17.2	21.5	28.27
0.60	15%	12.7	15.5	20.1	27.5
0.60	30%	10.4	13.8	18.3	25.17
0.60	45%	8.3	10.7	14.4	19.6

Appendix Table A3 Compressive strength of specimens tested at 7 days

w/b	VA (%)	Compressive strength (MPa)			
		1	2	3	average
0.50	0%	25.19	23.25	27.76	25.4
0.50	15%	23.25	21.52	12.53	19.1
0.50	30%	14.63	15.07	16.8	15.5
0.50	45%	14.21	12.92	10.97	12.7
0.55	0%	23.67	18.51	21.12	21.1
0.55	15%	18.08	18.08	14.24	16.8
0.55	30%	14.63	13.77	13.96	14.12
0.55	45%	10.76	10.33	9.24	10.11
0.60	0%	16.36	15.50	15.84	15.9
0.60	15%	15.50	13.99	9.21	12.7
0.60	30%	12.92	12.06	6.22	10.4
0.60	45%	8.61	7.97	8.32	8.3

Appendix Table A4 Compressive strength of specimens tested at 14 days

w/b	VA (%)	Compressive strength (MPa)			
		1	2	3	average
0.50	0%	29.28	28.41	33.21	30.3
0.50	15%	27.98	26.69	17.93	24.2
0.50	30%	20.21	18.06	20.83	19.7
0.50	45%	18.69	15.93	14.48	16.7
0.55	0%	26.26	26.69	26.55	26.5
0.55	15%	23.8	20.23	21.52	21.85
0.55	30%	16.36	18.08	19.56	18
0.55	45%	13.33	11.62	14.74	13.23
0.60	0%	18.08	16.36	17.16	17.2
0.60	15%	14.62	17.22	14.66	15.5
0.60	30%	15.05	12.92	13.43	13.8
0.60	45%	10.59	11.19	10.32	10.7

Appendix Table A5 Compressive strength of specimens tested at 28 days

w/b	VA (%)	Compressive strength (MPa)			
		1	2	3	average
0.50	0%	37.88	34.44	36.28	36.2
0.50	15%	31.43	31.82	28.85	30.7
0.50	30%	25.8	22.36	27.74	25.3
0.50	45%	22.79	23.22	21.19	22.4
0.55	0%	28.41	30.99	32.4	30.6
0.55	15%	26.66	28.51	25.83	27
0.55	30%	23.31	20.23	20.66	21.4
0.55	45%	15.07	16.34	15.39	15.6
0.60	0%	21.07	20.66	22.77	21.5
0.60	15%	20.23	20.23	19.84	20.1
0.60	30%	17.66	18.06	19.18	18.3
0.60	45%	15.05	12.92	15.23	14.4

Appendix Table A6 Compressive strength of specimens tested at 56 days

w/b	VA (%)	Compressive strength (MPa)			
		1	2	3	average
0.50	0%	38.7	40.97	36.55	38.74
0.50	15%	38.27	34.4	35.33	36
0.50	30%	29.24	30.1	30.96	30.1
0.50	45%	24.08	23.65	25.47	24.4
0.55	0%	36.12	36.55	37.1	36.59
0.55	15%	30.1	36.07	32.68	32.95
0.55	30%	29.24	29.67	28.9	29.27
0.55	45%	20.7	19.78	18.92	19.8
0.60	0%	30.1	29.24	25.47	28.27
0.60	15%	28.81	27.89	25.8	27.5
0.60	30%	24.08	24.94	26.49	25.17
0.60	45%	21.07	18.06	19.67	19.6

Appendix Table A7 Summary of test results of average flexural strength

w/b	VA (%)	Average flexural strength (MPa)			
		7 days	14 days	28 days	56 days
0.50	0%	3.72	4.48	4.71	5
0.50	15%	3.2	4	4.38	4.95
0.50	30%	2.84	3.69	3.98	4.63
0.50	45%	2.2	2.82	3.16	3.41
0.55	0%	3.31	3.66	4.39	4.5
0.55	15%	2.83	3.31	4.17	4.4
0.55	30%	2.45	2.93	3.82	4
0.55	45%	1.97	2.34	3.07	3.5
0.60	0%	2.76	3.1	3.45	3.8
0.60	15%	2.21	2.54	3.24	3.6
0.60	30%	2.07	2.39	3.17	3.53
0.60	45%	1.79	2.08	2.96	3.35

Appendix Table A8 Flexural strength of specimens tested at 7 days

w/b	VA (%)	Flexural strength (MPa)			
		1	2	3	average
0.50	0%	4.09	3.61	3.46	3.72
0.50	15%	3.77	2.84	2.99	3.2
0.50	30%	3.14	2.58	2.80	2.84
0.50	45%	2.51	2.07	2.02	2.2
0.55	0%	3.59	2.97	3.37	3.31
0.55	15%	3.29	2.58	2.62	2.83
0.55	30%	2.99	2.32	2.04	2.45
0.55	45%	2.39	1.81	1.71	1.97
0.60	0%	3.29	2.07	2.92	2.76
0.60	15%	2.69	2.20	1.74	2.21
0.60	30%	1.95	1.94	2.32	2.07
0.60	45%	1.80	1.81	1.76	1.79

Appendix Table A9 Flexural strength of specimens tested at 14 days

w/b	VA (%)	Flexural strength (MPa)			
		1	2	3	average
0.50	0%	4.39	4.65	4.40	4.48
0.50	15%	4.40	4.07	3.53	4.0
0.50	30%	3.35	3.87	3.85	3.69
0.50	45%	2.83	2.58	3.05	2.82
0.55	0%	3.87	3.61	3.50	3.66
0.55	15%	3.10	3.36	3.47	3.31
0.55	30%	2.99	2.91	2.89	2.93
0.55	45%	2.75	2.32	1.95	2.34
0.60	0%	3.10	3.36	2.84	3.1
0.60	15%	2.58	2.84	2.20	2.54
0.60	30%	2.39	2.32	2.46	2.39
0.60	45%	2.10	2.07	2.07	2.08

Appendix Table A10 Flexural strength of specimens tested at 28 days

w/b	VA (%)	Flexural strength (MPa)			
		1	2	3	average
0.50	0%	4.71	4.65	4.77	4.71
0.50	15%	4.26	4.78	4.10	4.38
0.50	30%	3.87	4.13	3.94	3.98
0.50	45%	2.97	3.36	3.15	3.16
0.55	0%	4.39	4.13	4.65	4.39
0.55	15%	3.87	4.39	4.25	4.17
0.55	30%	3.62	3.87	3.97	3.82
0.55	45%	3.41	2.96	2.84	3.07
0.60	0%	3.45	3.87	3.03	3.45
0.60	15%	3.38	2.84	3.50	3.24
0.60	30%	3.21	2.90	3.40	3.17
0.60	45%	3.08	2.80	3.0	2.96

Appendix Table A11 Flexural strength of specimens tested at 56 days

w/b	VA (%)	Flexural strength (MPa)			
		1	2	3	average
0.5	0%	4.90	5.17	4.90	5.0
0.5	15%	5.03	4.91	4.91	4.95
0.5	30%	4.65	4.65	4.59	4.63
0.5	45%	3.10	3.87	3.26	3.41
0.55	0%	4.52	4.65	4.33	4.5
0.55	15%	4.39	4.13	4.68	4.4
0.55	30%	4.13	3.87	4.0	4.0
0.55	45%	3.36	3.62	3.52	3.5
0.60	0%	4.0	3.87	3.53	3.8
0.60	15%	3.62	3.23	3.95	3.6
0.60	30%	2.97	3.62	4.0	3.53
0.60	45%	3.85	3.49	2.71	3.35

Appendix Table A12 Los Angeles Abrasion wear (%) of volcanic ash concrete at w/b=0.5

Los Angeles Abrasion wear (%)				
Age (days)	0%VA	15%VA	30%VA	45%VA
28	15.2	15.4	16.0	16.4
56	13.28	13.8	14.2	15.4

Appendix Table A13 Pore Size Distribution of OPC by Volume – Intrusion

Pressure [PSI]	Pore Diameter [µm]	Volume Intruded [cc/g]	Delta Volume [cc/g]	% Volume Intruded %	Dv(d) [cc/(µm-g)]	-dv/dlog(d) [cc/g]
0.972	2.19E+02	0.0000	0.0000	0.00	3.68E-06	2.96E-03
1.299	1.64E+02	0.0006	0.0006	0.24	4.87E-06	3.19E-03
1.665	1.28E+02	0.0012	0.0005	0.45	7.80E-06	3.19E-03
2.041	1.05E+02	0.0014	0.0002	0.54	1.16E-05	3.23E-03
2.420	8.82E+01	0.0016	0.0002	0.61	1.55E-05	3.08E-03
2.794	7.63E+01	0.0018	0.0002	0.67	1.98E-05	2.95E-03
3.164	6.74E+01	0.0020	0.0002	0.76	2.64E-05	3.11E-03
3.538	6.03E+01	0.0022	0.0002	0.82	2.48E-05	2.85E-03
3.913	5.45E+01	0.0023	0.0002	0.88	2.33E-05	2.66E-03
4.287	4.98E+01	0.0024	0.0001	0.90	2.48E-05	2.61E-03
4.657	4.58E+01	0.0024	0.0001	0.92	2.72E-05	2.66E-03
5.026	4.25E+01	0.0025	0.0001	0.95	3.05E-05	2.81E-03
5.393	3.96E+01	0.0026	0.0001	0.97	3.03E-05	2.73E-03
5.741	3.72E+01	0.0027	0.0001	1.00	3.20E-05	2.78E-03
6.090	3.50E+01	0.0027	0.0001	1.02	3.32E-05	2.81E-03
6.440	3.31E+01	0.0028	0.0001	1.05	3.80E-05	3.04E-03
6.790	3.14E+01	0.0029	0.0001	1.09	4.39E-05	3.31E-03
7.139	2.99E+01	0.0030	0.0001	1.12	9.59E-05	7.58E-03
7.490	2.85E+01	0.0030	0.0001	1.15	1.80E-04	1.38E-02
7.844	2.72E+01	0.0031	0.0001	1.17	2.97E-04	2.17E-02
8.183	2.61E+01	0.0032	0.0001	1.20	4.35E-04	3.00E-02
8.506	2.51E+01	0.0033	0.0001	1.23	5.95E-04	3.88E-02
8.830	2.42E+01	0.0041	0.0008	1.53	7.77E-04	4.81E-02
9.139	2.33E+01	0.0051	0.0011	1.93	9.83E-04	5.77E-02
9.465	2.25E+01	0.0065	0.0014	2.45	1.21E-03	6.76E-02
9.789	2.18E+01	0.0078	0.0014	2.96	1.47E-03	7.78E-02

Appendix Table A13 (Continued)

Pressure [PSI]	Pore Diameter [µm]	Volume Intruded [cc/g]	Delta Volume [cc/g]	% Volume Intruded %	Dv(d) [cc/(µm-g)]	-dv/dlog(d) [cc/g]
10.095	2.11E+01	0.0092	0.0013	3.47	1.82E-03	9.22E-02
10.386	2.05E+01	0.0105	0.0013	3.96	2.31E-03	1.14E-01
10.677	2.00E+01	0.0118	0.0013	4.46	2.65E-03	1.26E-01
10.968	1.95E+01	0.0131	0.0013	4.95	2.90E-03	1.34E-01
11.257	1.90E+01	0.0144	0.0013	5.45	3.08E-03	1.38E-01
11.562	1.85E+01	0.0163	0.0019	6.17	3.27E-03	1.42E-01
11.884	1.80E+01	0.0192	0.0029	7.24	3.46E-03	1.46E-01
12.205	1.75E+01	0.0213	0.0021	8.05	3.64E-03	1.48E-01
12.540	1.70E+01	0.0232	0.0019	8.76	3.82E-03	1.51E-01
12.875	1.66E+01	0.0247	0.0015	9.34	4.01E-03	1.53E-01
13.209	1.62E+01	0.0263	0.0015	9.93	4.21E-03	1.56E-01
13.559	1.57E+01	0.0278	0.0015	10.51	4.17E-03	1.50E-01
13.924	1.53E+01	0.0294	0.0015	11.09	3.68E-03	1.28E-01
14.287	1.49E+01	0.0309	0.0015	11.68	3.31E-03	1.11E-01
14.648	1.46E+01	0.0325	0.0015	12.26	2.98E-03	9.70E-02
15.005	1.42E+01	0.0340	0.0015	12.85	2.70E-03	8.47E-02
15.361	1.39E+01	0.0350	0.0010	13.21	2.38E-03	7.21E-02
15.716	1.36E+01	0.0350	0.0000	13.21	2.04E-03	5.97E-02
16.054	1.33E+01	0.0350	0.0000	13.21	1.67E-03	4.75E-02
16.393	1.30E+01	0.0350	0.0000	13.21	1.27E-03	3.49E-02
16.730	1.28E+01	0.0350	0.0000	13.21	8.20E-04	2.20E-02
17.066	1.25E+01	0.0350	0.0000	13.21	3.28E-04	8.56E-03
17.402	1.23E+01	0.0350	0.0000	13.21	0.00E+00	0.00E+00
17.735	1.20E+01	0.0350	0.0000	13.21	0.00E+00	0.00E+00
18.067	1.18E+01	0.0350	0.0000	13.21	0.00E+00	0.00E+00
18.398	1.16E+01	0.0350	0.0000	13.21	1.24E-06	4.37E-05

Appendix Table A13 (Continued)

Pressure [PSI]	Pore Diameter [µm]	Volume Intruded [cc/g]	Delta Volume [cc/g]	% Volume Intruded %	Dv(d) [cc/(µm-g)]	-dv/dlog(d) [cc/g]
18.727	1.14E+01	0.0350	0.0000	13.21	4.32E-06	1.73E-04
19.038	1.12E+01	0.0350	0.0000	13.21	8.76E-06	4.24E-04
19.916	1.07E+01	0.0350	0.0000	13.21	1.48E-05	8.74E-04
21.775	9.80E+00	0.0350	0.0000	13.21	2.55E-05	1.81E-03
25.897	8.24E+00	0.0350	0.0000	13.22	4.56E-05	3.33E-03
34.677	6.15E+00	0.0352	0.0002	13.29	9.58E-05	5.74E-03
51.011	4.18E+00	0.0357	0.0005	13.46	2.42E-04	9.47E-03
77.991	2.74E+00	0.0366	0.0009	13.81	6.76E-04	1.50E-02
117.714	1.81E+00	0.0384	0.0018	14.50	1.88E-03	2.27E-02
171.626	1.24E+00	0.0411	0.0027	15.53	4.85E-03	3.28E-02
239.130	8.92E-01	0.0450	0.0038	16.98	1.11E-02	4.52E-02
320.326	6.66E-01	0.0502	0.0052	18.94	2.28E-02	6.00E-02
414.879	5.14E-01	0.0570	0.0068	21.52	4.24E-02	7.69E-02
522.206	4.09E-01	0.0655	0.0085	24.73	7.32E-02	9.56E-02
642.605	3.32E-01	0.0755	0.0100	28.50	1.17E-01	1.15E-01
775.679	2.75E-01	0.0867	0.0112	32.74	1.78E-01	1.35E-01
919.430	2.32E-01	0.0988	0.0121	37.31	2.56E-01	1.55E-01
1071.963	1.99E-01	0.1114	0.0126	42.06	3.50E-01	1.72E-01
1231.182	1.73E-01	0.1240	0.0127	46.84	4.54E-01	1.86E-01
1394.991	1.53E-01	0.1363	0.0122	51.46	5.59E-01	1.96E-01
1562.592	1.37E-01	0.1479	0.0117	55.87	6.60E-01	2.01E-01
1734.634	1.23E-01	0.1588	0.0109	59.99	7.50E-01	2.01E-01
1911.068	1.12E-01	0.1686	0.0098	63.68	8.26E-01	1.97E-01
2092.241	1.02E-01	0.1771	0.0085	66.88	8.82E-01	1.90E-01
2278.354	9.36E-02	0.1841	0.0070	69.53	9.18E-01	1.80E-01
2468.558	8.64E-02	0.1899	0.0057	71.70	9.33E-01	1.68E-01

Appendix Table A13 (Continued)

Pressure [PSI]	Pore Diameter [µm]	Volume Intruded [cc/g]	Delta Volume [cc/g]	% Volume Intruded %	Dv(d) [cc/(µm-g)]	-dv/dlog(d) [cc/g]
2662.705	8.01E-02	0.1945	0.0046	73.46	9.26E-01	1.55E-01
2860.793	7.46E-02	0.1983	0.0038	74.89	9.00E-01	1.41E-01
3062.324	6.97E-02	0.2015	0.0032	76.12	8.63E-01	1.28E-01
3266.449	6.53E-02	0.2044	0.0029	77.20	8.21E-01	1.16E-01
3473.070	6.14E-02	0.2070	0.0025	78.16	7.86E-01	1.06E-01
3682.484	5.79E-02	0.2093	0.0023	79.04	7.60E-01	9.76E-02
3893.894	5.48E-02	0.2114	0.0021	79.85	7.50E-01	9.20E-02
4107.650	5.19E-02	0.2134	0.0020	80.60	7.52E-01	8.82E-02
4323.900	4.93E-02	0.2152	0.0018	81.28	7.61E-01	8.53E-02
4542.745	4.70E-02	0.2169	0.0017	81.91	7.75E-01	8.31E-02
4764.833	4.48E-02	0.2185	0.0016	82.52	7.93E-01	8.13E-02
4989.167	4.28E-02	0.2201	0.0016	83.13	8.14E-01	7.99E-02
5215.296	4.09E-02	0.2217	0.0015	83.71	8.38E-01	7.89E-02
5443.521	3.92E-02	0.2231	0.0014	84.25	8.61E-01	7.79E-02
5673.443	3.76E-02	0.2245	0.0014	84.78	8.92E-01	7.75E-02
5905.661	3.61E-02	0.2258	0.0013	85.29	9.27E-01	7.73E-02
6139.175	3.48E-02	0.2271	0.0013	85.77	9.62E-01	7.72E-02
6375.084	3.35E-02	0.2284	0.0013	86.25	9.86E-01	7.62E-02
6612.591	3.23E-02	0.2296	0.0012	86.70	1.01E+00	7.56E-02
6852.342	3.11E-02	0.2307	0.0012	87.14	1.04E+00	7.51E-02
7093.890	3.01E-02	0.2319	0.0011	87.58	1.07E+00	7.44E-02
7337.084	2.91E-02	0.2330	0.0011	88.00	1.10E+00	7.38E-02
7582.125	2.81E-02	0.2340	0.0010	88.37	1.13E+00	7.33E-02
7829.411	2.73E-02	0.2350	0.0010	88.76	1.15E+00	7.26E-02
8078.193	2.64E-02	0.2360	0.0010	89.13	1.18E+00	7.22E-02
8329.021	2.56E-02	0.2369	0.0009	89.48	1.21E+00	7.15E-02

Appendix Table A13 (Continued)

Pressure [PSI]	Pore Diameter [μm]	Volume Intruded [cc/g]	Delta Volume [cc/g]	% Volume Intruded %	Dv(d) [cc/(μm-g)]	-dv/dlog(d) [cc/g]
8581.597	2.49E-02	0.2378	0.0009	89.82	1.23E+00	7.08E-02
8836.116	2.41E-02	0.2387	0.0009	90.16	1.25E+00	6.98E-02
9092.085	2.35E-02	0.2396	0.0009	90.48	1.28E+00	6.93E-02
9350.846	2.28E-02	0.2405	0.0009	90.81	1.29E+00	6.81E-02
9610.954	2.22E-02	0.2413	0.0008	91.12	1.31E+00	6.69E-02
9873.359	2.16E-02	0.2421	0.0008	91.42	1.32E+00	6.57E-02
10137.310	2.10E-02	0.2428	0.0008	91.70	1.33E+00	6.47E-02
10403.210	2.05E-02	0.2435	0.0007	91.98	1.34E+00	6.33E-02
10671.100	2.00E-02	0.2442	0.0007	92.23	1.34E+00	6.17E-02
10941.090	1.95E-02	0.2448	0.0006	92.47	1.33E+00	5.99E-02
11213.070	1.90E-02	0.2455	0.0006	92.70	1.34E+00	5.85E-02
11487.200	1.86E-02	0.2461	0.0006	92.93	1.34E+00	5.72E-02
11763.230	1.81E-02	0.2466	0.0006	93.14	1.35E+00	5.66E-02
12041.850	1.77E-02	0.2472	0.0005	93.34	1.37E+00	5.60E-02
12321.820	1.73E-02	0.2477	0.0005	93.53	1.39E+00	5.58E-02
12604.430	1.69E-02	0.2482	0.0005	93.73	1.42E+00	5.57E-02
12888.440	1.66E-02	0.2487	0.0005	93.93	1.44E+00	5.55E-02
13174.690	1.62E-02	0.2493	0.0006	94.14	1.46E+00	5.51E-02
13469.530	1.58E-02	0.2498	0.0006	94.35	1.50E+00	5.53E-02
13772.700	1.55E-02	0.2504	0.0006	94.56	1.54E+00	5.54E-02
14084.95	1.52E-02	0.2509	0.0006	94.77	1.58E+00	5.57E-02
14406.18	1.48E-02	0.2515	0.0005	94.98	1.62E+00	5.56E-02
14728.91	1.45E-02	0.2520	0.0005	95.17	1.66E+00	5.55E-02
15054.09	1.42E-02	0.2525	0.0005	95.37	1.66E+00	5.42E-02
15381.01	1.39E-02	0.2530	0.0005	95.56	1.66E+00	5.30E-02
15710.47	1.36E-02	0.2535	0.0005	95.75	1.65E+00	5.16E-02

Appendix Table A13 (Continued)

Pressure [PSI]	Pore Diameter [µm]	Volume Intruded [cc/g]	Delta Volume [cc/g]	% Volume Intruded %	Dv(d) [cc/(µm-g)]	-dv/dlog(d) [cc/g]
16041.48	1.33E-02	0.2540	0.0005	95.93	1.64E+00	5.02E-02
16374.94	1.30E-02	0.2545	0.0005	96.11	1.64E+00	4.90E-02
16711.14	1.28E-02	0.2549	0.0004	96.26	1.63E+00	4.78E-02
17042.40	1.25E-02	0.2553	0.0004	96.40	1.61E+00	4.62E-02
17369.57	1.23E-02	0.2556	0.0004	96.53	1.58E+00	4.46E-02
17691.90	1.21E-02	0.2559	0.0003	96.66	1.54E+00	4.28E-02
18009.04	1.19E-02	0.2563	0.0003	96.78	1.51E+00	4.10E-02
18328.78	1.16E-02	0.2566	0.0003	96.90	1.47E+00	3.93E-02
18650.41	1.14E-02	0.2569	0.0003	97.01	1.46E+00	3.84E-02
18973.54	1.12E-02	0.2571	0.0003	97.11	1.44E+00	3.74E-02
19298.31	1.11E-02	0.2574	0.0003	97.21	1.43E+00	3.65E-02
19625.63	1.09E-02	0.2576	0.0002	97.30	1.42E+00	3.55E-02
19954.50	1.07E-02	0.2579	0.0002	97.39	1.39E+00	3.44E-02
20284.46	1.05E-02	0.2581	0.0003	97.48	1.39E+00	3.38E-02
20616.37	1.04E-02	0.2584	0.0002	97.57	1.38E+00	3.31E-02
20949.83	1.02E-02	0.2586	0.0002	97.66	1.40E+00	3.29E-02
21281.59	1.00E-02	0.2588	0.0002	97.74	1.41E+00	3.28E-02
21614.99	9.87E-03	0.2590	0.0002	97.82	1.42E+00	3.25E-02
21950.00	9.72E-03	0.2592	0.0002	97.90	1.43E+00	3.21E-02
22286.35	9.57E-03	0.2594	0.0002	97.98	1.41E+00	3.11E-02
22624.99	9.43E-03	0.2597	0.0002	98.06	1.40E+00	3.04E-02
22965.19	9.29E-03	0.2599	0.0002	98.14	1.39E+00	2.97E-02
23307.03	9.15E-03	0.2601	0.0002	98.22	1.38E+00	2.92E-02
23650.71	9.02E-03	0.2602	0.0002	98.28	1.39E+00	2.89E-02
23996.79	8.89E-03	0.2604	0.0002	98.34	1.37E+00	2.80E-02
24345.17	8.76E-03	0.2606	0.0002	98.40	1.37E+00	2.77E-02

Appendix Table A13 (Continued)

Pressure [PSI]	Pore Diameter [µm]	Volume Intruded [cc/g]	Delta Volume [cc/g]	% Volume Intruded %	Dv(d) [cc/(µm-g)]	-dv/dlog(d) [cc/g]
24695.54	8.64E-03	0.2607	0.0002	98.46	1.34E+00	2.68E-02
25050.90	8.52E-03	0.2609	0.0002	98.52	1.31E+00	2.58E-02
25408.61	8.40E-03	0.2610	0.0002	98.59	1.32E+00	2.56E-02
25768.21	8.28E-03	0.2612	0.0001	98.64	1.34E+00	2.57E-02
26129.75	8.16E-03	0.2613	0.0002	98.70	1.37E+00	2.60E-02
26493.35	8.05E-03	0.2615	0.0001	98.76	1.42E+00	2.65E-02
26859.39	7.94E-03	0.2616	0.0001	98.81	1.47E+00	2.71E-02
27226.82	7.84E-03	0.2618	0.0002	98.87	1.52E+00	2.76E-02
27596.81	7.73E-03	0.2620	0.0002	98.93	1.57E+00	2.83E-02
27968.48	7.63E-03	0.2621	0.0002	99.00	1.65E+00	2.92E-02
28342.25	7.53E-03	0.2623	0.0002	99.06	1.72E+00	3.00E-02
28717.67	7.43E-03	0.2625	0.0002	99.13	1.83E+00	3.16E-02
29095.39	7.33E-03	0.2627	0.0002	99.20	1.95E+00	3.33E-02
29475.35	7.24E-03	0.2629	0.0002	99.27	2.05E+00	3.45E-02
29857.55	7.15E-03	0.2631	0.0002	99.34	2.16E+00	3.59E-02
30241.46	7.05E-03	0.2632	0.0002	99.42	2.27E+00	3.72E-02
30627.70	6.97E-03	0.2635	0.0002	99.50	2.40E+00	3.89E-02
31015.99	6.88E-03	0.2637	0.0002	99.59	2.40E+00	3.83E-02
31403.01	6.79E-03	0.2639	0.0002	99.67	2.49E+00	3.90E-02
31792.33	6.71E-03	0.2642	0.0002	99.76	2.58E+00	3.95E-02
32185.53	6.63E-03	0.2644	0.0002	99.85	2.67E+00	4.02E-02
32579.94	6.55E-03	0.2647	0.0003	99.95	2.76E+00	4.09E-02
32980.61	6.47E-03	0.2648	0.0001	100.00	2.81E+00	4.08E-02

Appendix Table A14 Pore Size Distribution of 1VA45 by Volume – Intrusion

Pressure [PSI]	Pore Diameter [μm]	Volume Intruded [cc/g]	Delta Volume [cc/g]	% Volume Intruded %	Dv(d) [cc/(μm-g)]	-dv/dlog(d) [cc/g]
0.972	2.19E+02	0.0000	0.0000	0.00	3.33E-06	3.04E-03
1.299	1.64E+02	0.0004	0.0004	0.11	4.55E-06	3.35E-03
1.665	1.28E+02	0.0008	0.0004	0.20	7.67E-06	3.60E-03
2.041	1.05E+02	0.0011	0.0003	0.28	1.18E-05	3.80E-03
2.420	8.82E+01	0.0013	0.0003	0.36	1.68E-05	3.98E-03
2.794	7.63E+01	0.0016	0.0003	0.43	2.22E-05	4.07E-03
3.164	6.74E+01	0.0019	0.0003	0.51	3.09E-05	4.56E-03
3.538	6.03E+01	0.0022	0.0003	0.58	3.55E-05	4.80E-03
3.913	5.45E+01	0.0024	0.0002	0.64	4.06E-05	5.01E-03
4.287	4.98E+01	0.0026	0.0002	0.70	4.69E-05	5.29E-03
4.657	4.58E+01	0.0028	0.0002	0.75	5.28E-05	5.45E-03
5.026	4.25E+01	0.0030	0.0002	0.80	5.72E-05	5.42E-03
5.376	3.97E+01	0.0032	0.0002	0.84	6.11E-05	5.42E-03
5.708	3.74E+01	0.0033	0.0001	0.88	6.40E-05	5.36E-03
6.022	3.54E+01	0.0035	0.0001	0.92	6.59E-05	5.24E-03
6.338	3.37E+01	0.0036	0.0001	0.95	6.71E-05	5.07E-03
6.655	3.21E+01	0.0037	0.0001	0.98	6.94E-05	4.99E-03
6.953	3.07E+01	0.0038	0.0001	1.00	6.95E-05	4.76E-03
7.236	2.95E+01	0.0038	0.0001	1.02	6.85E-05	4.51E-03
7.520	2.84E+01	0.0039	0.0001	1.04	6.55E-05	4.13E-03
7.805	2.73E+01	0.0040	0.0001	1.06	6.05E-05	3.68E-03
8.075	2.64E+01	0.0040	0.0001	1.08	5.79E-05	3.41E-03
8.331	2.56E+01	0.0041	0.0000	1.09	5.70E-05	3.26E-03
8.588	2.48E+01	0.0041	0.0000	1.10	5.60E-05	3.16E-03
8.845	2.41E+01	0.0041	0.0000	1.10	5.62E-05	3.12E-03
9.120	2.34E+01	0.0042	0.0000	1.11	5.79E-05	3.16E-03

Appendix Table A14 (Continued)

Pressure [PSI]	Pore Diameter [µm]	Volume Intruded [cc/g]	Delta Volume [cc/g]	% Volume Intruded %	Dv(d) [cc/(µm-g)]	-dv/dlog(d) [cc/g]
9.378	2.28E+01	0.0042	0.0000	1.12	6.08E-05	3.25E-03
9.635	2.21E+01	0.0042	0.0000	1.12	6.28E-05	3.30E-03
9.908	2.15E+01	0.0043	0.0000	1.14	6.84E-05	3.51E-03
10.182	2.10E+01	0.0043	0.0000	1.15	7.41E-05	3.71E-03
10.439	2.04E+01	0.0044	0.0000	1.16	8.44E-05	4.10E-03
10.695	2.00E+01	0.0044	0.0000	1.18	1.12E-04	5.37E-03
10.968	1.95E+01	0.0045	0.0000	1.19	1.40E-04	6.61E-03
11.257	1.90E+01	0.0045	0.0001	1.21	1.71E-04	7.88E-03
11.562	1.85E+01	0.0046	0.0001	1.22	2.15E-04	9.71E-03
11.884	1.80E+01	0.0046	0.0001	1.24	2.61E-04	1.15E-02
12.205	1.75E+01	0.0048	0.0002	1.29	3.09E-04	1.32E-02
12.540	1.70E+01	0.0050	0.0002	1.34	3.62E-04	1.50E-02
12.875	1.66E+01	0.0052	0.0002	1.39	4.21E-04	1.68E-02
13.209	1.62E+01	0.0055	0.0003	1.46	4.81E-04	1.86E-02
13.559	1.57E+01	0.0057	0.0003	1.53	5.47E-04	2.04E-02
13.924	1.53E+01	0.0060	0.0003	1.60	6.18E-04	2.23E-02
14.287	1.49E+01	0.0063	0.0003	1.68	6.41E-04	2.23E-02
14.648	1.46E+01	0.0066	0.0003	1.75	6.56E-04	2.21E-02
15.005	1.42E+01	0.0068	0.0003	1.82	6.69E-04	2.18E-02
15.361	1.39E+01	0.0071	0.0003	1.89	7.51E-04	2.42E-02
15.700	1.36E+01	0.0073	0.0002	1.95	8.45E-04	2.68E-02
16.022	1.33E+01	0.0075	0.0001	1.99	9.72E-04	3.05E-02
16.327	1.31E+01	0.0076	0.0001	2.02	1.12E-03	3.45E-02
16.633	1.28E+01	0.0077	0.0001	2.05	1.27E-03	3.88E-02
16.938	1.26E+01	0.0081	0.0004	2.16	1.44E-03	4.32E-02
17.242	1.24E+01	0.0085	0.0004	2.26	1.62E-03	4.77E-02

Appendix Table A14 (Continued)

Pressure [PSI]	Pore Diameter [µm]	Volume Intruded [cc/g]	Delta Volume [cc/g]	% Volume Intruded %	Dv(d) [cc/(µm-g)]	-dv/dlog(d) [cc/g]
17.545	1.22E+01	0.0090	0.0005	2.39	1.80E-03	5.19E-02
17.846	1.20E+01	0.0095	0.0005	2.53	2.02E-03	5.68E-02
18.147	1.18E+01	0.0100	0.0005	2.67	2.25E-03	6.19E-02
18.445	1.16E+01	0.0105	0.0005	2.81	2.50E-03	6.72E-02
18.743	1.14E+01	0.0110	0.0005	2.94	2.42E-03	6.35E-02
19.054	1.12E+01	0.0116	0.0005	3.08	2.31E-03	5.91E-02
19.380	1.10E+01	0.0121	0.0005	3.22	2.14E-03	5.36E-02
19.718	1.08E+01	0.0126	0.0005	3.36	1.95E-03	4.76E-02
20.048	1.06E+01	0.0131	0.0005	3.50	1.74E-03	4.20E-02
20.695	1.03E+01	0.0132	0.0001	3.53	1.57E-03	3.84E-02
22.309	9.56E+00	0.0134	0.0001	3.57	1.49E-03	3.83E-02
26.088	8.18E+00	0.0136	0.0002	3.62	1.59E-03	4.22E-02
34.176	6.24E+00	0.0139	0.0004	3.72	2.03E-03	4.84E-02
47.922	4.45E+00	0.0154	0.0014	4.10	2.94E-03	5.63E-02
66.179	3.22E+00	0.0201	0.0047	5.35	3.96E-03	6.55E-02
88.247	2.42E+00	0.0292	0.0092	7.80	7.45E-03	8.23E-02
115.125	1.85E+00	0.0426	0.0133	11.35	1.37E-02	1.02E-01
150.405	1.42E+00	0.0587	0.0162	15.67	2.47E-02	1.24E-01
196.483	1.09E+00	0.0768	0.0181	20.50	4.43E-02	1.49E-01
255.161	8.36E-01	0.0965	0.0197	25.75	7.70E-02	1.75E-01
327.012	6.52E-01	0.1175	0.0210	31.34	1.24E-01	1.98E-01
412.534	5.17E-01	0.1395	0.0220	37.21	1.83E-01	2.13E-01
510.779	4.18E-01	0.1624	0.0229	43.31	2.47E-01	2.21E-01
620.501	3.44E-01	0.1857	0.0233	49.54	3.16E-01	2.24E-01
740.452	2.88E-01	0.2087	0.0230	55.68	3.90E-01	2.25E-01
872.677	2.44E-01	0.2290	0.0203	61.09	4.66E-01	2.23E-01

Appendix Table A14 (Continued)

Pressure [PSI]	Pore Diameter [μm]	Volume Intruded [cc/g]	Delta Volume [cc/g]	% Volume Intruded %	Dv(d) [cc/(μm-g)]	-dv/dlog(d) [cc/g]
1018.074	2.10E-01	0.2454	0.0163	65.45	5.42E-01	2.17E-01
1175.747	1.81E-01	0.2579	0.0126	68.80	6.12E-01	2.09E-01
1342.799	1.59E-01	0.2680	0.0100	71.48	6.65E-01	1.97E-01
1516.737	1.41E-01	0.2765	0.0085	73.75	6.90E-01	1.82E-01
1696.164	1.26E-01	0.2837	0.0072	75.67	6.79E-01	1.64E-01
1880.132	1.14E-01	0.2898	0.0061	77.30	6.53E-01	1.47E-01
2067.392	1.03E-01	0.2950	0.0052	78.69	6.31E-01	1.33E-01
2258.046	9.45E-02	0.2995	0.0045	79.88	6.22E-01	1.23E-01
2451.294	8.70E-02	0.3035	0.0040	80.94	6.20E-01	1.14E-01
2647.736	8.06E-02	0.3069	0.0034	81.86	6.17E-01	1.07E-01
2846.272	7.50E-02	0.3099	0.0030	82.66	6.15E-01	9.98E-02
3047.155	7.00E-02	0.3126	0.0027	83.37	6.14E-01	9.39E-02
3250.383	6.56E-02	0.3150	0.0024	84.01	6.17E-01	8.93E-02
3455.705	6.17E-02	0.3171	0.0022	84.59	6.22E-01	8.55E-02
3663.374	5.82E-02	0.3191	0.0019	85.11	6.27E-01	8.19E-02
3872.888	5.51E-02	0.3209	0.0018	85.59	6.36E-01	7.92E-02
4084.748	5.22E-02	0.3225	0.0017	86.03	6.49E-01	7.72E-02
4299.201	4.96E-02	0.3242	0.0017	86.48	6.66E-01	7.56E-02
4515.901	4.72E-02	0.3258	0.0016	86.91	6.87E-01	7.45E-02
4734.696	4.51E-02	0.3273	0.0015	87.30	7.11E-01	7.39E-02
4955.336	4.31E-02	0.3287	0.0014	87.69	7.42E-01	7.38E-02
5178.523	4.12E-02	0.3301	0.0014	88.06	7.76E-01	7.40E-02
5403.205	3.95E-02	0.3315	0.0013	88.42	8.17E-01	7.47E-02
5629.984	3.79E-02	0.3328	0.0013	88.77	8.52E-01	7.49E-02
5858.808	3.64E-02	0.3341	0.0013	89.12	8.89E-01	7.52E-02
6089.029	3.50E-02	0.3354	0.0013	89.45	9.32E-01	7.59E-02

Appendix Table A14 (Continued)

Pressure [PSI]	Pore Diameter [µm]	Volume Intruded [cc/g]	Delta Volume [cc/g]	% Volume Intruded %	Dv(d) [cc/(µm-g)]	-dv/dlog(d) [cc/g]
6321.196	3.38E-02	0.3366	0.0012	89.78	9.74E-01	7.64E-02
6555.060	3.25E-02	0.3378	0.0012	90.12	1.02E+00	7.69E-02
6790.969	3.14E-02	0.3390	0.0012	90.44	1.06E+00	7.76E-02
7028.226	3.04E-02	0.3402	0.0012	90.75	1.11E+00	7.81E-02
7267.828	2.94E-02	0.3414	0.0012	91.06	1.15E+00	7.84E-02
7509.375	2.84E-02	0.3425	0.0011	91.36	1.20E+00	7.87E-02
7752.370	2.75E-02	0.3436	0.0011	91.65	1.24E+00	7.88E-02
7997.461	2.67E-02	0.3447	0.0011	91.94	1.27E+00	7.86E-02
8244.348	2.59E-02	0.3457	0.0010	92.21	1.30E+00	7.79E-02
8492.481	2.51E-02	0.3467	0.0010	92.49	1.33E+00	7.73E-02
8743.110	2.44E-02	0.3477	0.0010	92.75	1.35E+00	7.61E-02
8995.734	2.37E-02	0.3487	0.0010	93.01	1.38E+00	7.55E-02
9250.205	2.31E-02	0.3496	0.0009	93.25	1.41E+00	7.51E-02
9506.223	2.24E-02	0.3504	0.0008	93.48	1.43E+00	7.44E-02
9764.735	2.19E-02	0.3513	0.0008	93.70	1.46E+00	7.38E-02
10025.143	2.13E-02	0.352	0.0008	93.90	1.49E+00	7.31E-02
10287.697	2.07E-02	0.3529	0.0008	94.12	1.51E+00	7.26E-02
10552.197	2.02E-02	0.3537	0.0008	94.34	1.53E+00	7.19E-02
10818.893	1.97E-02	0.3545	0.0008	94.55	1.56E+00	7.12E-02
11087.784	1.92E-02	0.3552	0.0008	94.75	1.59E+00	7.10E-02
11358.820	1.88E-02	0.3560	0.0007	94.95	1.62E+00	7.05E-02
11631.703	1.83E-02	0.3567	0.0007	95.15	1.66E+00	7.04E-02
11912.668	1.79E-02	0.3574	0.0007	95.34	1.67E+00	6.91E-02
12195.729	1.75E-02	0.3581	0.0007	95.53	1.66E+00	6.71E-02
12480.737	1.71E-02	0.3588	0.0007	95.72	1.66E+00	6.53E-02
12773.928	1.67E-02	0.3595	0.0007	95.89	1.65E+00	6.34E-02

Appendix Table A14 (Continued)

Pressure [PSI]	Pore Diameter [µm]	Volume Intruded [cc/g]	Delta Volume [cc/g]	% Volume Intruded %	Dv(d) [cc/(µm-g)]	-dv/dlog(d) [cc/g]
13075.450	1.63E-02	0.3602	0.0007	96.07	1.64E+00	6.15E-02
13385.356	1.59E-02	0.3608	0.0006	96.23	1.62E+00	5.92E-02
13704.394	1.56E-02	0.3613	0.0005	96.37	1.60E+00	5.71E-02
14025.426	1.52E-02	0.3618	0.0005	96.51	1.57E+00	5.49E-02
14348.504	1.49E-02	0.3623	0.0005	96.65	1.54E+00	5.27E-02
14673.528	1.45E-02	0.3628	0.0005	96.78	1.51E+00	5.05E-02
15000.798	1.42E-02	0.3633	0.0005	96.90	1.47E+00	4.81E-02
15323.926	1.39E-02	0.3637	0.0004	97.02	1.45E+00	4.65E-02
15649.300	1.36E-02	0.3641	0.0004	97.12	1.45E+00	4.53E-02
15976.668	1.34E-02	0.3645	0.0004	97.23	1.44E+00	4.42E-02
16299.946	1.31E-02	0.3649	0.0004	97.33	1.43E+00	4.31E-02
16619.082	1.28E-02	0.3652	0.0003	97.42	1.41E+00	4.18E-02
16933.328	1.26E-02	0.3655	0.0003	97.50	1.41E+00	4.08E-02
17242.734	1.24E-02	0.3659	0.0003	97.59	1.39E+00	3.98E-02
17554.436	1.22E-02	0.3662	0.0003	97.67	1.39E+00	3.90E-02
17867.984	1.19E-02	0.3665	0.0003	97.75	1.39E+00	3.84E-02
18183.381	1.17E-02	0.3667	0.0003	97.82	1.40E+00	3.80E-02
18500.820	1.15E-02	0.3670	0.0003	97.90	1.43E+00	3.82E-02
18820.305	1.13E-02	0.3673	0.0003	97.97	1.45E+00	3.82E-02
19141.439	1.11E-02	0.3675	0.0003	98.04	1.48E+00	3.81E-02
19464.666	1.10E-02	0.3678	0.0003	98.11	1.50E+00	3.83E-02
19789.490	1.08E-02	0.3681	0.0003	98.18	1.54E+00	3.85E-02
20115.562	1.06E-02	0.3684	0.0003	98.26	1.58E+00	3.90E-02
20443.131	1.04E-02	0.3687	0.0003	98.34	1.64E+00	3.97E-02
20768.705	1.03E-02	0.3689	0.0003	98.41	1.69E+00	4.03E-02
21095.273	1.01E-02	0.3692	0.0003	98.48	1.73E+00	4.07E-02

Appendix Table A14 (Continued)

Pressure [PSI]	Pore Diameter [µm]	Volume Intruded [cc/g]	Delta Volume [cc/g]	% Volume Intruded %	Dv(d) [cc/(µm-g)]	-dv/dlog(d) [cc/g]
21423.643	9.96E-03	0.3695	0.0003	98.56	1.76E+00	4.05E-02
21753.557	9.81E-03	0.3698	0.0003	98.63	1.77E+00	4.00E-02
22085.117	9.66E-03	0.3701	0.0003	98.71	1.75E+00	3.91E-02
22418.424	9.52E-03	0.3703	0.0003	98.78	1.75E+00	3.83E-02
22753.676	9.38E-03	0.3706	0.0003	98.85	1.74E+00	3.76E-02
23090.477	9.24E-03	0.3708	0.0002	98.91	1.70E+00	3.62E-02
23429.521	9.11E-03	0.3710	0.0002	98.97	1.67E+00	3.49E-02
23770.361	8.97E-03	0.3712	0.0002	99.02	1.63E+00	3.36E-02
24113.799	8.85E-03	0.3714	0.0002	99.07	1.57E+00	3.20E-02
24462.623	8.72E-03	0.3716	0.0002	99.12	1.51E+00	3.03E-02
24813.992	8.60E-03	0.3718	0.0002	99.17	1.46E+00	2.89E-02
25167.057	8.48E-03	0.3719	0.0002	99.21	1.44E+00	2.82E-02
25522.918	8.36E-03	0.3721	0.0002	99.26	1.43E+00	2.76E-02
25880.273	8.24E-03	0.3723	0.0002	99.30	1.43E+00	2.73E-02
26239.627	8.13E-03	0.3724	0.0001	99.34	1.42E+00	2.66E-02
26600.926	8.02E-03	0.3726	0.0001	99.38	1.41E+00	2.61E-02
26964.119	7.91E-03	0.3727	0.0002	99.42	1.41E+00	2.58E-02
27329.158	7.81E-03	0.3729	0.0002	99.46	1.42E+00	2.55E-02
27696.846	7.70E-03	0.3730	0.0002	99.50	1.42E+00	2.53E-02
28065.932	7.60E-03	0.3732	0.0001	99.54	1.43E+00	2.51E-02
28437.156	7.50E-03	0.3733	0.0001	99.58	1.45E+00	2.51E-02
28810.480	7.40E-03	0.3734	0.0001	99.61	1.47E+00	2.52E-02
29185.699	7.31E-03	0.3736	0.0001	99.65	1.48E+00	2.51E-02
29562.367	7.22E-03	0.3737	0.0001	99.69	1.49E+00	2.49E-02
29941.127	7.13E-03	0.3739	0.0001	99.72	1.50E+00	2.47E-02
30321.938	7.04E-03	0.3740	0.0001	99.76	1.53E+00	2.49E-02

Appendix Table A14 (Continued)

Pressure [PSI]	Pore Diameter [μm]	Volume Intruded [cc/g]	Delta Volume [cc/g]	% Volume Intruded %	Dv(d) [cc/(μm-g)]	-dv/dlog(d) [cc/g]
30704.889	6.95E-03	0.3741	0.0001	99.80	1.54E+00	2.47E-02
31090.139	6.86E-03	0.3743	0.0001	99.83	1.54E+00	2.44E-02
31473.441	6.78E-03	0.3744	0.0001	99.87	1.57E+00	2.44E-02
31859.918	6.70E-03	0.3745	0.0001	99.90	1.59E+00	2.43E-02
32248.322	6.62E-03	0.3747	0.0001	99.94	1.63E+00	2.44E-02
32641.229	6.54E-03	0.3748	0.0001	99.97	1.65E+00	2.43E-02
33036.590	6.46E-03	0.3749	0.0001	100.00	1.66E+00	2.41E-02

Appendix Table A15 Pore Size Distribution of 56VA45 by Volume – Intrusion

Pressure [PSI]	Pore Diameter [μm]	Volume Intruded [cc/g]	Delta Volume [cc/g]	% Volume Intruded %	Dv(d) [cc/(μm-g)]	dv/dlog(d) [cc/g]
1.192	1.79E+02	0.0000	0.0000	0.00	2.37E-04	1.19E-01
1.465	1.46E+02	0.0451	0.0451	13.87	2.71E-04	1.19E-01
1.785	1.20E+02	0.0544	0.0094	16.77	3.55E-04	1.04E-01
2.201	9.69E+01	0.0587	0.0042	18.06	4.76E-04	9.31E-02
2.634	8.10E+01	0.0610	0.0024	18.80	6.31E-04	8.42E-02
3.068	6.95E+01	0.0626	0.0016	19.28	7.99E-04	7.68E-02
3.477	6.14E+01	0.0689	0.0063	21.23	1.05E-03	7.71E-02
3.902	5.47E+01	0.0692	0.0002	21.30	3.83E-04	3.16E-02
4.341	4.91E+01	0.0694	0.0002	21.36	2.67E-04	2.19E-02
4.795	4.45E+01	0.0695	0.0002	21.41	2.40E-04	1.79E-02
5.241	4.07E+01	0.0697	0.0001	21.45	2.32E-04	1.53E-02
5.683	3.75E+01	0.0698	0.0001	21.48	2.31E-04	1.34E-02
6.122	3.48E+01	0.0698	0.0001	21.50	4.14E-05	3.05E-03

Appendix Table A15 (Continued)

Pressure [PSI]	Pore Diameter [µm]	Volume Intruded [cc/g]	Delta Volume [cc/g]	% Volume Intruded %	Dv(d) [cc/(µm-g)]	-dv/dlog(d) [cc/g]
6.560	3.25E+01	0.0699	0.0001	21.52	3.95E-05	2.76E-03
6.996	3.05E+01	0.0700	0.0001	21.55	3.80E-05	2.52E-03
7.411	2.88E+01	0.0700	0.0001	21.56	3.67E-05	2.33E-03
7.808	2.73E+01	0.0701	0.0001	21.58	3.68E-05	2.24E-03
8.184	2.61E+01	0.0701	0.0001	21.60	3.73E-05	2.19E-03
8.561	2.49E+01	0.0702	0.0000	21.61	3.87E-05	2.18E-03
8.937	2.39E+01	0.0702	0.0000	21.62	3.89E-05	2.09E-03
9.314	2.29E+01	0.0702	0.0000	21.63	3.86E-05	2.00E-03
9.672	2.21E+01	0.0703	0.0000	21.64	3.71E-05	1.84E-03
10.009	2.13E+01	0.0703	0.0000	21.65	3.46E-05	1.66E-03
10.348	2.06E+01	0.0703	0.0000	21.66	3.21E-05	1.49E-03
10.687	2.00E+01	0.0704	0.0000	21.66	3.16E-05	1.41E-03
11.025	1.94E+01	0.0704	0.0000	21.67	3.08E-05	1.34E-03
11.382	1.87E+01	0.0704	0.0000	21.67	2.99E-05	1.25E-03
11.757	1.81E+01	0.0704	0.0000	21.68	2.83E-05	1.15E-03
12.150	1.76E+01	0.0704	0.0000	21.68	2.62E-05	1.04E-03
12.540	1.70E+01	0.0704	0.0000	21.68	2.55E-05	1.00E-03
12.927	1.65E+01	0.0704	0.0000	21.69	2.67E-05	1.04E-03
13.313	1.60E+01	0.0704	0.0000	21.69	2.80E-05	1.08E-03
13.716	1.56E+01	0.0705	0.0000	21.69	3.20E-05	1.20E-03
14.118	1.51E+01	0.0705	0.0000	21.70	3.66E-05	1.33E-03
14.498	1.47E+01	0.0705	0.0000	21.70	4.21E-05	1.48E-03
14.878	1.43E+01	0.0705	0.0000	21.71	4.78E-05	1.63E-03
15.237	1.40E+01	0.0705	0.0000	21.72	5.39E-05	1.79E-03
15.596	1.37E+01	0.0705	0.0000	21.72	5.71E-05	1.83E-03
15.936	1.34E+01	0.0706	0.0000	21.73	6.05E-05	1.88E-03

Appendix Table A15 (Continued)

Pressure [PSI]	Pore Diameter [µm]	Volume Intruded [cc/g]	Delta Volume [cc/g]	% Volume Intruded %	Dv(d) [cc/(µm-g)]	-dv/dlog(d) [cc/g]
16.577	1.29E+01	0.0706	0.0000	21.74	6.34E-05	1.87E-03
16.897	1.26E+01	0.0706	0.0000	21.75	6.29E-05	1.82E-03
17.216	1.24E+01	0.0706	0.0000	21.75	6.17E-05	1.75E-03
17.533	1.22E+01	0.0706	0.0000	21.75	6.03E-05	1.67E-03
17.866	1.19E+01	0.0707	0.0000	21.76	5.80E-05	1.58E-03
18.216	1.17E+01	0.0707	0.0000	21.76	5.53E-05	1.48E-03
18.563	1.15E+01	0.0707	0.0000	21.76	5.05E-05	1.33E-03
18.927	1.13E+01	0.0707	0.0000	21.77	4.44E-05	1.15E-03
19.287	1.11E+01	0.0707	0.0000	21.77	4.22E-05	1.07E-03
19.663	1.09E+01	0.0707	0.0000	21.77	3.92E-05	9.73E-04
135.161	1.58E+00	0.0708	0.0001	21.81	1.48E-04	1.45E-03
179.069	1.19E+00	0.0710	0.0002	21.86	3.16E-04	2.13E-03
237.548	8.98E-01	0.0712	0.0002	21.93	6.70E-04	3.02E-03
311.045	6.86E-01	0.0715	0.0003	22.03	1.38E-03	4.19E-03
399.561	5.34E-01	0.0720	0.0004	22.16	2.74E-03	5.78E-03
502.846	4.24E-01	0.0725	0.0006	22.33	5.16E-03	7.87E-03
620.601	3.44E-01	0.0732	0.0007	22.54	9.15E-03	1.07E-02
751.030	2.84E-01	0.0740	0.0008	22.79	1.54E-02	1.44E-02
893.284	2.39E-01	0.0750	0.0010	23.09	2.55E-02	1.96E-02
1045.717	2.04E-01	0.0762	0.0012	23.46	4.16E-02	2.67E-02
1208.129	1.77E-01	0.0776	0.0015	23.90	6.64E-02	3.62E-02
1380.870	1.55E-01	0.0794	0.0018	24.46	1.04E-01	4.87E-02
1556.455	1.37E-01	0.0816	0.0022	25.13	1.60E-01	6.49E-02
1732.738	1.23E-01	0.0844	0.0028	25.99	2.40E-01	8.53E-02
1909.670	1.12E-01	0.0878	0.0034	27.03	3.50E-01	1.10E-01
2085.604	1.02E-01	0.0920	0.0042	28.32	4.96E-01	1.40E-01

Appendix Table A15 (Continued)

Pressure [PSI]	Pore Diameter [µm]	Volume Intruded [cc/g]	Delta Volume [cc/g]	% Volume Intruded %	Dv(d) [cc/(µm-g)]	-dv/dlog(d) [cc/g]
2261.189	9.43E-02	0.0970	0.0050	29.87	6.83E-01	1.74E-01
2436.026	8.76E-02	0.1030	0.0060	31.71	9.13E-01	2.11E-01
2609.515	8.18E-02	0.1100	0.0070	33.86	1.19E+00	2.51E-01
2784.002	7.66E-02	0.1180	0.0081	36.35	1.50E+00	2.93E-01
2957.990	7.21E-02	0.1271	0.0090	39.13	1.85E+00	3.34E-01
3132.777	6.81E-02	0.1369	0.0098	42.16	2.23E+00	3.73E-01
3307.663	6.45E-02	0.1473	0.0104	45.37	2.61E+00	4.08E-01
3483.348	6.12E-02	0.1583	0.0110	48.74	2.98E+00	4.37E-01
3661.129	5.83E-02	0.1694	0.0111	52.17	3.34E+00	4.59E-01
3840.555	5.55E-02	0.1805	0.0111	55.58	3.65E+00	4.74E-01
4023.724	5.30E-02	0.1914	0.0108	58.92	3.90E+00	4.79E-01
4210.486	5.07E-02	0.2017	0.0104	62.11	4.10E+00	4.77E-01
4401.389	4.85E-02	0.2115	0.0098	65.13	4.22E+00	4.67E-01
4597.432	4.64E-02	0.2206	0.0091	67.93	4.27E+00	4.49E-01
4796.717	4.45E-02	0.2288	0.0082	70.44	4.25E+00	4.26E-01
5001.242	4.27E-02	0.2361	0.0074	72.71	4.17E+00	3.99E-01
5209.259	4.10E-02	0.2427	0.0065	74.72	4.04E+00	3.70E-01
5421.817	3.94E-02	0.2484	0.0058	76.49	3.87E+00	3.40E-01
5638.266	3.78E-02	0.2534	0.0050	78.02	3.67E+00	3.10E-01
5858.059	3.64E-02	0.2577	0.0043	79.34	3.46E+00	2.81E-01
6081.695	3.51E-02	0.2615	0.0038	80.52	3.25E+00	2.55E-01
6308.124	3.38E-02	0.2649	0.0034	81.57	3.04E+00	2.30E-01
6537.597	3.26E-02	0.2680	0.0031	82.51	2.85E+00	2.09E-01
6769.365	3.15E-02	0.2707	0.0027	83.34	2.68E+00	1.90E-01
7003.977	3.05E-02	0.2731	0.0024	84.09	2.55E+00	1.75E-01
7240.834	2.95E-02	0.2753	0.0022	84.77	2.45E+00	1.64E-01

Appendix Table A15 (Continued)

Pressure [PSI]	Pore Diameter [µm]	Volume Intruded [cc/g]	Delta Volume [cc/g]	% Volume Intruded %	Dv(d) [cc/(µm-g)]	-dv/dlog(d) [cc/g]
7480.137	2.85E-02	0.2773	0.0020	85.38	2.37E+00	1.54E-01
7722.484	2.76E-02	0.2791	0.0018	85.95	2.30E+00	1.45E-01
7966.326	2.68E-02	0.2809	0.0017	86.48	2.24E+00	1.37E-01
8212.515	2.60E-02	0.2825	0.0017	86.99	2.20E+00	1.31E-01
8460.897	2.52E-02	0.2842	0.0017	87.51	2.18E+00	1.26E-01
8710.527	2.45E-02	0.2858	0.0016	88.00	2.16E+00	1.22E-01
8962.405	2.38E-02	0.2872	0.0015	88.45	2.17E+00	1.19E-01
9216.227	2.32E-02	0.2886	0.0014	88.88	2.18E+00	1.16E-01
9472.395	2.25E-02	0.2900	0.0013	89.29	2.19E+00	1.13E-01
9730.357	2.19E-02	0.2912	0.0012	89.67	2.19E+00	1.11E-01
9990.767	2.14E-02	0.2924	0.0012	90.05	2.18E+00	1.07E-01
10253.171	2.08E-02	0.2936	0.0012	90.41	2.16E+00	1.03E-01
10517.221	2.03E-02	0.2948	0.0011	90.76	2.16E+00	1.01E-01
10783.118	1.98E-02	0.2959	0.0011	91.10	2.15E+00	9.81E-02
11051.012	1.93E-02	0.2969	0.0010	91.41	2.15E+00	9.58E-02
11320.850	1.88E-02	0.2978	0.0009	91.69	2.15E+00	9.35E-02
11593.033	1.84E-02	0.2987	0.0009	91.97	2.16E+00	9.14E-02
11866.965	1.80E-02	0.2996	0.0009	92.25	2.15E+00	8.92E-02
12149.028	1.76E-02	0.3005	0.0009	92.52	2.15E+00	8.73E-02
12439.723	1.72E-02	0.3013	0.0009	92.79	2.15E+00	8.52E-02
12732.313	1.68E-02	0.3022	0.0008	93.04	2.16E+00	8.37E-02
13026.753	1.64E-02	0.3030	0.0008	93.30	2.18E+00	8.27E-02
13329.723	1.60E-02	0.3038	0.0008	93.55	2.20E+00	8.16E-02
13640.925	1.56E-02	0.3046	0.0008	93.80	2.20E+00	7.96E-02
13961.31	1.53E-02	0.3054	0.0008	94.04	2.19E+00	7.74E-02
14283.69	1.49E-02	0.3062	0.0008	94.28	2.19E+00	7.53E-02

Appendix Table A15 (Continued)

Pressure [PSI]	Pore Diameter [µm]	Volume Intruded [cc/g]	Delta Volume [cc/g]	% Volume Intruded %	Dv(d) [cc/(µm-g)]	-dv/dlog(d) [cc/g]
14608.763	1.46E-02	0.3069	0.0007	94.51	2.19E+00	7.37E-02
14935.634	1.43E-02	0.3077	0.0007	94.74	2.18E+00	7.16E-02
15264.798	1.40E-02	0.3083	0.0006	94.93	2.17E+00	6.96E-02
15589.872	1.37E-02	0.3089	0.0006	95.11	2.14E+00	6.73E-02
15910.156	1.34E-02	0.3094	0.0006	95.28	2.12E+00	6.54E-02
16232.585	1.31E-02	0.3100	0.0006	95.45	2.09E+00	6.31E-02
16557.211	1.29E-02	0.3105	0.0005	95.61	2.06E+00	6.10E-02
16877.146	1.26E-02	0.3110	0.0005	95.76	2.04E+00	5.93E-02
17192.789	1.24E-02	0.3114	0.0005	95.90	2.04E+00	5.85E-02
17503.494	1.22E-02	0.3119	0.0004	96.04	2.07E+00	5.83E-02
17816.193	1.20E-02	0.3123	0.0004	96.16	2.09E+00	5.78E-02
18130.59	1.18E-02	0.3127	0.0004	96.29	2.12E+00	5.77E-02
18446.682	1.16E-02	0.3131	0.0004	96.42	2.15E+00	5.77E-02
18764.869	1.14E-02	0.3136	0.0004	96.55	2.21E+00	5.84E-02
19085.055	1.12E-02	0.3140	0.0004	96.69	2.30E+00	5.96E-02
19406.734	1.10E-02	0.3144	0.0004	96.82	2.38E+00	6.08E-02
19726.371	1.08E-02	0.3149	0.0004	96.95	2.47E+00	6.20E-02
20047.055	1.06E-02	0.3153	0.0004	97.08	2.55E+00	6.31E-02
20369.482	1.05E-02	0.3158	0.0005	97.22	2.62E+00	6.37E-02
20693.359	1.03E-02	0.3162	0.0005	97.37	2.69E+00	6.43E-02
21019.281	1.02E-02	0.3167	0.0005	97.52	2.76E+00	6.49E-02
21346.701	9.99E-03	0.3172	0.0005	97.66	2.82E+00	6.52E-02
21675.867	9.84E-03	0.3176	0.0004	97.79	2.85E+00	6.48E-02
22006.928	9.69E-03	0.3180	0.0004	97.92	2.89E+00	6.47E-02
22339.984	9.55E-03	0.3184	0.0004	98.05	2.88E+00	6.35E-02
22674.439	9.41E-03	0.3189	0.0004	98.18	2.85E+00	6.18E-02

Appendix Table A15 (Continued)

Pressure [PSI]	Pore Diameter [µm]	Volume Intruded [cc/g]	Delta Volume [cc/g]	% Volume Intruded %	Dv(d) [cc/(µm-g)]	-dv/dlog(d) [cc/g]
23011.590	9.27E-03	0.3192	0.0004	98.30	2.81E+00	6.02E-02
23354.527	9.13E-03	0.3196	0.0004	98.42	2.79E+00	5.87E-02
23699.711	9.00E-03	0.3200	0.0004	98.53	2.77E+00	5.74E-02
24047.188	8.87E-03	0.3203	0.0003	98.64	2.75E+00	5.63E-02
24396.961	8.74E-03	0.3207	0.0003	98.74	2.73E+00	5.51E-02
24748.33	8.62E-03	0.3210	0.0003	98.83	2.70E+00	5.37E-02
25101.594	8.50E-03	0.3213	0.0003	98.93	2.68E+00	5.25E-02
25456.654	8.38E-03	0.3216	0.0003	99.03	2.66E+00	5.16E-02
25814.061	8.26E-03	0.3219	0.0003	99.12	2.63E+00	5.03E-02
26173.363	8.15E-03	0.3222	0.0003	99.22	2.63E+00	4.95E-02
26534.564	8.04E-03	0.3225	0.0003	99.31	2.62E+00	4.86E-02
26897.656	7.93E-03	0.3228	0.0003	99.40	2.62E+00	4.80E-02
27262.898	7.83E-03	0.3231	0.0003	99.49	2.60E+00	4.69E-02
27630.336	7.72E-03	0.3234	0.0003	99.57	2.55E+00	4.54E-02
27999.518	7.62E-03	0.3236	0.0003	99.64	2.55E+00	4.48E-02
28367.271	7.52E-03	0.3238	0.0002	99.72	2.56E+00	4.42E-02
28738.404	7.42E-03	0.3241	0.0003	99.80	2.57E+00	4.35E-02
29111.703	7.33E-03	0.3243	0.0002	99.86	2.58E+00	4.29E-02
29488.588	7.23E-03	0.3245	0.0002	99.92	2.59E+00	4.22E-02
29866.936	7.14E-03	0.3248	0.0002	100.00	2.61E+00	4.18E-02
29866.936	7.14E-03	0.3248	0.0002	100.00	2.61E+00	4.18E-02

Appendix Table A16 Compressive strength of standard motor at 7 days

Mix No	VA/FA (%)	Compressive strength (MPa)				Normalized compressive strength %
		1	2	3	Average	
1	0%	26.09	22.61	20.20	22.97	100
2	15% FA	21.2	29.07	17.03	22.43	97.65
3	30%FA	24.27	16.75	19.85	20.29	88.33
4	45%FA	14.55	14.55	15.36	14.82	64.5
5	15%VA	24.63	19.14	21.32	21.70	94.47
6	30%VA	13.28	16.79	16.10	15.39	67.00
7	45%VA	13.15	7.63	10.22	10.33	44.97

Appendix Table A17 Compressive strength of standard motor at 28 days

Mix No	FA/VA (%)	Compressive strength (MPa)				Normalized compressive strength %
		1	2	3	Average	
1	0%	24.08	26.78	25.12	25.33	100
2	15%FA	22.81	27.57	33.89	28.09	110.9
3	30%FA	25.42	31.55	31.73	29.57	116.74
4	45%FA	24.94	24.13	24.66	24.58	97.04
5	15%VA	22.38	25.92	25.90	24.73	97.66
6	30%VA	22.58	19.39	20.87	20.95	82.71
7	45%VA	14.00	10.54	15.16	13.23	52.24

Appendix Table A18 Water demand for 100% flow standard motor for compressive strength and water absorption tests

Mix No	FA/VA (%)	Cement (gram)	FA/VA (gram)	Sand (gram)	Water (ml)
1	0%	500	0	1375	254
2	15%FA	425	75	1375	252
3	30%FA	350	150	1375	247
4	45%FA	275	225	1375	237
5	15%VA	425	75	1375	255
6	30%VA	350	150	1375	256
7	45%VA	275	225	1375	258

Appendix Table A19 Water absorption of standard motor at 28 days

Mix No	FA/VA (%)	Absorption (%)			
		1	2	3	Average
1	0%	8.74	8.76	8.41	8.64
2	15%FA	9.48	9.38	9.66	9.51
3	30%FA	9.41	9.47	9.86	9.58
4	45%FA	9.75	9.68	9.48	9.64
5	15%VA	9.08	9.22	8.75	9.02
6	30%VA	9.37	9.97	10.05	9.8
7	45%VA	10.27	10.5	10.62	10.46

Appendix B

Photos of the experiments

Appendix Figure B1 Testing consistency of cement and volcanic ash mix paste

Appendix Figure B2 Curing of specimens in water

Appendix Figure B3 Testing Los Angeles abrasion

Appendix Figure B4 Testing compressive strength with ELE testing machine

Appendix Figure B5 Testing flexural strength of VA concrete

Appendix Figure B6 Mixing mortar

Appendix Figure B7 Measuring flow of mortar

Appendix Figure B8 Testing compressive strength of mortar with Universal Testing Machine

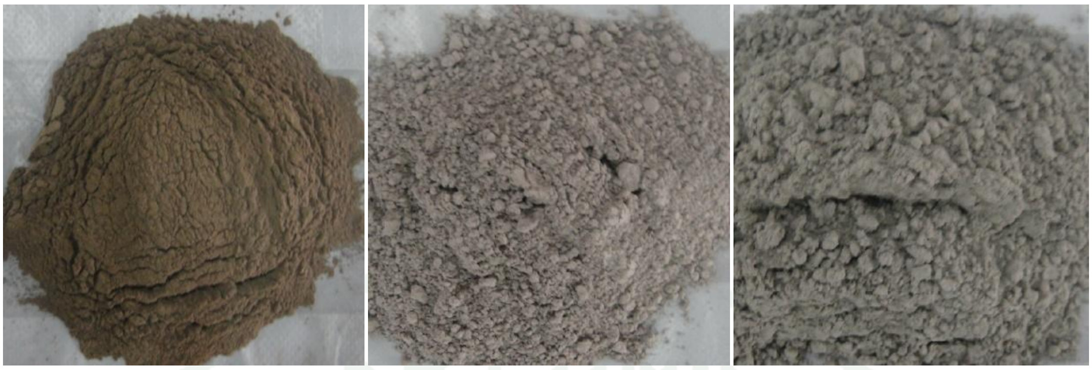

Fly ash volcanic ash cement

Appendix Figure B9 Photos of fly ash, volcanic ash and cement powders

CURRICULUM VITAE

NAME **:** Miss Ei Ei Mon

BIRTH DATE **:** May 13, 1975

BIRTH PLACE : Chauk, the Republic of the Union of Myanmar

EDUCATION **:**

YEAR	**INSTITUTE**	**DEGREE/DIPLOMA**
2002	Mandalay Technological University, Myanmar	B.Eng (Civil Engineering)
2011	Kasetsart University, Thailand	M.Eng (Civil Engineering)

POSITION/TITLE : Assistant Engineer (Civil)

WORKPLACE : Public Works, Ministry of Construction, Naypyitaw, the Republic of the Union of Myanmar

SCHOLARSHIP/AWARDS: Thai Government Scholarship 2009-2011